

UNITED STATES DEPARTMENT OF THE INTERIOR
GEOLOGICAL SURVEY

ELECTRIC LOGGING AND ELECTRICAL PROPERTIES OF
ROCKS IN RAINIER MESA AREA,
NEVADA TEST SITE, NEVADA

By

R.D. Carroll

Open-File Report 90-31

Prepared in cooperation with the
Nevada Operations Office
U.S. Department of Energy
(Interagency Agreement DE-AI08-86NV10583)
and the
Defense Nuclear Agency

1990

This report is preliminary and has not been reviewed for conformity with U.S. Geological Survey editorial standards and stratigraphic nomenclature. Company names are for descriptive purposes only and do not constitute endorsement by the U.S. Geological Survey

UNITED STATES DEPARTMENT OF THE INTERIOR
GEOLOGICAL SURVEY

**ELECTRIC LOGGING AND ELECTRICAL PROPERTIES OF
ROCKS IN RAINIER MESA AREA,
NEVADA TEST SITE, NEVADA**

By

R.D. Carroll

CONTENTS

	Page
Abstract.....	1
Introduction.....	2
Acknowledgments.....	8
Geology and hydrology.....	8
Geologic implications from electric logs obtained in Rainier Mesa.....	13
Correlation based on log character.....	15
Top of zeolitization.....	17
General aspects of electric logging in Rainier Mesa.....	18
Borehole temperatures and the geothermal regime.....	20
Resistivity of Rainier Mesa pore water.....	24
Quantitative interpretation of electric logs.....	32
Saturated tuff.....	33
Effect of clay on electrical resistivity.....	45
Unsaturated zone.....	53
Clay content versus resistivity.....	56
Effect of zeolites on electrical resistivity.....	60
Laboratory measurements.....	64
Other electrical properties obtained in logging.....	69
Magnetic susceptibility.....	71
Induced polarization.....	72
Spontaneous potential.....	74
Dielectric constant.....	77
Resistivity of rocks in Rainier Mesa area.....	82
Summary and conclusions.....	83
References cited.....	85

ILLUSTRATIONS

Figure		Page
1.	Map of locations of vertical drill holes in Rainier Mesa area in which electric logs are available.....	3
2.	General stratigraphy of Rainier Mesa area, Nevada Test Site.....	9
3.	Generalized north-south cross section through Rainier Mesa area.....	10
4.	Lithologic and electric logs obtained in holes in northern Aqueduct Mesa.....	In pocket
5.	Lithologic and electric logs obtained in holes in southern Aqueduct Mesa.....	In pocket
6.	Lithologic and electric logs obtained in holes in northern N-tunnel area.....	In pocket
7.	Lithologic and electric logs obtained in holes in central Rainier Mesa.....	In pocket
8.	Lithologic and electric logs obtained in holes in southern Rainier Mesa.....	In pocket
9.	Lithologic and electric logs obtained in HTH#1.....	In pocket
10.	Electric log obtained entirely in dolomite in Dolomite Hill hole.....	14
11.	Electric logs obtained in Rainier Mesa area illustrating character correlation in tunnel beds 3 and 4.....	16
12.	Generalized thermal regime in Rainier Mesa.....	21
13.	Graphs of temperatures recorded on electric logs from Rainier Mesa area as a function of (a) bottom-hole elevations and (b) hole depths.....	23
14.	Plot of locations of samples obtained in t#3 for pore-water chemistry.....	26
15.	Graphs of conductivity of Rainier Mesa fracture waters versus (a) total ion content and (b) calculated values from equivalent NaCl content.....	28
16.	Graph of resistivity versus total dissolved solids for Rainier Mesa fracture waters.....	29
17.	Graph of behavior of tuff conductivity versus pore-saturant conductivity for a clean rock and rock containing clay-bound water.....	35
18.	Plots of formation factor-porosity relationship for tuff samples obtained in Rainier Mesa tunnel beds.....	36
19.	Schematic of rock constituents affecting electric and neutron logs.....	43
20.	Plot of surface area versus cation exchange capacity for several rock types.....	46
21.	Histograms of CEC, Qv, and porosity distribution for 140 clayey sandstones used to derive WS model.....	49
22.	Plots of relationships among Qv, CEC, and porosity for 140 clayey sandstones used to derive WS model.....	50
23.	Electric (ELOG) and density (DENS) logs obtained in tunnel beds in e#3	52
24.	Electric (ELOG) and density (DEN) logs obtained in unsaturated zone in e#3	55

ILLUSTRATIONS--Continued

	Page
25. Graphs of range of resistivities as a function of clay content predicted by WS model for tuffs in the saturated tunnel beds.....	58
26. Graphs of range of resistivities as a function of clay content predicted by WS model for tuffs in the unsaturated zone.....	59
27. Graphs of theoretical electric log resistivities and Qv which would be observed in the tunnel beds in e#3 for an average tuff CEC of 80 meq/100 g.....	62
28. Waxman-Smiths plots of conductivity of core versus saturant reported for three zeolites.....	63
29. Plots of conductivity of selected tuff samples from Rainier Mesa area versus (a) zeolite content and (b) clay content.....	68
30. Plots of calculated WS conductivity of selected tuff samples from Rainier Mesa area versus measured conductivity for (a) all samples using measured Qv and (b) samples using only the clay component with assumed CEC = 1 meq/g.....	70
31. Density, electric, induced polarization, and magnetic susceptibility logs obtained in e#3.....	In pocket
32. Schematic of ideal SP response in sand-clay sequence.....	75
33. Electric log obtained in Hagestad hole illustrating SP response in tuffs.....	In pocket
34. Histogram of mud resistivities recorded from pit or tank samples obtained on Rainier Mesa.....	78
35. Plots of dielectric constant and resistivity as a function of frequency for four saturated zeolitized tuff samples.....	80
36. Plots of dielectric constant and resistivity as a function of frequency for welded Tub Spring Member.....	81

TABLES

Table	1. Vertical drill holes in Rainier Mesa area in which electric logs are available.....	4
	2. Chemical analyses of fracture and interstitial water from Rainier Mesa.....	27
	3. Measured and calculated resistivity of fracture waters in tunnels and interstitial water from t#3 tuff samples.....	31
	4. X-ray analyses of selected tuff samples from Rainier Mesa area.....	38
	5. Minerals found in Rainier Mesa area volcanic rocks which exhibit CEC or contain chemically bound hydrogen.....	41
	6. Results of X-ray diffraction analyses of tuff samples on which electrical resistivity measurements were made.....	66
	7. Physical properties, electrical resistivity, and cation exchange capacity of selected tuff samples.....	67
	8. Magnetic susceptibility of samples from units in Rainier Mesa.....	72

**ELECTRIC LOGGING AND ELECTRICAL PROPERTIES OF
ROCKS IN RAINIER MESA AREA,
NEVADA TEST SITE, NEVADA**

By

R.D. Carroll

ABSTRACT

Electric logs obtained in 33 drill holes in the Rainier Mesa region were evaluated. Aside from the usual character correlations associated with densely welded tuffs, correlations over considerable distances in the ash-fall tuffs may be noted at the horizons of tunnel bed subunits 4J and 3D, and at the contact of tunnel bed subunit 3A and the Tub Spring Member of the Belted Range Tuff. The latter correlation is the most widespread in the bedded tuffs in the area. Although diagnostic in several holes drilled in Aqueduct Mesa, the electric log does not universally reflect the top of zeolitization within holes drilled in Rainier Mesa.

Quantitative interpretation of electric logs in terms of saturation and porosity is hampered by lack of extensive knowledge of several parameters, the most significant being pore-water chemistry and resistivity. Analyses of pore-water chemistry obtained from 18 samples in one hole indicate a resistivity of 35 ohm-meters, a value not significantly different from that produced from fractures. This value is over an order of magnitude greater than reported previously by Keller (1962).

The effect of counterions on the resistivity of the volcanic rocks is significant. Resistivity measurements on samples from one horizontal hole indicate bound-water resistivities an order of magnitude lower than the pore-water resistivity exist in many of these rocks. The application of the Waxman-Smiths model for electrical conduction in montmorillonite-bearing sands appears sufficient to explain the magnitude of the resistivities observed on electric logs in Rainier Mesa if clay is ubiquitous in the zeolitized and vitric zones. Clay in the amount of a few percent is generally all that is required, and limited X-ray diffraction data appear to confirm the widespread presence of montmorillonite in these amounts.

The contribution of the zeolites to the electrical resistivity appears second order at best, particularly in the presence of moderate amounts of clay. Thus, the much greater cation exchange capacities exhibited by zeolitic tuff samples do not appear effective in contributing to lowering the resistivity in accordance with the Waxman-Smiths model. The contribution of these zeolites is estimated to be equivalent to that of a few percent clay.

These observations are confirmed by electrical resistivity measurements made on 26 vitric and zeolitized tuff samples containing clay in amounts as high as 66 percent and clinoptilolite in amounts as high as 80 percent. Resistivities measured with a fresh-water saturant indicate agreement with the Waxman-Smiths model when only the clay content is used as the source of counterions. No relationship exists between predicted and calculated resistivity based on a Q_v including the cation exchange capacity of both clay and zeolites. The resistivity appears to bear little relationship to zeolite

content, actually being greatest for several of the samples with higher zeolite contents.

The Waxman-Smits model predicts a relatively large theoretical range in resistivity for small amounts of montmorillonite contained within the porosity and saturation ranges representative of the Rainier Mesa tuffs. At high clay contents the resistivity becomes insensitive to clay. Using realistic tuff parameters in the Waxman-Smits model, the 20 and 10 ohm-meter resistivity thresholds historically used with electric logs as an empirical indication of clay compare favorably. However, these values may yield liberal or conservative estimates of clay depending on the saturation and porosity limits one places on high clay contents in situ. The small counterion contribution of zeolites in lowering resistivity would also tend to make this predictor conservative.

Magnetic susceptibility and induced polarization logs have been run in Rainier Mesa and dielectric constant measurements have been reported for zeolitized tuff samples. These data indicate that geophysical logs employing these measurement techniques are worthy of further study.

The behavior of the SP log cannot be quantified without laboratory data, however, the SP deflections are often similar to those observed in petroleum lithologies, indicating positive deflections opposite postulated clay zones in the zeolitized tuff. Because the mud is postulated as less resistive than the pore water, this behavior is attributed to the presence of divalent cations in the formation waters.

INTRODUCTION

This report, the final in a trilogy of reports dealing with rock properties interpreted chiefly from geophysical logs, examines the electrical measurements obtained in 33 vertical drill holes in the Rainier Mesa area, Nevada. Earlier reports dealt with seismic velocity and density (Carroll and Magner, 1988; Carroll, 1989).

The Rainier Mesa area, located about 90 mi northwest of Las Vegas, Nevada, is the location for nuclear weapon effects tests fielded by the Defense Nuclear Agency at the Nevada Test Site (NTS). Rainier Mesa was the site of the first successfully contained underground nuclear explosion in 1957. A brief chronology of testing in the tunnel complexes in this area was reported by Carroll and Magner (1988). The locations of all vertical drill holes in which electric logs have been obtained in the Rainier Mesa area are shown on figure 1 and listed in table 1. The data cover the period 1957 through 1987, and with exceptions as noted in table 1, the logs are reproduced in this report. Standard electric logs were obtained in practically all holes; where other types of electrical logs were run these are also listed. The majority of the holes listed in table 1 are 4-in. diameter and were drilled using bentonite mud. Lost circulation was characteristic in these holes, with an attendant absence of rigid controls on mud characteristics.

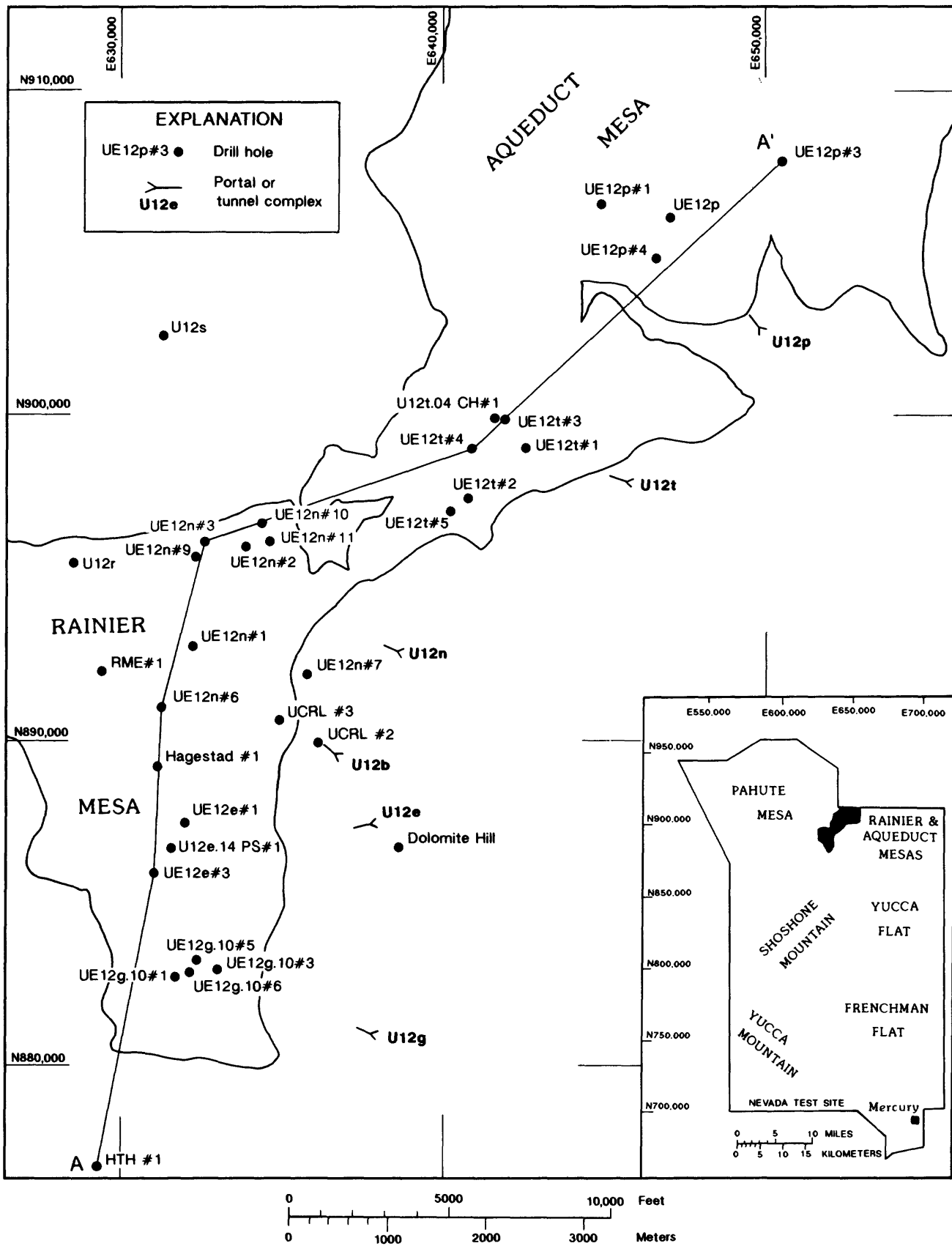


Figure 1.--Locations of vertical drill holes in Rainier Mesa area in which electric logs are available.

Table 1.--Vertical drill holes in Rainier Mesa area in which electric logs are available¹

[See figure 1 for hole locations]

Hole	Coordinates		Surface elevation (feet)	Depth (feet)	Completion date	Electric log coverage, ³ (feet)	Remarks
	N. E.						
Hagestad #1	N. 889,190 E. 631,132		7485	1952	7/57	354--1932 (8) (34)	Induction log and microresistivity log also run.
Mac Exp. Co. #1 (Dolomite Hill)	N. 886,712 E. 638,632		6399	1200	6/59	40--1010 (10)	In dolomite. Induction log and microresistivity log also run.
Rainier Mesa Expl. #1 (RME) (U12b,07C)	N. 892,097 E. 629,404		7361	3833	8/63	1300--3599 (7)	Focused log also run.
UCRL#2 (U12b#2)	N. 889,947 E. 636,111		6795	1043	4/57	---4	Reported by Keller (1959b). Not presented.
UCRL#3 (U12b#3)	N. 890,617 E. 634,913		7495	1074	4/57	---4	Reported by Keller (1959b). Not presented.
USGS HTH#1 (Stockade Wash)	N. 876,855 E. 629,310		6156	4206	8/62	438--1596 (9) 1600--3704 3713--4199	Induction logs, focused logs, and microresistivity logs also run. Final run in dolomite.
UE12e#1	N. 887,459 E. 632,001		7431	2000	8/73	424--1997 (8)	
UE12e#3	N. 885,923 E. 631,038		7465	2199	1/74	656--2195 (8) (31)	USGS also ran 4-in. normal resistivity, magnetic susceptibility, and induced polarization logs.
U12e.14PS#1	N. 886,670 E. 631,549		7458	873	7/74	See remarks	Only 100 ft of hole logged. Not presented.
UE12g.10#1	N. 882,715 E. 631,729		7528	1522	7/68	See remarks	Only 222 ft of hole logged. Not presented.
UE12g.10#3	N. 882,944 E. 633,034		7530	1425	3/74	686--1420 (8)	
UE12g.10#5	N. 883,237 E. 632,370		7571	1402	7/76	See remarks	Only 192 ft of hole logged. Not presented.
UE12g.10#6	N. 882,870 E. 632,160		7555	1450	6/77	634--1368 (8)	
UE12n#1	N. 892,867 E. 632,209		7321	2001	3/73	250--1998 (6)	

Table 1.--Vertical drill holes in Rainier Mesa area in which electric logs are available¹--Continued

Hole	Coordinates N. E.	Surface elevation (feet)	Depth (feet)	Completion date	Electric log, coverage ^{2,3} (feet)	Remarks
UE12n#2	N. 895,938 E. 633,839	7344	1779	4/73	100-1764 (6)	
UE12n#3	N. 896,075 E. 632,559	7479	1409	8/73	1034-1398 (6)	
UE12n#6	N. 891,000 E. 631,250	7420	2317	11/73	1110-2304 (7)	USGS also ran 4-in. normal and induced polarization logs.
UE12n#7	N. 892,004 E. 635,755	6893	832	8/73	204- 830 (7)	
UE12n#9	N. 895,600 E. 632,309	7383	1550	3/76	See remarks	Only 290 ft of hole logged. Not presented. USGS also ran a discrete spacing scratcher-electrode log in the interval 25-1536 ft. Reported by Carroll and others (1979).
UE12n#10	N. 896,655 E. 634,354	7384	1877	2/77	1300-1854 (6)	
UE12n#11	N. 896,074 E. 634,582	7309	1882	7/78	430- 765 (6) 1258-1828	
UE12p.01 (UE12p)	N. 906,011 E. 646,971	6337	1848	3/67	844-1420 (4) 1440-1759	Hole size 2.4 to 3.0 in.
UE12p#1	N. 906,432 E. 644,827	6477	2165	12/69	520-1160 (4)	
UE12p#3	N. 907,719 E. 650,425	6332	2601	3/70	260-1045 (4) 1950-2585	Second run in 2.3-in. hole.
UE12p#4	N. 904,748 E. 646,551	6396	1781	10/86	332- 872 (4) 1064-1764	Second run in 3.5-in. hole; resistivity considered only representative of character on second run.
UE12t#1	N. 898,949 E. 642,521	6762	2262	5/67	894-1182 (5) 1204-2252	Logs of poor quality; excessive noise; possibly in error.
UE12t#2	N. 897,406 E. 640,740	7008	1684	10/69	316-1060 (5)	
UE12t#3	N. 899,833 E. 641,874	6777	2176	2/73	622-2173 (5)	

Table 1.--Vertical drill holes in Rainier Mesa area in which electric logs are available¹--Continued

Hole	Coordinates N. E.	Surface elevation (feet)	Depth (feet)	Completion date	Electric log coverage ^{2,3} (feet)	Remarks
UE12t#4	N. 898,930 E. 640,840	6924	2290	10/73	1010-2280 (5)	
UE12t#5	N. 897,020 E. 640,192	7059	1611	6/74	1190-1600 (5)	
U12t.04 CH#1	N. 899,876 E. 641,542	6796	1187	6/83	See remarks	36-in. hole; induction and 16-in. normal logs run. Not presented.
U12r	N. 895,401 E. 628,500	7514	2520	10/62	See remarks	Induction log in 12.25-in. hole. Not presented.
U12s (Gold Meadows Stock)	N. 902,407 E. 631,260	6794	1596	4/68	See remarks	52-in. hole; no mud sample; decentralized tool. Not presented.

¹Does not include holes drilled from tunnel level.

²All logs are standard electrical logs unless otherwise noted in remarks.

³Number in parentheses refers to figure where data are presented.

⁴Exact depths not available. Logs reproduced on figure b-3 of Keller (1959b).

The electric log is the least understood, in a quantitative sense, of all the logs presently run at the Nevada Test Site. Electric logs are presently used as a correlation tool and to define zones of low resistivity that might be indicative of clay, especially the smectites. The definition of clay zones is of significance in Rainier Mesa because of possible adverse effects on the stability of mined tunnels and in predicting the movement during ground shock of tuff blocks bound by clay along bedding planes. In holes drilled for nuclear tests elsewhere at the NTS, large amounts of clay are considered hazardous to containment of nuclear events because of associated low shear strength and possible high water content. Thus, the identification of clay zones is a matter of some significance. The electrical properties of the volcanic rocks may also relate quantitatively to exchange capacity and, by extension, to radionuclide absorption, permeability, and differences in seismic coupling in the zeolitized zone. The necessary laboratory measurements to confirm or deny such relationships are quite involved and no overriding concerns have necessitated such investigations to date.

On the other hand, adequate estimates of oil in place in clay-altered rocks in petroleum reservoirs are of significant economic importance. In the presence of invasion, the electric log is the only device with sufficient depth of investigation to most easily obtain estimates of saturation. Thus the great emphasis in understanding electrical response in clay sands is readily understood. One purpose of this report is to investigate the application of oil-field resistivity models to the volcanic rocks in Rainier Mesa.

Because electrical logging measurements in recent years have progressed to techniques considerably beyond the routine measurement of electrical resistivity obtained from standard electric logs, we have also attempted to include data concerning the application of dielectric constant, magnetic susceptibility, and induced polarization measurements to the rocks in Rainier Mesa.

The application of electrical techniques to the derivation of porosity and saturation in the Rainier Mesa area is hampered by an absence of laboratory studies necessary to model the mechanism of current conduction in volcanic rocks. The major emphasis in the literature is focused on petroliferous environments where the chief cause of deviation from basic models describing rock resistivity is clay. Although clay exists in varying amounts in the volcanic rocks in Rainier Mesa, and can be a major concern in mining when encountered in significant volume, the most universal alteration products present in these rocks are zeolites, primarily clinoptilolite. Whether zeolites can be treated using existing shaly sand models is not apparent based on existing studies. Another purpose of this report is to investigate the role of zeolites on electric log response.

To facilitate use of this report, usage of certain terms and the elimination of repetitious text will be employed using the following guidelines:

- (a) Prefixes for drill hole descriptors will be dropped, e.g., UE12t#3 will generally be shown as t#3.

- (b) The area encompassed by the drill holes shown on figure 1 will be referred to as the Rainier Mesa area unless specific reference is required. This is in accordance with general usage at NTS. The area in general is that encompassed by the Rainier Mesa Quadrangle Map (Gibbons and others, 1963).
- (c) All depth references in this report are in feet in order to facilitate use of these data with other logging and drilling information. To convert from feet to meters multiply by 0.3048.
- (d) At NTS the term tunnel or tunnel complex is commonly applied to complexes of drifts which are accessed by adits. This common usage of referring to underground workings as tunnels will be retained.

Finally, the reader should note that the focus of this report is directed toward topics we consider of particular interest to the Defense Nuclear Agency's tunnel testing program, the funding source for this work.

Acknowledgments

J.E. Kibler, U.S. Geological Survey (USGS), aided in computer compilation of many of the illustrations in this report. M.F. Duncan, USGS, provided much help regarding drafting of illustrations. X-ray analyses provided by S.J. Chipera of Las Alamos National Laboratory were of key importance in describing the results of the laboratory tests. Of particular aid was J.E. Magner, USGS, whose general knowledge of the Rainier Mesa geotechnical environment was invaluable. The aid of the Defense Nuclear Agency, the funding agency for this work, is greatly appreciated, particularly that of Barbara Harris-West and J.W. LaComb. D.R. Townsend of Fenix & Scisson of Nevada (FSN) provided fruitful discussions on aspects of the geology. Finally, note must be taken of the logging organizations, chiefly Birdwell, Inc., without whose efforts no data would be available.

GEOLOGY AND HYDROLOGY

The first detailed mapping of the volcanic rocks at the NTS was done at Rainier Mesa (Gibbons and others, 1963; Sargent and Orkild, 1973). The general stratigraphy of the Rainier Mesa area is shown on figure 2, and a generalized geologic cross section is shown on figure 3. The overwhelming majority of the rocks penetrated in drill holes in the area are of volcanic origin; the tuff sections penetrated in RME#1 and HTH#1 being in excess of 3,600-ft thick. Prior to erosion, the original volcanic section in the area of HTH#1 is estimated to have been at least 5,000-ft thick.

The Tertiary-age volcanic rocks rest unconformably on Paleozoic and Precambrian miogeosynclinal carbonate and clastic rocks. Quartz monzonite of the Gold Meadows Stock is exposed at the surface in the northwest area of figure 1. The U12s hole was collared in the stock and nearly 500 ft of the stock was penetrated in the bottom of U12r. Limited thicknesses (less than 160 ft) of quartz monzonite have been penetrated atop precambrian quartzite in holes RME#1, and n#10.

EXPLANATION

- Fault showing relative direction of displacement
- △ △ △ △ Thrust fault with teeth on upper plate
- Approximate top of saturated volcanic rocks
- UE12e#3 Drill hole
- ① Tp & Tpc
- ② Tp & Tpw
- ③ Tp
- ④ Tt5, Tt4 & Tt3
- ⑤ Tt2, Tyf, Tt1, Trv, Tf & Tot
- ⑥ Tt2 & Tyf
- ⑦ Tt2 & Tc
- ⑧ Tt2, Tt1 & Tot
- ⑨ Tt2, Tyf, Tt1, Tot & Tc

(See fig.2 for explanation of symbols)

A' South North

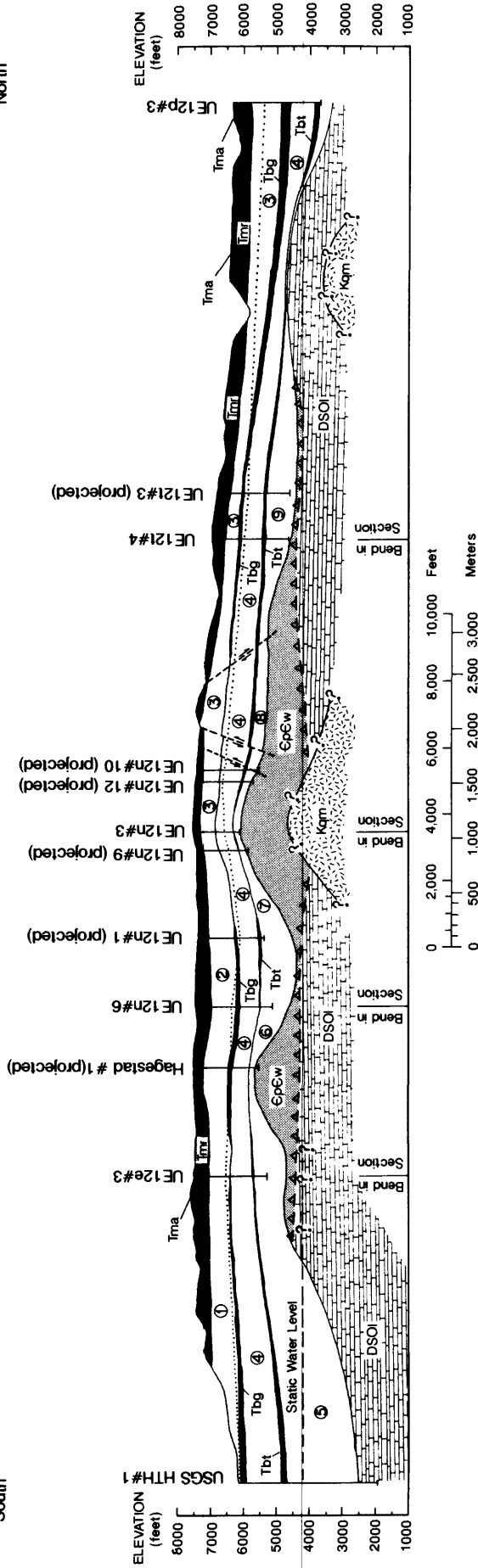


Figure 3.--Generalized north-south cross section through Rainier Mesa area. (See fig. 1 for location of section)

Other basement rocks in the area consist of limestone and dolomite (penetrated in UE12p, p#4, t#1, t#2, t#5, and HTH#1) and quartzite (penetrated in p#1, n#2, n#3, n#9, n#10, RME#1, and Hagestad). The non-clastic rocks are overthrust in places by the CP fault over the younger limestones and dolomites. The root of this fault is believed to underlie Rainier Mesa.

Resistivities of rock in the Rainier Mesa area range from a few ohm-meters to several thousand ohm-meters. These are also the extremes of resistivity found at the NTS, with carbonates, quartzites, and some volcanic flows accounting for the highest resistivities. Pre-Tertiary rocks also exhibit the highest resistivities in the Rainier Mesa region. Tuffs with pervasive clay mineral alteration exhibit the lowest resistivities both on Rainier Mesa and elsewhere at NTS. The rocks in the overlying volcanic section range from densely welded ash flows to friable, reworked, vitric and zeolitized ash-fall tuffs. In order of decreasing resistivity the rocks in the section can be broadly divided into carbonates, quartzites, and granite; welded ash flows; unsaturated nonwelded and generally unaltered, or vitric, volcanics; and zeolitized and clayey bedded tuffs. Although a distinct change in density and velocity frequently occurs at the top of the zone of generally pervasive zeolitization of the tuff, this demarcation is often, but not always, poorly developed on electric logs. This will be discussed in the section concerning log correlations.

The process of zeolitization in Rainier Mesa has resulted in an increase in induration and saturation of the tuff. In the drill holes covered by this report, the top of pervasive zeolitization is often an easily recognizable geologic and physical-property boundary, occurring as either a sharp demarcation within a few vertical feet separating vitric from zeolitized tuff, or characterized by a series of zones of alternating partially zeolitized and zeolitized material extending for as much as 180 ft prior to encountering pervasively zeolitized material.¹ These complicated zeolitization patterns are possibly associated with paleotopography. The behavior of the top of zeolitization as an acoustic impedance and density horizon has been discussed in detail (Carroll and Magner, 1988; Carroll, 1989). Zeolitization in the Rainier Mesa area has been discussed by several authors (Hoover, 1968; Claassen and White, 1979; White and others, 1980).

¹This horizon is our geophysical definition of the "top" of zeolitization. This boundary is believed to be closely coincident with the top of saturated volcanic rock in the perched water zone in the Rainier Mesa area; with the onset of the pervasively zeolitized tuff section described in lithologic logs; and with the approximate base of the unsaturated or vitric tuff. All of these definitions are interchangeably used in this report. It is the distinct density and velocity increase often found in the vicinity of this boundary upon which we base our definition. Our use of the term "zeolitized" is meant to apply to the saturated tuffs below this boundary.

A broader geologic definition of zeolitized tuff would recognize a transition zone above our "top" extending from the first onset of visible coatings on shards through beds of variable induration and alteration (D.L. Hoover, USGS, written commun., 1986). Hoover logged nearly 700 ft of thickness for this transition zone in n#6 and n#8.

Where drilled the zeolitized tuffs range in thickness from in excess of 3,000 ft in the southern part of the area (HTH#1) to slightly over 500 ft over the paleotopographic high in n#3. The depth to the top of zeolitization is generally about 800 to 1,000 ft below the top of the mesa in these drill holes, although it is over 1,200 ft in n#1. The shallower depths may bear some relationship to paleotopography. The approximate top of zeolitization, or saturation in the perched water zone, is shown on figure 3.

Where the zeolitization process is due to downward percolating ground water, as it is believed to be in the Rainier Mesa area, alteration progresses upward from permeability barriers such as welded tuffs or clastic rocks (Hoover, 1968). At some locations in the Rainier Mesa area, such as in the e#1, e#3, and Hagestad holes, partially zeolitized zones of relatively low density and limited vertical extent occur at the top of tunnel bed 5 directly beneath the welded Grouse Canyon Member of the Belted Range Tuff and at some vertical distance from the "top" of pervasive zeolitization. A possible explanation for this phenomenon is that the inherent pumice-rich nature and high permeability of tunnel bed 5 coupled with the bridging effect of the overlying welded Grouse Canyon render this unit less subject to induration and (or) zeolitization than other tunnel beds.

The reduced permeability in the pervasively zeolitized zone has resulted in the tuffs being nearly saturated in a perched water zone above the basement rocks.² However, intervals in the tuff above this horizon may also be nearly saturated because of the intermittent nature of alteration above pervasive zeolitization at some locations. Thus, it may not be unreasonable, because of the high capillary retention resulting from these alteration processes, to find intervals of high water saturation at several locations within the unsaturated zone.

The regional water table is generally deeper than the base of the volcanic section beneath eastern Rainier Mesa in the area of the tunnels, but occurs within the volcanic rocks in HTH#1 and probably within the thicker volcanic sections in western Rainier Mesa. Based on a measurement at an elevation of 4,189 ft in HTH#1 (fig. 3), the regional water table is estimated to be about 1,800 ft beneath tunnel level in eastern Rainier Mesa proper. The pre-Tertiary rocks are not saturated immediately below the volcanic rocks on the eastern edge of the mesa, the zeolitic zone acting as a confining bed permitting drainage to the pre-Tertiary water table through existing fracture

²Actually, partial saturation exists in the perched water zone but the amount of gas voids in the rock is generally less than 2 percent. At two tunnel locations, however, gas voids in excess of 5 percent have been encountered within the pervasively zeolitized zone (Carroll and Cunningham, 1980). Relatively low water saturations have also been observed in samples obtained in the zeolitized zone near tunnel portals (Byers, 1962). Because of the relatively low gas voids we choose to call this the "saturated" zone, although a strict hydrologic definition requires that pore water be under pressure greater than atmospheric to apply this definition. Although definitive measurements are lacking, the fact that all fractures at tunnel level are not water bearing suggests that pore pressures significantly above atmospheric should not be expected in the zeolitized tuff at tunnel level.

systems. The geologic structure to the west and north, however, suggests the presence of volcanic rocks for several hundred feet below an elevation of 4,189 ft as is evident in RME#1 and p#3. A detailed report on the hydrologic regime in the area has been written by Thordarson (1965).

Two lithologies within the unsaturated zone are densely welded. The Rainier Mesa Member of the Timber Mountain Tuff forms the resistant cap rock on the mesas throughout the region, and the welded Grouse Canyon Member of the Belted Range Tuff is present in structural lows.

In northern Rainier Mesa and southern Aqueduct Mesa the top of pervasive zeolitization is generally found in the zone between the base of the Paintbrush Tuff and the top of tunnel bed 4. Proceeding southward from the vicinity of n#6, additional ash-flow and ash-fall tuffs are found between the Paintbrush Tuff and the Grouse Canyon Member. The welded Grouse Canyon is within the zone of zeolitization in the southern part of the region and is found near tunnel level in the G-tunnel area (fig. 3). Zeolitization extends for a considerable distance above the Grouse Canyon in northern Aqueduct Mesa.

With rare exception, all underground nuclear tests in tunnels in the Rainier Mesa area have been conducted in pervasively zeolitized rock. The main testing media, tunnel beds units 3 and 4, consist of pervasively zeolitized, bedded and reworked ash-fall tuffs stratigraphically overlying the Tub Spring Member. Beneath the Tub Spring Member of the Belted Range Tuff are a series of ash-flow and ash-fall zeolitized tuffs, the former often exhibiting dense welding. Densely welded sections of ash-flow units beneath the Tub Spring Member are found in the Tuff of Red Rock Valley and the Fraction Tuff. A paleocolluvial layer, separating the volcanic rocks from the basement rocks, varies greatly in thickness throughout the area. The thickest penetration occurs in n#11 which bottomed in 181 ft of paleocolluvial material. By contrast, the n#3 hole, drilled over a paleotopographic high of quartzite, penetrated only 2 ft of paleocolluvium.

A report describing the geology in the holes listed in this report is recommended as an adjunct to use of the resistivity data (Maldonado and others, 1979).

GEOLOGIC IMPLICATIONS FROM ELECTRIC LOGS OBTAINED IN RAINIER MESA

The 16-in. normal electric logs obtained in the Rainier Mesa area are reproduced on figures 4 through 9 (in pocket) and figure 10. All the logs were reproduced from analogue records digitized on 1.0 ft intervals. Similar to log data previously reported for density and velocity, these logs are plotted by area and with respect to true elevation for each hole. The areas represented are northern and southern Aqueduct Mesa (figs. 4 and 5), northern N-tunnel (fig. 6), central Rainier Mesa (fig. 7), southern Rainier Mesa (fig. 8), and HTH#1 drilled south of Rainier Mesa in Stockade Wash (fig. 9). Figure 10 is the log from the Dolomite Hill hole, which was drilled totally in dolomite.

The lithology depicted on these logs is chiefly that reported by Maldonado and others (1979) and D. R. Miller (USGS, written commun., 1970). Some lithology has been updated based upon additional studies by the USGS,

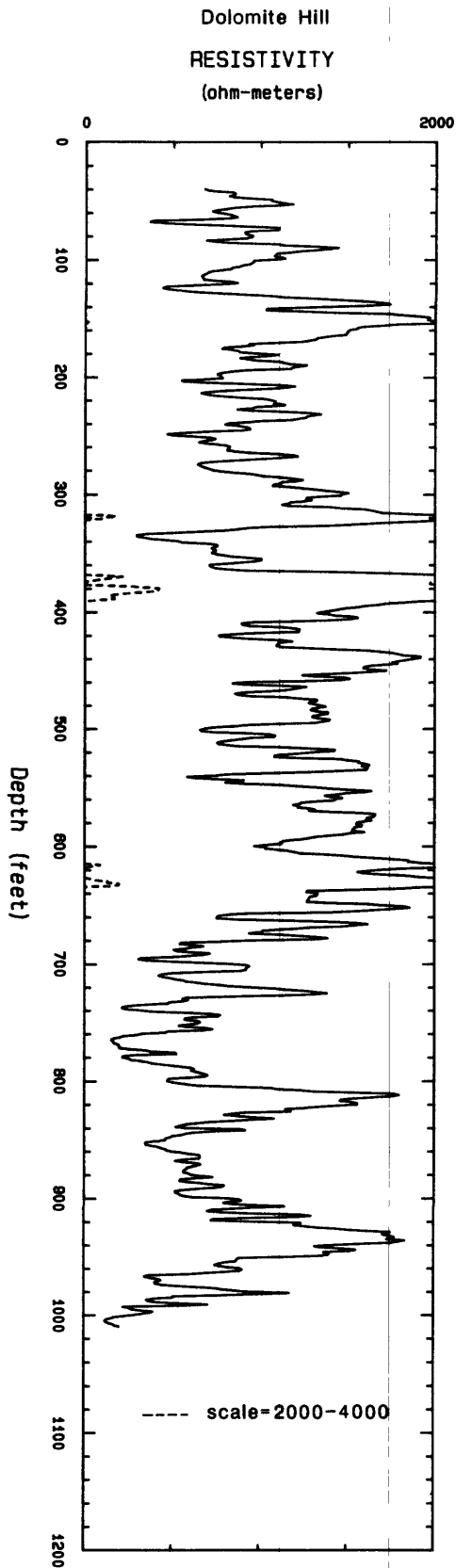


Figure 10.--Electric log obtained entirely in dolomite in Dolomite Hill hole.
Elevation of collar is 6,399 ft.

FSN, and in the case of the Hagestad #1 hole, by utilizing character correlations indicated by the logs. The horizons labeled A, D, and J on the figures are discussed below in connection with correlation. The top of zeolitization shown on the logs was derived from velocity and density logs where available, or from geologic estimates.

Correlation Based on Log Character

Electric logs have important uses in correlating the stratigraphic section by exhibiting characteristic signatures in most lithologies. These signatures are generally most readily obtained in sedimentary sequences where the character of the rock may be similar over considerable distances. In volcanic sequences character correlations can be subtle and subject to lateral changes and local depositional peculiarities over short distances. Where high-resistivity, low-porosity welded units are present, such as the Grouse Canyon and the Tub Spring Members in the Rainier Mesa area, they serve as excellent marker horizons. However, these units may be absent over topographic highs such as in the N-tunnel area, or lose character at the distal end of ash flows. Consequently, with widely spaced exploratory holes, character can be extremely subtle or absent in all but the welded units.

Density logs correlate well at several horizons in the bedded tuffs in the Rainier Mesa area (Carroll, 1989). Correlations are also found on electric logs, particularly in tunnel beds units 3 and 4 (Fig. 11). The section included between the Tub Spring Member and tunnel bed subunit 4J frequently exhibits a saw-tooth signature with resistivity lows in subunits 3A, 3D, and 4J. The signature is most frequently seen as a ramp between tunnel beds subunits 3A and 3D. The best example of the 3A/3D/4J correlation signature on figure 11 is in e#3. Of these three horizons (labeled A, D, and J on figs. 4-9), the most consistent and prominent correlation is the low resistivity zone at the Tub Spring/3A contact. This resistivity low occurs despite the presence or absence of dense welding in the Tub Spring, which is welded only in t#4 and p#3 on figure 11. The marker within the 4J subunit is also diagnostic in eastern and southern Rainier Mesa due to a thin, high-resistivity streak seen on the 16-in. normal but not on the 64-in. normal. This relatively high resistivity streak within subunit 4J is also seen on logs obtained in horizontal holes drilled from tunnel level and logged with a 3-ft or 4-ft Wenner array.

The most southern hole shown on figure 11 is e#3, which is 8.9 km from p#3 and 5.0 km from t#4. The geology in p#3 has not been subject to reexamination since drilling in 1970. Whether subunits 4J and 3D are recognizable or even present in this hole is undetermined. Thus, the lithology in the resistivity low at 2,100 ft in p#3 is unidentified. The nearest hole south of e#3 that penetrates the tunnel beds is HTH#1 at a distance of 2.8 km in Stockade Wash (fig. 1). The correlations shown on figure 11 are not strikingly evident on the electric log from HTH#1 (fig. 9) and the availability of only cuttings for the first 1,992 ft of HTH#1, limited core further downhole, and a 1962 drilling date make judgments on the exact location of subunits within the tunnel beds in that hole somewhat speculative.

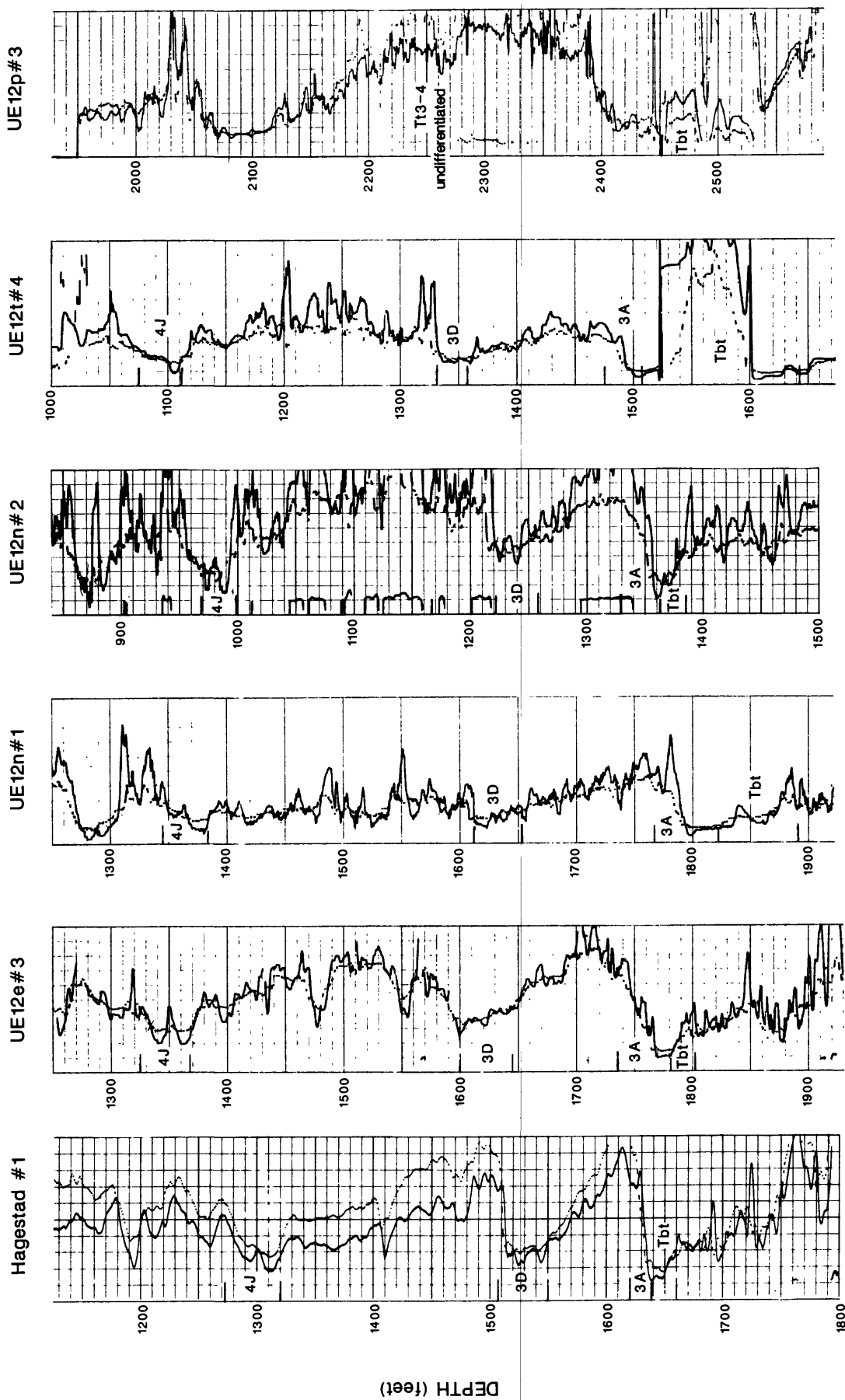


Figure 11.--Electric logs obtained in Rainier Mesa area illustrating character correlation in tunnel beds 3 and 4. Logs are 16- and 64-in. normals. Scales are 0-100, 0-1,000 ohm-meters.

Correlation signatures of the type seen on figure 11 appear to be losing character toward the extreme north and south in the Rainier Mesa area and possibly over a much shorter distance to the west in Rainier Mesa proper in n#6 and RME#1 (figs. 6 and 7). Although the 3D/4J signatures appear muted in these holes, the muted character correlates between the two logs. The unusually low resistivity on the log of n#6, indicating bedded tuffs of less than 20 ohm-meters generally throughout the hole, leads to a suspicion of the correctness of the log scale. However, the log character agrees well with the log obtained in RME#1. Although the apparent resistivity in RME#1 is about twice that of n#6, these resistivities are sufficiently low to suggest that resistivity of the zeolitized tuff may be decreasing to the west in Rainier Mesa. (An alternate explanation of extremely low mud resistivity causing the lower observed resistivities in these holes seems remote given the muds normally used in drilling. No mud sample was obtained in RME#1. Mud resistivity in n#6 from a pit sample was 12 ohm-meters at 20 °C.)

Top of Zeolitization

The top of zeolitization is shown on figures 4 through 9. Because there are more electric logs available than density or velocity logs, the location of the top of zeolitization with respect to area and elevation is more extensively seen on these figures than on those contained in the velocity and density reports previously cited. The data concerning the location of the top of zeolitization were obtained from several sources. Because velocity and (or) density logs are not available or interpretable in many holes, some of the data listed on figures 9 through 11 are from geologic estimates of the first indication of the onset of pervasive zeolitization in the tuff. Several of these estimates were provided by D.R. Townsend, FSN and D.L. Hoover, USGS. A top of intermittent zeolitization as well as a top of pervasive zeolitization is only shown for those holes which indicate such a condition on density logs (Carroll, 1989).

The behavior of electric logs as indicators of the top of zeolitization is interesting. In all the holes in northern Aqueduct Mesa where there are electric logs through this zone, the log appears to be fairly diagnostic (fig. 4). Elsewhere, with the exception of n#2 (fig. 6), they do not. Although several holes lack electric logs through this zone, the absence of a distinct drop in electrical resistivity at this horizon should not be unexpected. It is probable that saturation and clay alteration are sufficient above this horizon at many locations to mask any reflection of pervasive zeolitization. As will be discussed in the section on "Quantitative Interpretation of Electric Logs", clay content is more significant than zeolite content in lowering the electrical resistivity of the tuffs. The velocity and density logs are understandably more sensitive to increases in induration (which the top of pervasive zeolitization in the bedded tuffs essentially represents) than is the electric log, which is sensitive to water content, water chemistry, and alteration. How these actually vary near the top of zeolitization in, for example, the northern Aqueduct Mesa holes shown on figure 4, is unknown. A relatively abrupt transition in these parameters is suggested at some locations and not at others.

Examination of the relative position of the top of zeolitization shown on figures 4 to 9 allows observations to be made on this phenomenon in addition to the remarks already presented. Locally zeolitization appears at the

highest elevation at the edge of Rainier Mesa in n#7 (fig. 7) and over paleotopographic highs in t#1, t#5, and n#3 (figs. 5 and 6). The Hagestad hole appears to be an exception, exhibiting a relatively deep top of zeolitization over a quartzite high (fig. 8). Zeolitization appears deepest in western Rainier Mesa in RME#1, n#1, and n#6 (figs. 7 and 8). The lowest elevation in the region is apparent at 5,400 to 5,600 ft in northern Aqueduct Mesa (fig. 4). In Rainier Mesa the highest elevation is near 6,700 ft in n#7 and e#1, the lowest near 6,000 ft in RME#1 and n#1. The highest elevation in Aqueduct Mesa is near 6,500 ft in t#5 (fig. 5).

GENERAL ASPECTS OF ELECTRIC LOGGING IN RAINIER MESA

Electric logging is the oldest of the geophysical logging techniques, dating back to the 1920's. The continuing importance of electric logging lies in the fact that it is often the only logging tool from which one can obtain a measurement of the formation undisturbed by invasion, and consequently, is the primary logging tool used to determine saturation, the major goal in estimating oil in place. The first electric logs appear to have been obtained in Rainier Mesa in 1957 in connection with the initial exploration of the area (the first nuclear test at the NTS was in 1951). There is a record of an electric log obtained in a water well in the Groom Lake area northeast of NTS in 1954 (Moore, 1960). The first geophysical logging (gamma ray) at the NTS appears to have been in 1950.

The traditional application of electric logs has been the determination of water content in both saturated and unsaturated rocks. In the Rainier Mesa area the rocks from the surface to the top of zeolitization shown on figure 3 are partially saturated, with porosities in the nonwelded tuff ranging from about 20 to 50 percent. Saturation in this zone is not well defined, with estimates ranging from 60 to over 90 percent based on core and log data from various holes and tunnels. The problems inherent in determining saturation from geophysical logs have been discussed by Carroll (1989), and the variation of water content is not well documented in this zone.

Based on numerous sample measurements, we may consider the zeolitized tuffs to be saturated although the effect on resistivity of the generally less than 2 percent (connected?) gas voids in the these rocks is not documented. The average porosity in tunnel beds 3 and 4, the chief media in which nuclear tests are conducted, is about 35 percent. In the pre-Tertiary rocks the dominant mechanism controlling resistivity is not matrix porosity, which is less than 2 percent, but fractures. Methods for determining quantitative values of water content within fractured rocks are poorly defined and electric logs in this environment are basically correlation tools.

The distinction between saturated and partially saturated tuff is important because the relationships for determining water content from resistivity differ for these two conditions. For unaltered rocks these equations are the well known Archie equations;

$$R_o/R_w = F = \phi^{-m} \quad (1)$$

for saturated rock, and

$$R_t/R_o = I = S_w^{-n} \quad (2)$$

for partially saturated rock. Here R_o = saturated rock resistivity; R_w = resistivity of the saturating fluid; R_t = resistivity of the partially saturated rock; S_w = saturation; ϕ = rock intergranular porosity; I = resistivity index, F = formation factor, a normalized constant which is theoretically the same for all values of R_w given a constant ϕ . The constants "m" and "n" are usually empirically determined and frequently assumed to be 2.0 in consolidated formations. In theory "m" may be derived directly from geophysical logs and ϕ either constant may be derived from laboratory measurements on core.³

The caveat must again be emphasized that these equations apply only in rocks which do not have an appreciable alteration component. In petroleum environments alteration occurs chiefly in the form of smectite clays. Alteration in the Rainier Mesa volcanic tuffs is chiefly in the form of zeolites,⁴ with clay generally a minor component in most of the stratigraphic section. The effect of alteration on electrical resistivity will be discussed shortly. First, some of the variables in equations 1 and 2 need to be examined with regard to the Rainier Mesa environment.

In applying equations 1 and 2 we obtain R_o directly from the log in the zeolitized zone, or R_t from the electric log at the depth of interest above zeolitization. This may be a complex procedure in the presence of thin beds and invasion. Another correction needed is the effect of the borehole mud on the resistivity recorded by the log. This is accomplished with the aid of standard correction charts, a procedure not addressed in this report (Dresser Atlas, 1982; Schlumberger, 1987). The mud correction involves the mud temperature at the depth of interest which is affected by the geothermal regime in Rainier Mesa.

Borehole Temperatures and the Geothermal Regime

The mud temperature is a significant parameter in electric log

³In logging practice, porosity is more easily determined from logging devices other than the electric log. However, because we are addressing the application of electric logs in volcanic rocks and not an overall approach to physical property determinations using the full array of geophysical logs, we proceed as if equations 1 and 2 are the only available approaches.

⁴At isolated locations the occurrence of 30 to 50 percent smectite clay in large volumes within Rainier Mesa has been of concern with regard to tunnel stability. This is rare, as it is zeolites which normally comprise 30 to 50 percent of the tuff. Discussion of clay in this regard has been reported (Carroll and Cunningham, 1980). None of the logs presented in this report penetrate such zones, except possibly at the base of the tuff section overlying permeable pre-Tertiary rocks, e.g., HTH#1 (fig. 9).

interpretation. For normal logs, which comprise almost all the logs available in Rainier Mesa, a temperature correction is required in order to derive the true resistivity of the tuff because the resistivity recorded is a function of the ratio of the borehole fluid resistivity and the true formation resistivity. This requires that the mud resistivity be known at the depth of interest. The mud resistivity is generally obtained by recording the maximum temperature observed in the hole, measuring the resistivity of a mud sample, and correcting the resistivity for temperature by assuming a temperature gradient.

The resistivity of 25 drilling mud samples obtained in Rainier Mesa over the time period covered by this report ranges from 1.4 to 29 ohm-meters (20°C). All these holes were drilled under "lost circulation" conditions, and with the exception of a bailer sample obtained in g.10#6 hole (11 ohm-meters), all samples were obtained from the mud pit or tank. Thus the degree to which these samples represent the actual resistivity of the mud in the hole is subject to question.

Of additional interest is the degree to which the maximum recorded temperatures in these holes represent the true geothermal gradient. Lachenbruch and others (1987) have reported on the thermal regime in Rainier Mesa based on measurements in the UCRL#3, UCRL#4, and Hagestad holes. They found that the effects of drilling on the temperature regime were still evident a year after the drilling of the Hagestad hole. They made measurements over a sufficient time period, however, to obtain reliable estimates of true geothermal gradients. They report geothermal gradients in the range $31^{\circ}\text{C}/\text{km}$ to $38^{\circ}\text{C}/\text{km}$, the lower number obtained in the Hagestad hole. This was the only hole that penetrated a thick volcanic section wherein the temperatures measured were not affected by mesa topography. The range in gradient obtained for these volcanic rocks is notably higher than the $13^{\circ}\text{C}/\text{km}$ to $28^{\circ}\text{C}/\text{km}$ reported by Hearst and Nelson (1985, p. 71) as representative of the sedimentary rocks normally encountered in well logging. The thermal regime derived by Lachenbruch and others in Rainier Mesa is shown on figure 12.

The Rainier Mesa cap rock, about 285-ft thick in the Hagestad hole, was found to be at a uniform temperature, thus two contours at 10°C are shown near the surface on figure 12. The depth of seasonal temperature change in these rocks is estimated not to exceed 60 ft, and the absence of a geothermal gradient to depths as great as 300 ft in the Hagestad hole is attributed by Lachenbruch and others to possible downward circulation of water and air in the highly fractured welded tuff. The data on figure 12 are remarkably consistent with the temperature of 20°C measured by the author at an elevation of about 6,066 ft in the N.07 tunnel using thermistors grouted in a 35-ft horizontal hole.

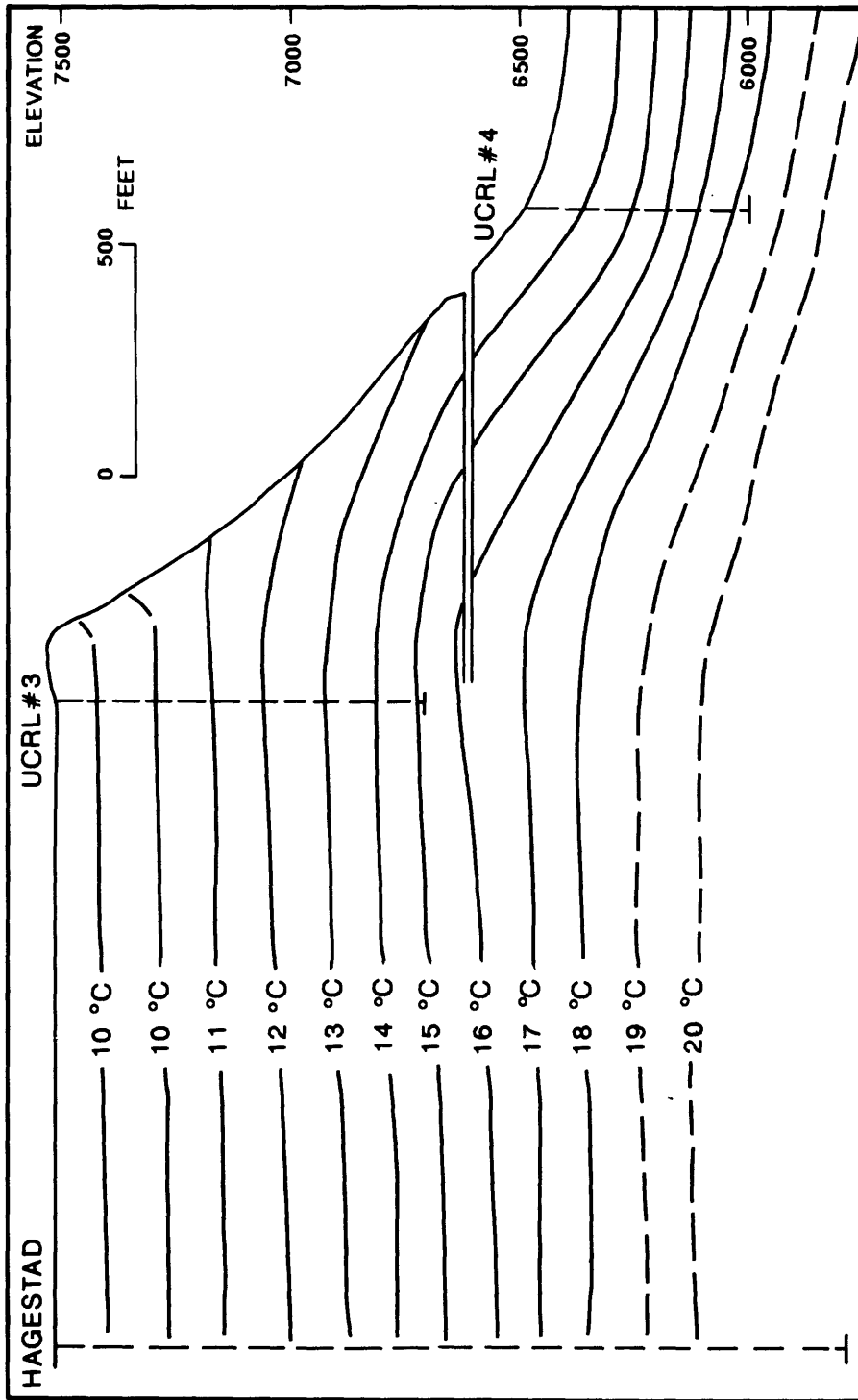


Figure 12.--Generalized thermal regime in Rainier Mesa. (After Lachenbruch and others, 1987.)

In order to compare the maximum temperatures listed on electric logs with the actual geothermal regime, the measured gradient of 31⁰C/km obtained in the Hagestad hole can be combined with the observed 20⁰C temperature at 6,066 ft to obtain,

$$T = 20^{\circ}\text{C} + (6066 - E)(0.00945) \quad (3)$$

where T is the temperature and E is the elevation of interest. This equation enables one to obtain an estimate of the temperature at any desired elevation in the volcanic section between the base of the cap rock and the top of the pre-Tertiary rocks.

Figure 13a is a plot of equation 3 compared with bottom hole-temperatures (from a maximum recording thermometer) recorded on 27 electric logs obtained in the Rainier Mesa area. Only holes drilled from the top of the mesa and removed from topographic effects are listed. Figure 13b is a plot of the data as a function of hole depth. The equation shown on figure 13b was derived using the average of the hole collar elevations to obtain,

$$T = 0.00945Z + 10.6 \quad (4)$$

where T is the temperature and Z the depth of interest (ft). The temperature at depth at any hole location can be estimated from,

$$T = 0.00945(Z - E) + 77.3 \quad (5)$$

where Z and E are depth and elevation (ft). Again it should be emphasized that these estimates are only applicable to the volcanic section and only below the base of the cap rock. Equation 4 is somewhat arbitrary because it is based on the average collar elevation (7,055 ft) of holes on both Rainier and Aqueduct Mesas. Thus the intercept at 10⁰C appears contradictory to the data on figure 12. Utilizing the average collar elevation of only the Rainier Mesa holes (7,356 ft vs 6,618 ft for Aqueduct Mesa) would result in an intercept at 10⁰C of 231 ft, which is in good agreement with figure 12. In a similar context, on figure 13a it should be noted that the actual collar elevation of the Hagestad hole is 7,485 ft.

Figure 13 indicates that the temperatures listed on electric logs do not appear to provide a reliable estimate of the geothermal regime. This, of course, does not detract from their intended purpose of determining true resistivity from normal logs because the resistivity of the mud is the quantity affecting the electric log response, not the steady-state geothermal regime.

A detailed review of the effect of temperature on both fluid and saturated rock resistivities may be found in Ucock (1979).

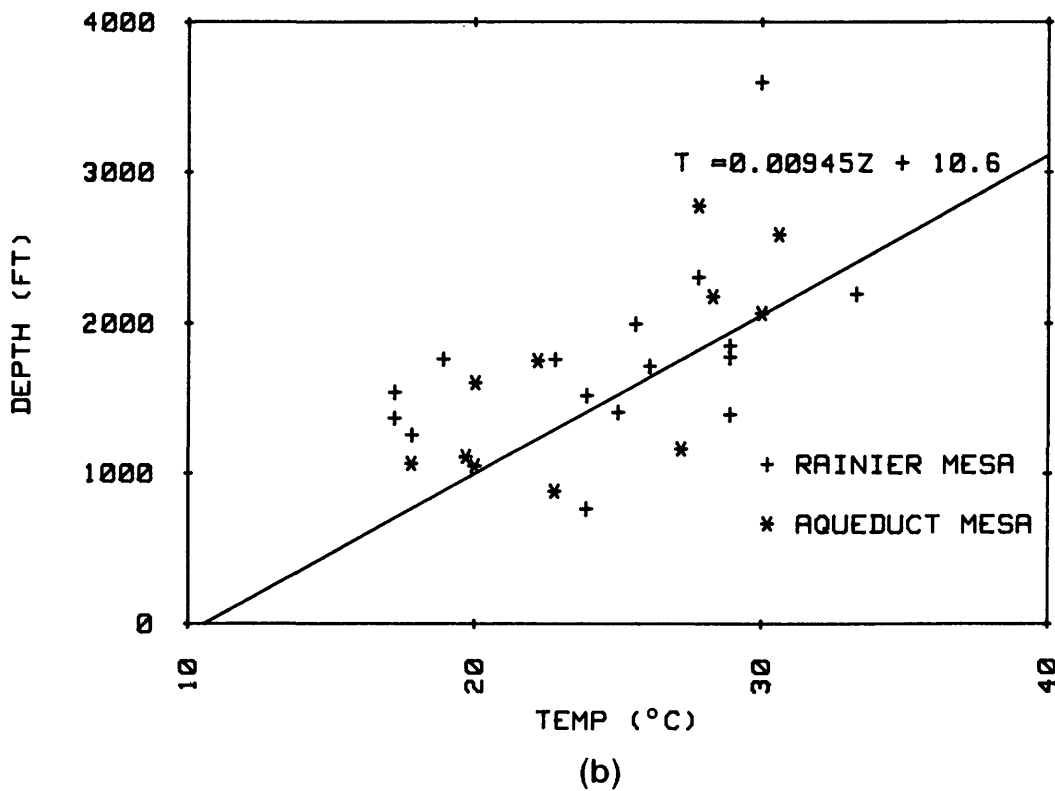
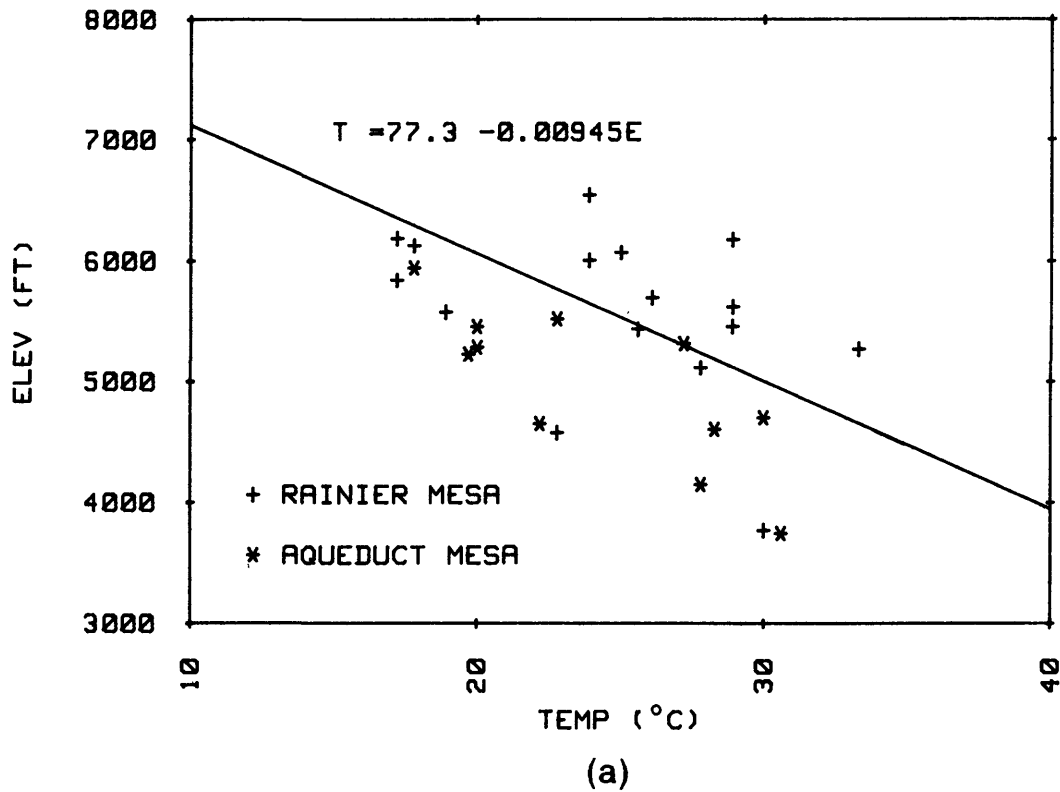


Figure 13.--Temperatures recorded on electric logs from Rainier Mesa area as a function of (a) bottom-hole elevations and (b) hole depths.

Resistivity of Rainier Mesa Pore Water

There are several difficulties in evaluating the unknowns in equations 1 and 2 in the volcanic rocks in Rainier Mesa. One of the seemingly more innocuous is a knowledge of the formation water resistivity, R_w . Regardless of the electrical model applicable to these rocks, R_w may be expected to be a dominant parameter. The normal procedure in logging is to obtain R_w from the spontaneous potential log or from a direct measurement on a sample. Two important considerations arise. First, the waters at the NTS, aside from complicating the model by being fresh, contain several ion species and are not NaCl. Thus, many of the models in the geophysical logging literature dependent on NaCl as the R_w parameter are not directly applicable. Second, and more importantly, in spite of numerous measurements of the resistivity of water samples, the water resistivity actually dominating current conduction in the Tertiary rock pores is unknown. This seeming contradiction is due to the fact that water samples obtained in Rainier Mesa and elsewhere are from fractures, and fractures generally comprise a miniscule volume compared to the pore volume in the pre-Tertiary rocks in Rainier Mesa. Thus, the contribution of fracture water to rock resistivity is trivial. The zeolitized tuffs generally do not produce interstitial water because of their extremely low permeability. We know of no attempts to determine actual pore-water resistivity in Rainier Mesa, although pore-water chemistry has been determined for one suite of samples (White and others, 1980).

Clebsch (1961) estimated the retention time of water in fractures in Rainier Mesa from the surface to tunnel level in E-tunnel as 0.8 to 6 years. This short period, when compared with what may be the retention time in the zeolitized tuff pores, raises concerns as to the validity of employing a value for R_w based on fracture water in resistivity calculations. Keller (1962) reported a value of 1.6 ohm-meter for the pore-water resistivity in Rainier Mesa based on a comparison of electrical measurements made in tunnels with those made on core saturated with salt water. However, Keller's results are in question as they are based on the assumption that the conduction model at in-situ conditions is similar to that obtained with a very low resistivity saturant, i.e., that equations 1 and 2 hold for all saturant resistivities. This is not true in the presence of rock with the capacity for ion exchange. A more reliable estimate of the value for R_w prevalent in the volcanic rocks is needed. This may be accomplished by examining the fracture-water chemistry and resistivity data available in Rainier Mesa, deriving a resistivity/chemistry relationship, and utilizing this to estimate the resistivity of the one available set of interstitial water chemistry data obtained in the area.

White and others (1980) obtained chemical analyses and conductivity measurements of water from fractures at several locations in the tunnels in Rainier Mesa, including in their report several earlier analyses reported by Clebsch and Barker (1960). In this study (of the effect of dissolution of volcanic glass on water chemistry) they also analyzed the pore-water chemistry of 18 natural state samples obtained in the interval 441 to 1,748 ft in the t#3 vertical hole (fig. 14). The pore water was obtained by centrifuging or squeezing the samples in triaxial compression. The results of these analyses are listed in table 2 in addition to the fracture-water chemistry derived.

We note several things in the data which might affect resistivity. The ion species in the vertical hole indicates some variation with depth. The chemistry of the samples from B tunnel also confirm this, in that this tunnel was above the top of zeolitization where sampled. No conductivity measurements are available for the interstitial water samples and the significance of these differences with regard to resistivity is not immediately obvious.

The presence of mixed ion species complicates the determination of resistivity from the chemistry and almost all logging literature deals with sodium chloride solutions. Equations for NaCl and other single salts allow the resistivity to be easily calculated from data in the International Critical Tables (National Research Council, 1929) and charts abound relating the amount of solute NaCl to its resistivity. For mixed ion species, one empirical method of obtaining resistivity is to plot total dissolved solids (TDS) against the measured electrical conductivity of the fracture waters listed in table 2. This is shown on figure 15a, and the results appear to be a good approximation to the mass of the data. An approach similar to this was used by Alger (1966) using data from fresh-water wells in several localities. Alger notes that most fresh-water plots of this nature fall between the lines for pure NaHCO_3 and NaCl. Such a plot of the resistivities of Rainier Mesa fracture waters is shown on figure 16.⁵ The data on figure 16 suggest that a second approach to approximating the resistivity from the dissolved solids is to use the NaHCO_3 curve with an appropriate offset.

⁵The conductivity data for fracture waters recorded in table 2 are not all laboratory measurements and field measurements were only made as a check. The field data were converted to conductivities at 25°C by the use of a KCl conductivity/temperature curve assuming 2 percent change in conductivity/degree C (H. Claassen, USGS, oral commun., 1987). Such estimates are not rigidly correct for mixed ion species but will not detract significantly from empirical estimates if ranges in the data are not broad.

UE12t#3

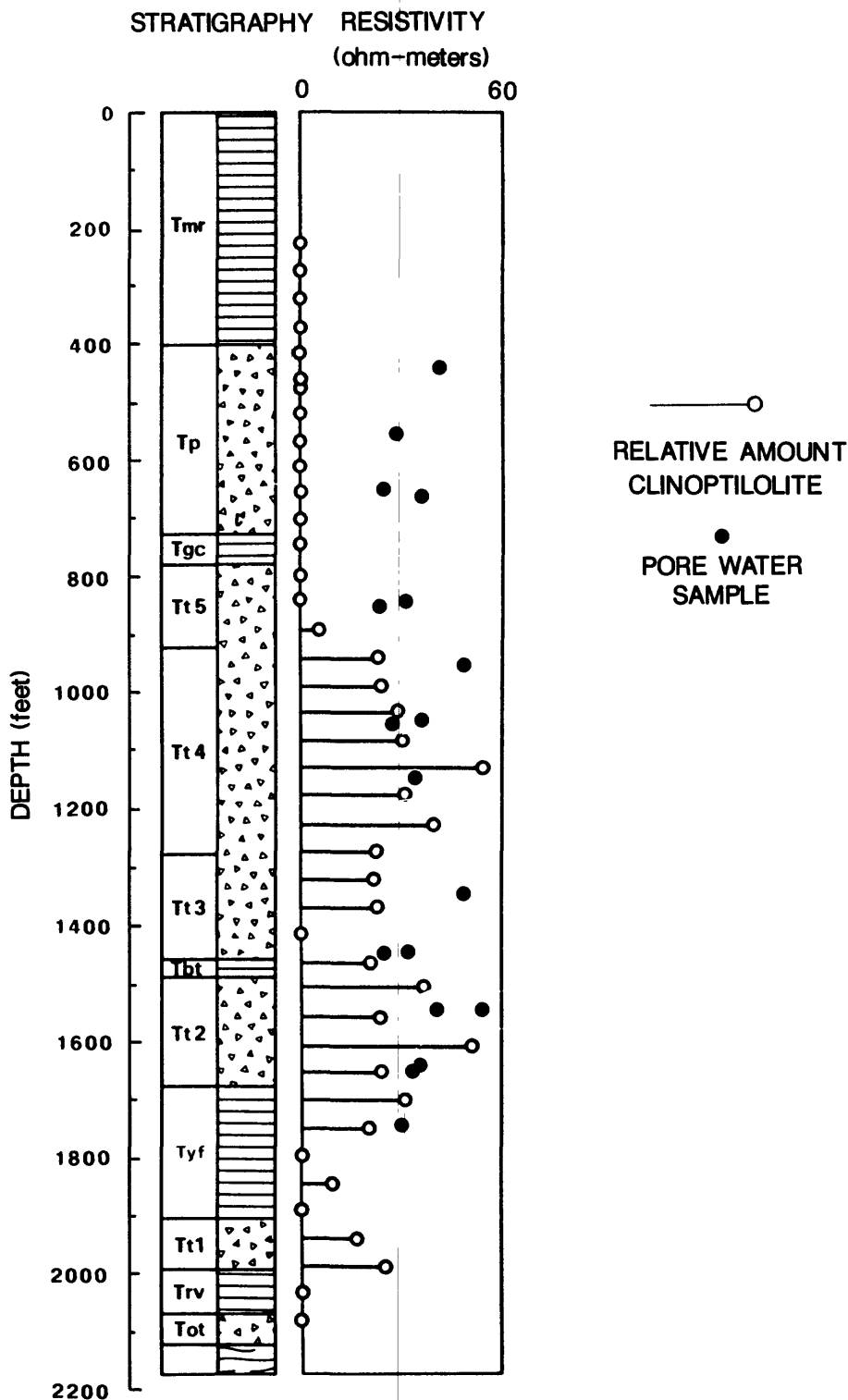


Figure 14.--Locations of samples obtained in t#3 for pore water chemistry. Relative values (no scale) of clinoptilolite from X-ray analyses. Resistivity of pore water was derived from chemistry for this report (modified from White and others, 1980; see fig. 2 for explanation of stratigraphy).

Table 2.--Chemical analyses of fracture and interstitial water from Rainier Mesa. Quantities are in millimoles/L

[Modified from White and others, 1980; leaders (--) indicate quantity not measured]

Fracture water from Rainier Mesa tunnels										
Tunnel ¹	Location ²	TDS ³ (calc)	Sodium	Potassium	Calcium	Magnesium	Bicarbonate	Sulfate	Chloride	Conductivity (umhos/cm)
U12n.05B	16+00	263	1.91	0.24	0.18	0.02	2.29	0.06	0.16	246
U12n.05	21+44	326	2.65	.28	.23	.02	2.85	.15	.37	408
U12n.05	21+39B	389	3.04	.33	.40	.06	3.39	.28	.37	339
U12n	3+00	480	2.70	.19	1.15	.28	3.62	.66	.90	570
U12n.07B	4+94	121	.96	.01	.01	.00	.87	.05	.06	97
U12n.02	UG#1	260	2.04	.14	.18	.01	2.25	.09	.20	237
U12t.02B	19+65	119	.96	.00	.01	.00	.92	.00	.02	97
U12t.02	XC-2	134	1.09	.01	.03	.01	1.08	.00	.05	114
U12t.02B	6+50	137	1.13	.02	.07	.00	.82	.18	.05	158
U12t	18+05	281	2.83	.09	.02	.01	2.44	.14	.28	287
U12t.03	UG#2	308	1.44	.14	.50	.21	2.23	.18	.27	267
U12t.03	UG#1	221	1.39	.14	.22	.06	1.46	.19	.31	217
U12t.04	UG#1	226	1.44	.13	.24	.08	1.61	.16	.28	218
U12t.03	UG#1	281	1.30	.17	.50	.17	2.18	.16	.31	280
U12t.03	UG#1	243	1.65	.17	.23	.06	1.85	.16	.28	227
U12t.03	UG#3	280	1.13	.14	.51	.19	2.15	.17	.26	263
U12e.07	4+15	246	1.13	.15	.43	.17	2.00	.15	.06	248
U12e.04	16+68	125	1.04	.02	.01	.00	.79	.13	.10	98
U12e	29+35	157	1.13	.09	.06	.00	.87	.12	.17	136
U12e	40+82	157	1.04	.20	.06	.00	.93	.10	.11	139
U12e.04	3+02	136	1.26	.01	.04	.00	.88	.09	.17	139
U12e.03	9+20	158	1.35	.10	.04	.00	1.15	.09	.06	147
U12e	35+75	174	.87	.17	.20	.08	.92	.18	.23	152
U12e.02	6+10	162	1.39	.06	.00	.00	.98	.12	.27	162
U12e.05	18+45	198	1.44	.08	.06	.00	1.05	.12	.28	169
U12e.03	10+25.5	205	1.74	.03	.06	.00	1.34	.12	.25	195
U12e.03	10+25	207	1.74	.07	.04	.00	1.38	.12	.23	198
U12e.07	10+25	207	1.13	.15	.43	.12	2.00	.15	.11	248
U12e	48+05	237	2.04	.28	.10	.00	1.77	.15	.34	258
U12e	54+32	263	1.61	.20	.40	.04	2.00	.15	.34	268
U12e	9+71	378	3.04	.07	.08	.00	2.10	.33	.45	308
U12b	14+65	197	.78	.07	.32	.04	1.21	.12	.14	164
U12b.03	3+70	159	.65	.07	.24	.06	.79	.09	.21	144
U12b.04	3+26	189	.96	.08	.20	.34	.98	--	.34	169

Sample depth (ft)	Interstitial water from t#3 core samples									

440.9			1.07	0.26	0.274	0.12	0.95	0.21	0.76	--
556.4			1.51	.36	.05	.29	2.25	.38	.90	--
653.5			1.89	.26	.57	.26	2.25	.42	.76	--
664			1.02	.11	.42	.17	.44	.42	1.07	--
845.1			1.30	.12	.40	.20	.43	.40	1.47	--
853			1.41	.14	.65	.30	.37	.74	1.75	--
1448.2			2.00	.36	.22	.029	1.09	.54	.56	--
1451.4			2.42	.49	.27	.041	1.07	.87	.56	--
956			1.11	.12	.20	.086	.79	.23	.59	--
1050.9			1.36	.19	.23	.07	.84	.47	.85	--
1054.1			1.54	.21	.70	.18	1.29	.52	.82	--
1150.9			1.01	.15	.32	.09	.97	.57	.85	--
1349.1			1.34	.14	.14	.034	.61	.34	.45	--
1544			1.74	.038	.005	.002	.91	.22	.27	--
1549.9			2.27	.031	.005	.004	1.41	.34	.31	--
1646			2.62	.031	.055	.006	1.72	.32	.34	--
1650.9			2.83	.023	.045	.006	1.84	.31	.48	--
1748			3.09	.097	.025	.005	1.90	.38	.48	--

¹Tunnel or drift. B = bypass drift.

²Construction station where sampled.

³Total dissolved solids.

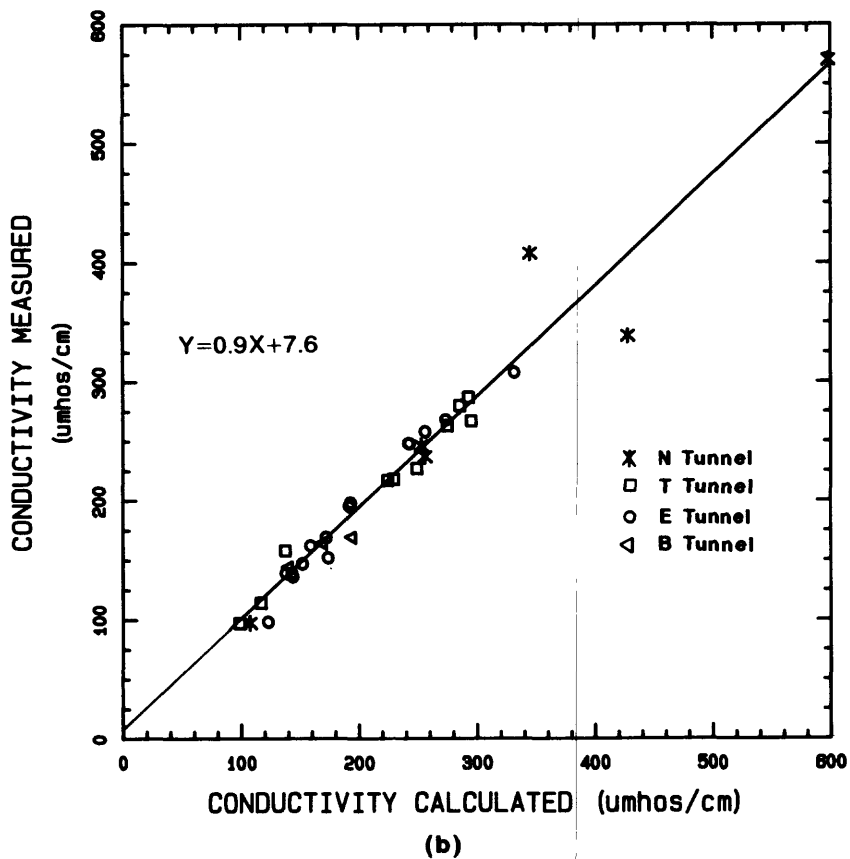
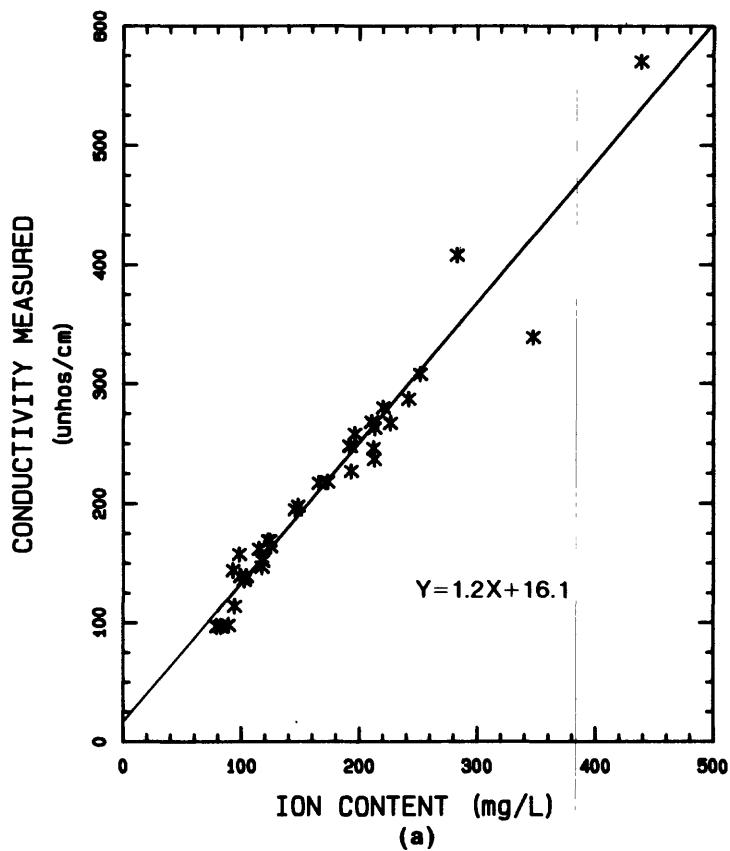


Figure 15.--Conductivity of Rainier Mesa fracture waters versus (a) total ion content and (b) calculated values from equivalent NaCl content. SiO_2 and F1 not included in total ion content.

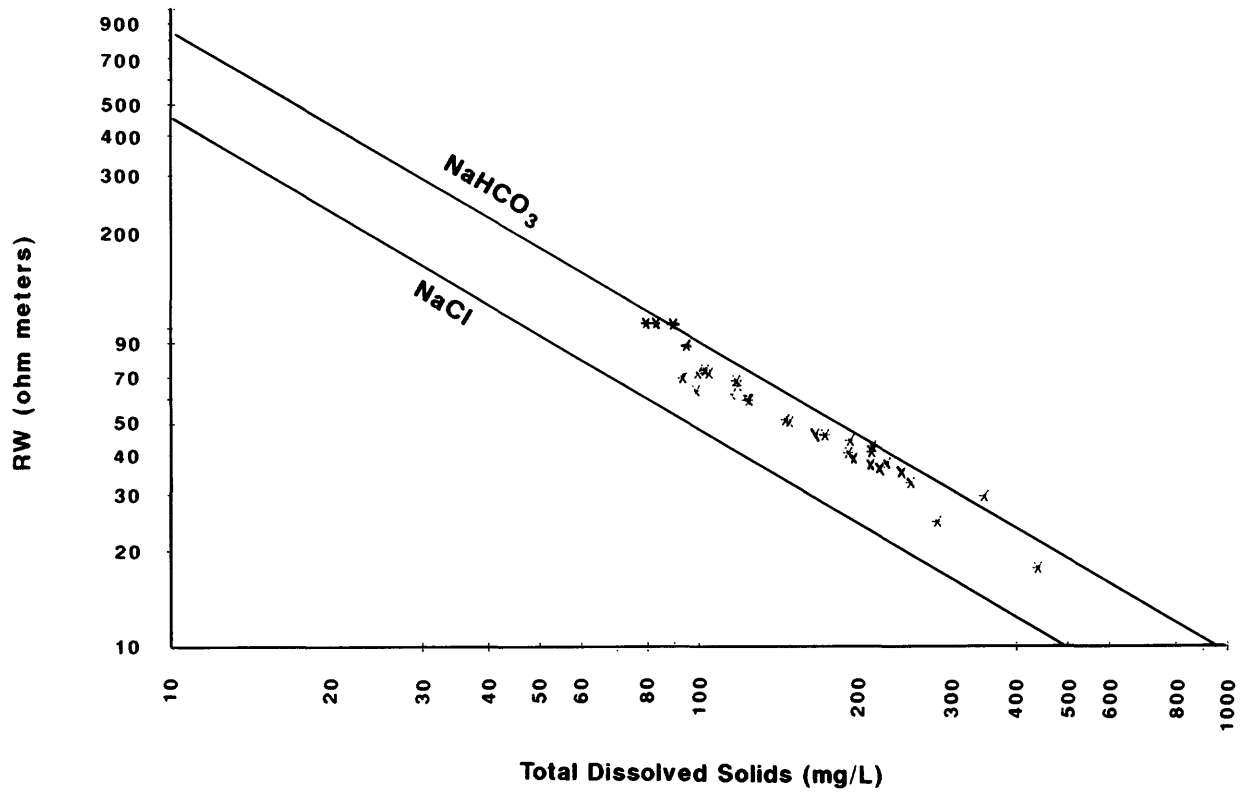


Figure 16.--Resistivity versus total dissolved solids for Rainier Mesa fracture waters.

A third approach to the determination of water conductivity from the water chemistry is to utilize resistivity relationships derived between the dissolved solids content of mixed ion species and equivalent NaCl solutions. Such relationships provide the relative resistivity contribution of each ion species in terms of a multiplying factor, and sum the results to obtain an equivalent NaCl total dissolved solids. The earlier logging practice of assuming a constant factor for each species regardless of concentration has been shown by Desai and Moore (1969) to be incorrect. Desai and Moore developed a series of polynomials for deriving the appropriate factors as a function of concentration. Schlumberger (Chart Gen-8, 1979) has published correction factors for various concentrations of mixed ion species in solution.⁶ Using factors estimated from this chart to calculate the equivalent NaCl dissolved solids and comparing with the measured values of fracture-water conductivity results in the plot of figure 15b. The resulting plot is also a fair fit to the fracture data, and thus, either technique demonstrated on figure 15 may be used to obtain an estimate of the pore-water conductivities of the samples from t#3. A comparison of water conductivity by tunnel location is listed in table 3.

The equivalent NaCl content may be converted to conductivity at 25°C using data from the International Critical Tables. These data are reported frequently in chart form but seldom as the more exact equation of fit. For R_w ranging from about 5 to 300 ohm-meters, these relationships for NaCl are

$$\text{Conductivity} = 1.978\text{TDS} + 14.976 \quad (6)$$

for NaHCO_3 ,

$$\text{Conductivity} = 1.014\text{TDS} + 10.413 \quad (7)$$

where conductivities are in mhos/cm, and TDS is in mg/L.

In the resistivity form presented on figure 16, for NaCl,

$$\text{Log } R_w = -0.978 \text{ Log TDS} + 3.637 \quad (8)$$

and, for NaHCO_3 ,

$$\text{Log } R_w = -0.973 \text{ Log TDS} + 3.903 \quad (9)$$

where R_w is in ohm-meters.

Data published by Jacobson and others (1986) on conductivities of samples obtained from fractures in N tunnel also fit the data on figure 15a when temperature corrected. The mean value for 21 of their measurements is 32 ohm-meters compared with the 43 ohm-meters listed for N-tunnel fracture water in table 3.

⁶Schlumberger references Desai and Moore as the source of their correction chart, however, some concentrations indicated by Schlumberger are considerably below the lower range published by Desai and Moore. We could not locate the reference applicable to these lower ranges. The multiplying factors interpolated from the Schlumberger chart to obtain equivalent NaCl were: Na=Cl=1.0; K=0.95; Ca=1.26; Mg=1.82; $\text{HCO}_3=0.34$; and $\text{SO}_4=0.76$. Dresser Atlas (1982) has published a similar chart which differs somewhat from the Schlumberger chart at low concentrations.

Table 3.--Measured and calculated resistivity of fracture waters in tunnels and interstitial water from t#3 tuff samples

[Values in ohm meters. Values for tunnel samples calculated from results on figure 15b. Values for t#3 samples calculated from equivalent NaCl conductivity of ion species. Leaders (--) indicate no data]

t#3 hole	B-tunnel		E-tunnel		N-tunnel		T-tunnel	
	Measured	Calculated	Measured	Calculated	Measured	Calculated	Measured	Calculated
41	61	60	40	41	41	40	103	101
29	69	72	102	81	24	29	88	85
25	59	52	74	69	29	23	63	72
36	--	--	72	70	18	17	35	34
31	--	--	72	72	103	93	37	34
24	--	--	68	66	42	39	46	44
31	--	--	66	58	--	--	46	44
25	--	--	62	63	--	--	36	35
48	--	--	59	58	--	--	44	40
35	--	--	51	52	--	--	38	36
27	--	--	51	52	--	--	--	--
34	--	--	40	41	--	--	--	--
48	--	--	39	39	--	--	--	--
54	--	--	37	37	--	--	--	--
40	--	--	32	30	--	--	--	--
35	--	--	--	--	--	--	--	--
33	--	--	--	--	--	--	--	--
30	--	--	--	--	--	--	--	--
Mean	63	61	58	54	43	40	54	53

Quantitative applications of resistivity measurements require an adjustment of R_w to the depth of interest because of temperature increase in the earth with depth. Because the value of R_o or R_t is found directly from the log, R_w must be temperature corrected to the depth of interest. For NaCl, this is accomplished by the use of the Arps equation frequently quoted in logging company literature (Arps, 1953);

$$R_{w2} = (R_{w1}) (T_1 + 21.5)/(T_2 + 21.5) \quad (10)$$

where the subscripts 1 and 2 refer to the two temperature states, R_w is in ohm-meters, and T in degrees Celsius. For the temperature ranges of interest at NTS, equation 10 is accurate to less than 1 percent. There is inadequate temperature range in the International Critical Tables to derive the temperature dependence of NaHCO_3 , however, equation 10 predicts the conductivity of NaHCO_3 within 2 to 4 percent from 18 to 25°C for dissolved solids in the range similar to those of Rainier Mesa waters. Interpretation charts of commercial logging companies imply that the use of the temperature dependence charts for NaCl with the NaCl equivalent dissolved solids for mixed ion species is adequate. Insight on the adequacy of this assumption may be found in Ucock (1979).

The data in table 3 indicate little difference between fracture and interstitial water resistivity in Rainier Mesa in the samples examined. The interstitial water appears to be slightly lower in resistivity, but order of magnitude differences as might be inferred from the results of Keller (1962) are not supported by these analyses.

A plot of the pore-water resistivities derived from the above techniques for the samples from t#3 is shown as a function of depth on figure 14. The t#3 pore-water data appear to yield a smaller range in resistivity than do fracture data. There is little evidence for any systematic depth dependence in the data, particularly where crossing the zeolitization boundary. Two things should be kept in mind. These resistivities do not reflect differences in individual ion species that may occur with depth or locally. A depth dependence of ion species related to the dissolution of glass was demonstrated by White and others (1980). This may be a factor in local differences in cation exchange capacity and their effect on electrical resistivity. Secondly, the sampling is inadequate to assign the observed resistivity range to all locations in the Rainier Mesa area, however, these are the only data we are aware of addressing pore-water resistivities at NTS. They are of considerable value in that they suggest that low resistivity pore waters do not generally exist in the Rainier Mesa tuff.

QUANTITATIVE INTERPRETATION OF ELECTRIC LOGS

Attempts to quantitatively interpret electric logs obtained in Rainier Mesa require some assumptions because of inadequate laboratory data concerning the parameters affecting the rock resistivity. In this regard, the first major assumption is that the value of 35 ohm-meters determined for the interstitial pore-water resistivity in the tuff is generally representative.

The average porosity in tunnel beds 3 and 4 in Rainier Mesa is about 35 percent with a two standard deviation range of about 25 to 45 percent (Brethauer and others, 1980). The resistivity observed on electric logs in

the tunnel beds is in the range 8 to 80 ohm-meters. It is therefore immediately apparent that an R_w of 35 ohm-meters involving these porosities cannot come close to satisfying equation 1, as resistivities in the range 172 to 560 ohm-meters would be required using the commonly accepted value for the cementation exponent "m" as 2. A similar situation exists in the unsaturated zone above the top of zeolitization where resistivities in the nonwelded tuff are in the range 20 to 100 ohm-meters. However, equation 2 also predicts much higher resistivities for saturations in the range of 60 to 90 percent, the range observed in limited core data obtained from the unsaturated zone in Rainier Mesa (Carroll, 1989). Thus, the discrepancy must be attributed to the presence of conductive mechanisms not accounted for in equations 1 and 2.

The major focus on modeling such mechanisms has been in petroleum source rocks where clays have been the major mineralogy responsible for the inapplicability of these equations. Clays have been found to impart an additional conductive fluid path in parallel with the pore water. This excess conductivity, or surface conductivity, is due to the counterions developed on the surface of clay particles arising from unsatisfied charges.

Saturated Tuff

Equation 1 may be modified to generally represent saturated rocks where a double layer of charge exists by including the additional parallel conductive component as,

$$C_o = C_w/F + X \quad (11)$$

where $C_o = 1/R_o$, $C_w = 1/R_w$, and X represents the conductance due to the additional charges on the rock surface.⁷

Equation 1 is now represented by the first term on the right in equation 11. The difference between equations 1 and 11 is demonstrated on figure 17. Equation 1 is represented by the plot through the origin where, theoretically for a saturated rock containing no surfaces with unsatisfied charge, the material obeys Archie's Law regardless of the resistivity of the saturant. The addition of surface-conductive solids in the form of clay counterions increases the rock conductivity as might be expected of parallel resistances. As the pore water (C_w) becomes more conductive it overwhelms the effect of the surface-conductive solids and a straight line of slope $1/F$ results. When pore waters become fresh the interaction of the two conductivities results in curvature of the plot at low values of C_w . The point at which the curvature deviates from a straight line (C_1 on fig. 17) is of interest. In actuality, almost all rocks show some curvature in the C_o - C_w plot as the pore water becomes fresher due to unsatisfied charges along broken bonds. Although treated laboratory materials have been noted to obey Archie's

⁷Conductivities are used in many of the equations involving double-layer models because linearity of C_o vs C_w plots results in more readily grasped concepts. Because much of our historical perspective at NTS is in units of resistivity this adds a certain unavoidable reciprocating of units. The author proposes to use resistivity where possible because of greater familiarity of these units for those engaged in Rainier Mesa logging.

equation for saturants of several thousand ohm-meters, in nature it is probable that C_1 occurs somewhere between 1 and 10 ohm-meters in the least altered rocks. Patnode and Wyllie (1950) report no more than about a 10 percent deviation for a 23 ohm-meter pore water saturating a "clean" sandstone. At $R_w = 389$ ohm-meters, the deviation becomes 40 percent. Not much attention has been focused in the logging literature in the fresh water range below C_1 on figure 17 because of the general absence of petroleum in fresh-water environments. The upper limit of C_1 is stated by Hill and Millburn (1950) as 0.1 ohm-meter, above which any effect of shale on the conductivity plot is suppressed. More recently, Clavier and others (1984) theoretically derived a value of 0.4 molal NaCl (approximately 0.3 ohm-meter) as the limiting value of C_1 for smectites. Experimental data of Waxman and Smits (1968) indicate a value of about 0.2 ohm-meter.

The behavior of Rainier Mesa tuffs in this context is shown on figure 18. The samples were from the U12n.10 UG-1 hole, a 1,401-ft horizontal hole drilled from tunnel level in Rainier Mesa, which penetrated tunnel beds subunits 3A through 4G. The tuff samples were all ash-fall tuffs and tuffaceous sandstones, containing varying amounts of alteration products, chiefly zeolites and minor amounts of clay (USGS, 1979). The samples on figure 18a were saturated with fresh water similar to that produced from fractures at tunnel level in Rainier Mesa. There is no correlation with equation 1 because the double-layer contribution is a significant portion of the effective pore-water resistivity. However, saturating the samples with salt water of resistivity 0.15 ohm-meter (fig. 18b) sufficiently shunts the contribution of X in equation 11 to yield good agreement with Archie's equation.

An approximate estimate of the magnitude, A , of the contribution of the double-layer fluid conductivity compared with C_w may be obtained at the mean porosity value using,

$$A = F/F_a - 1 \quad (12)$$

where F and F_a are the formation factors at low and high resistivity saturants, respectively. (This equation, valid for small amounts of clay, does not obviously follow from equation 11, but from the Waxman-Smits form of this equation which is discussed in the next section.) The data indicate that the counterions in the tuff double layer are an order of magnitude more conductive than the pore water.

The models derived for electric logging which attempt to quantify X do so by employing a relationship between the cation exchange capacity of the rock and the resistivity of the pore water. It behooves us, therefore, to identify those minerals within Rainier Mesa rocks which exhibit exchange capacity.

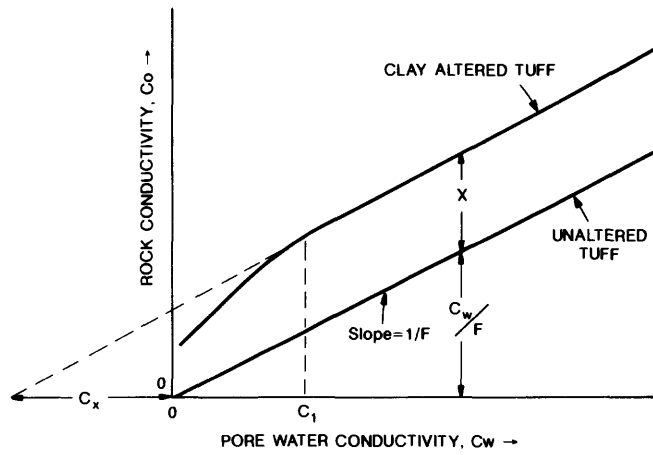


Figure 17.--Behavior of tuff conductivity versus pore saturant conductivity for a clean rock and rock containing clay-bound water. (Modified from Worthington, 1985)

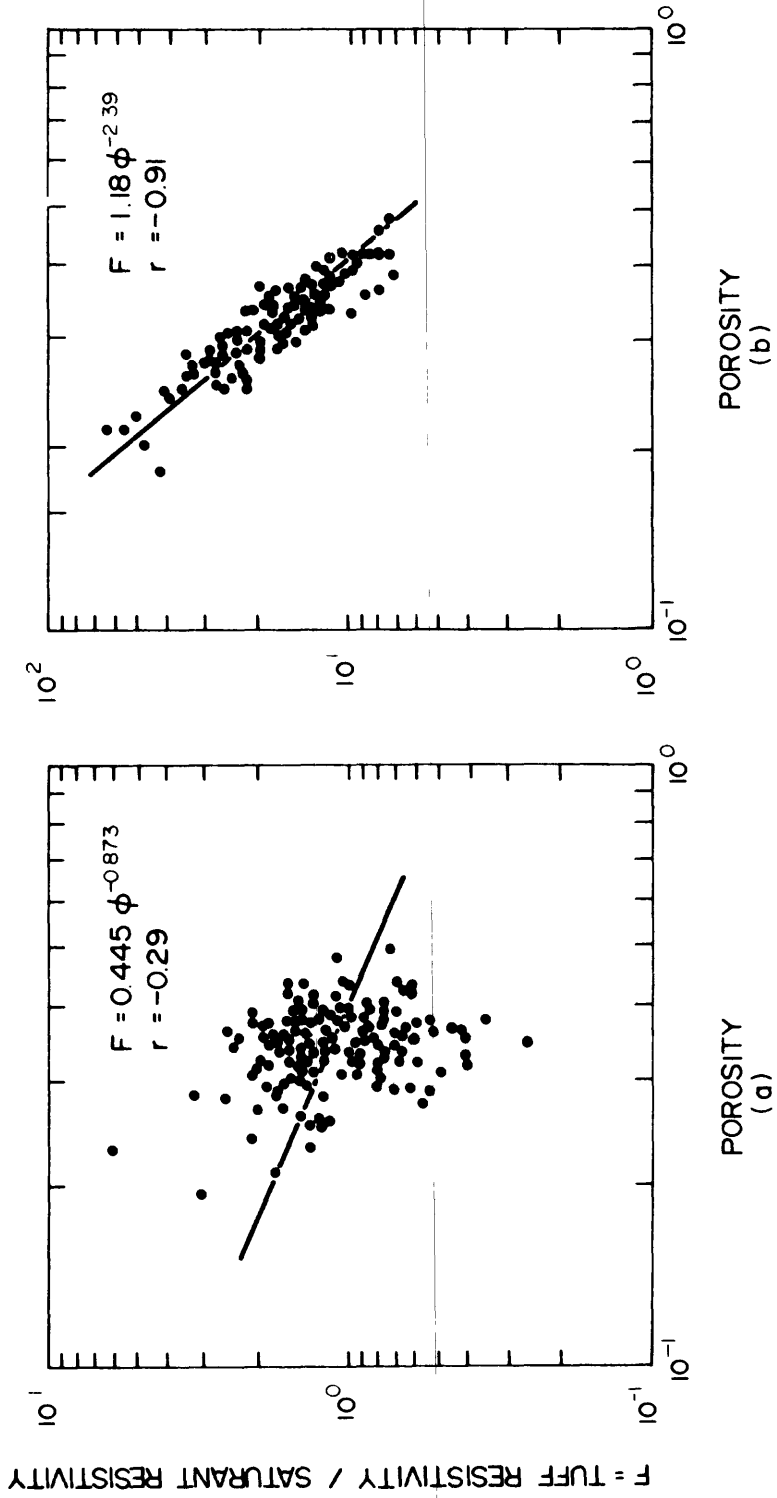


Figure 18.--Formation factor-porosity relationship for tuff samples obtained in Rainier Mesa tunnel beds. Samples in (a) were saturated with fresh water, and (b) with salt water. Correlation coefficient = r . (Modified from Carroll and Cunningham, 1980.)

Table 4 lists the results of limited X-ray diffraction analyses obtained to date on samples from the Rainier Mesa area. Because many of the samples listed were not systematically selected, the data should not be construed to represent any detailed description of subunit mineralogy.⁸ The majority of the clay samples were obtained in subunit 4K in the vicinity of a depositional syncline in the N-tunnel area, where structural conditions have resulted in considerable clay alteration of the tuff at tunnel level. The mineralogy within subunit 4K elsewhere in Rainier Mesa is more typically represented by the other samples listed in the table for that subunit.

Montmorillonite, illites, and mixed-layer clays appear to be the chief clays found in Rainier Mesa. A feature of note in these data is the almost universal presence of clay, both in the zeolitized zone and in the vitric tuff. They are believed to be ubiquitous in the volcanic rocks in Rainier Mesa as has been observed in volcanic rocks elsewhere at NTS (Bish and Vaniman, 1985). Small amounts in the context of electric logging means trace amounts. Clay universally present at levels near 5 percent will dramatically lower the resistivity in fresh water environments as we shall soon demonstrate.

Table 5 lists not only those minerals exhibiting cation exchange capacity (CEC) but also includes those minerals which may be expected to affect the response of neutron logs because of chemically contained hydrogen in the crystal structure. The hydrogen content of these hydrated minerals affects neutron log interpretation because the log sees this hydrogen as porosity. The neutron log response in tuff differs slightly from the physical concept generally associated with its response in clays. The neutron log, although beyond the scope of this report, would undoubtedly be involved in any logging program attempting to resolve water content and mineralogy in the volcanic

⁸Log interpretation techniques are derived from knowledge of the response of logging tools to the mineral constituents present in the formation. In Rainier Mesa this knowledge is not complete. Although there is adequate knowledge of the general mineralogy of the tuff, details necessary to relate mineralogy to geophysical logs in detail or to develop alteration models are lacking. Thus, although we know, for example, that clay is a prevalent mineral in the tuffs, how ubiquitously it is present in individual units and in what amounts is unknown. Yucca Mountain is the only area we are aware of at NTS wherein extensive X-ray mineralogy has been systematically obtained in the vertical geologic section (Bish and Vaniman, 1985). The different locale, different nature of the rocks, and different vertical alteration pattern in Yucca Mountain tuffs do not allow a direct application of the data to the Rainier Mesa area. Regardless, vertical and lateral variability of mineralogy within individual units may render definition of these variations using geophysical log techniques difficult.

Table 4.--X-ray analyses of selected tuff samples from Rainier Mesa area--Continued

Sample no.	Lithology	Montmorillonite ¹	Illite mixed layer	Illite-mica	Clinoptilolite	Quartz	Feldspar	Cristobalite- opaline silica	Amorphous (ash)	Carbonate	Sepiolite	Amphibole	Magnetite	Kaolinite	Hematite
<u>Vitric tuff</u>															
e#1 - 539	Tp	1	---	Tr.	---	Tr.	1	Tr.	7+	---	---	---	---	---	---
- 639	do	1	---	Tr.	Tr.	<1	2	Tr.	6	---	---	---	---	---	---
- 712	do	1+	---	Tr.	---	<1	3+	Tr.	4	---	---	---	---	---	---
- 745	do	1	---	---	---	Tr.	2	Tr.	5+	---	---	---	---	---	---
- 786	do	1	---	Tr.	Tr.	Tr.	2+	<1	5	---	---	---	---	---	---
<u>Clayey tuff</u>															
n05ug2 - 1202	Tt4K	1	3	---	2+	Tr.	<1	2	---	---	---	Tr.	---	---	---
- 1208	do	1	2+	---	2+	Tr.	<1	2+	---	---	Tr.	---	---	---	---
- 1210	do	1	2+	---	2+	Tr.	1	2+	---	---	---	Tr.	---	---	---
n03ug7 - 3.8	Tt4K	5 (20-35)	---	Tr.	<1	Tr.	2	1+	Tr.	Tr.	---	---	---	---	---
- 30	do	4+(30-40)	---	Tr.	1	Tr.	2+	<1	1+	Tr.	---	---	---	---	---
- 77.6	do	2+(20-30)	---	Tr.	2+	Tr.	3+	<1	1+	Tr.	---	---	---	---	---
- 80	do	2+(30-40)	---	Tr.	2	Tr.	4	<1	<1	Tr.	---	---	---	---	---
- 94	do	3+(20-30)	---	Tr.	1+	Tr.	2+	<1	1	Tr.	---	---	---	---	---
n05ug8 - 135	Tt4K	5+	---	Tr.	Tr.	Tr.	2+	Tr.	<1	Tr.	---	---	---	---	---
- 145.5	do	5	---	Tr.	Tr.	Tr.	2+	Tr.	1	Tr.	---	---	---	---	---
n#2 - 1362.5	Tt3A	3+(25-35)	---	Tr.	1+	Tr.	2+	Tr.	1+	Tr.	---	---	---	Tr.	---

¹Number in parentheses is percent illite mixed layer in samples.

²Includes mordenite.

³Red-colored portion of core.

⁴White-colored portion of core.

Table 4.--X-ray analyses of selected tuff samples from Rainier Mesa area--Continued

Sample location	Lithology	Montmorillonite ¹	Montmorillonite- illite mixed layer	Illite-mica	Clinoptilolite	Quartz	Feldspar	Cristobalite- opaline silica	Amorphous (ash)	Carbonate	Sepiolite	Amphibole	Magnetite	Kaolinite	Hematite
gi0ug1-222.7	Tt 4F	<1	<1	Tr.	4	1	2	1+	---	---	Tr.	---	---	---	---
t04 - 1+23	do	2 (10-50)	---	---	3	---	2	2	<1	Tr.	---	---	---	---	---
- B 5+04	do	2+(5-15)	---	---	3+	Tr.	1	2	<1	---	---	---	---	---	---
- B 6+19	do	1+(10-20)	---	---	2+	Tr.	2+	2	1	---	---	---	---	---	---
- B 6+56	do	<1 (5-25)	---	---	3+	<1	2+	2	<1	---	---	---	---	---	---
- 7+15	do	2+(10-20)	---	---	3	<1	2	1+	Tr.	Tr.	---	---	---	---	---
- 7+32	do	1+(5-15)	---	Tr.	3+	<1	2	1+	<1	Tr.	---	---	---	---	---
- 0+22	do	1+(5-15)	---	Tr.	5+	Tr.	1+	<1	<1	---	---	---	---	---	---
n18 - SS0+90	Tt3BC	1 (5-15)	---	Tr.	2+	<1	4+	---	1+	---	---	---	---	---	---
n02ug1 - 2615	Tt4K	1+(25-35)	---	Tr.	4+	Tr.	1+	1+	1	Tr.	---	---	---	---	---
n17 - 6+85	Tt4F	1 (5-15)	---	Tr.	2 ₅	Tr.	2	1+	Tr.	---	---	---	---	---	---
n15 - 1+35	do	<1 (10-20)	---	Tr.	6+	Tr.	2	---	Tr.	---	---	---	---	---	---
e20ug3 - 10.3	Tt4J	1+(15-25)	---	Tr.	4	<1	1+	<1	1	Tr.	---	---	---	---	---
e14ug10 - 908.4	do	<1	---	Tr.	5+	Tr.	1+	1	<1	Tr.	---	---	---	---	---
- 908.0	do	1	---	---	4+	Tr.	2	1+	<1	Tr.	---	---	---	---	---
n11g11 - 5.1	Tt4C0	Tr.	---	Tr.	4+	Tr.	2	2	<1	Tr.	---	---	---	---	---
g17 - 3.1	do	<1 (15-25)	---	---	6+	Tr.	1	<1	<1	Tr.	---	---	---	---	---
e20ug2 - 20	Tt4K	Tr.	---	Tr.	5+	<1	2	1+	Tr.	Tr.	---	---	---	---	---
- 230	Tt4H	1+(25-35)	---	---	4+	<1	1+	1+	<1	Tr.	---	---	---	---	---

Table 4.--X-ray analyses of selected tuff samples from Rainier Mesa area

[Analyses obtained by Paul Blackmon, USGS. Tr. = trace <5%; <1 = 5-9%; Leaders (---) indicate not determined; see figure 2 for explanation of lithologic symbols]

Sample location	Lithology	Montmorillonite ₁	Montmorillonite-mixed layer	Illite-mica	Clinoptilolite	Quartz	Feldspar	Cristobalite-opaline silica	Amorphous (ash)	Carbonate	Sepiolite	Amphibole	Magnetite	Kaolinite	Hematite
Zeolitized tuff															
t04 ugl-1156.8	Tt4ABCD	Tr.	---	---	7+	Tr.	<1	1	---	---	---	---	---	---	---
-1630.4	Tt38C	1	---	---	7+	---	1	1	---	---	---	---	---	---	---
-1799.5	do	<1	---	---	7+	---	<1	1+	---	---	---	---	---	---	---
n1UDnex2 - 36.5	Tt38C	Tr.	---	---	8	Tr.	1+	Tr.	Tr.	---	---	---	---	---	---
- 80.0	do	Tr.	---	---	7+	Tr.	Tr.	1+	<1	---	---	---	---	---	---
n15 - WP	Tt3A	Tr.	---	Tr.	2 ₅	<1	2+	Tr.	1	Tr.	---	---	---	---	---
- WP	do	Tr.	---	Tr.	2 ₅ +	1	2	Tr.	<1	Tr.	---	---	---	---	---
- 0+7	do	Tr.	---	Tr.	6	Tr.	2	Tr.	<1	Tr.	---	---	---	---	---
- 12+59	do	Tr.	---	Tr.	2 ₆ +	Tr.	2	Tr.	<1	Tr.	---	---	---	---	---
- B 8+25	Tt3D	2+ (10-20)	---	---	4+	Tr.	2	Tr.	<1	Tr.	---	---	---	---	---
- B 8+80	do	Tr. (10-20)	---	Tr.	2 ₆ +	Tr.	2	<1	Tr.	Tr.	---	---	---	---	---
e10 Slifer1-35	Tt4E	---	Tr	Tr	3+	<1	3	2+	---	---	---	---	---	---	---
e10 Slifer2-46.6	do	Tr.	---	<1	6+	Tr.	2	Tr.	---	---	---	---	Tr.	---	---
-46.6	do	Tr.	---	<1	4+	<1	4	Tr.	---	---	---	---	Tr.	---	---
n02NP-FACE	Tt4H	---	2+	Tr.	3	<1	<1	3	---	---	---	---	---	---	---
n#2 - 975.5	Tt4J	<1	Tr.	---	6	Tr.	1+	<1	Tr.	Tr.	---	---	---	---	---
- 983	do	Tr.	Tr.	---	4+	<1	1+	2	Tr.	Tr.	---	---	---	---	---
- 990	do	Tr.	Tr.	---	6	Tr.	1	1	<1	Tr.	---	---	---	---	---
- 1360.9	Tt3A	---	Tr.	Tr.	2+	<1	5+	Tr.	---	---	---	---	---	---	Tr.
e20ug3-122.5	Tt4K	1	---	Tr.	2 ₄	1	2+	Tr.	1	---	---	---	---	---	---
e20 -2+77	do	1	---	Tr.	2 ₅	<1	1+	<1	<1	---	---	---	---	---	---
n14ug1-764	Tt 4J	2 (15-25)	---	Tr.	1	Tr.	5	Tr.	<1	---	---	---	---	---	---
829.7	do	1+(25-35)	---	Tr.	3	Tr.	4	Tr.	<1	Tr.	---	---	---	---	---
848	do	1+(25-35)	---	Tr.	3	Tr.	3	1	<1	Tr.	---	---	---	---	---

Table 5.--Minerals found in Rainier Mesa area volcanic rocks which exhibit CEC or contain chemically bound hydrogen

[Leaders (--) indicate not determined]

Mineral	Formula ¹	CEC ¹ mg/100 g	Hydrogen ² index	Density (g/cc)
Zeolites				
Clinoptilolite	(Na ₂ K ₂ CaMg)[Al ₂ Si ₁₀ O ₂₄] · 8H ₂ O	170-200	0.25-0.40	2.16
Mordenite	(NaK)[Al ₁₅ O ₁₂] · 3H ₂ O	230	0.23	³ 2.39
Analcime	Na [AlSi ₂ O ₆] · H ₂ O	450	0.17-0.23	³ 2.45
Clays				
Montmorillonites	(1/2 Ca,Na) _{0.7} (Al,Mg,Fe) ₄ (Si,Al) ₈ O ₂₀ (OH) ₄	80-150	0.20-0.24	2.53
Illites	K _{1-1.5} Al ₄ [Si _{7-6.5} Al _{1-1.5} O ₂₀] (OH) ₄	10- 40	0.15-0.24	2.65
Mixed layer	--	--	0.10-0.29	2.56-2.7
Kaolinite	Al ₄ [Si ₄ O ₁₀] (OH) ₈	3- 15	0.33-0.36	2.44
Sepiolite	Mg [Si ₂ O ₅] ₃ (OH) ₂ · 6H ₂ O	20-30	--	1.0 -2.0
Other				
Opals	SiO ₂ · nH ₂ O	--	0.02-0.11	2.04-2.16
Micas	(K,Na,Ca)(Mg,Fe,Li,Al) ₂₋₃ [AlSi ₃ O ₁₀] (OH,F) ₄	--	0.12-0.13	2.69-2.31

¹Formulas and CEC for zeolites from Daniels and others, 1982; clays from Juhasz, 1979; sepiolite and others from Bates and Jackson, 1980.

²Hydrogen index and density from Edmundson and Raymer, 1979; clinoptilolite hydrogen index estimated from Ransom, 1977.

³These densities about 0.2 g/cc greater than reported by Breck (1973).

rocks. Thus we also include as a matter of record those minerals which may be expected to have influence on the neutron log as well as the electric log.⁹

Zeolites are easily the most abundant alteration product in the Rainier Mesa area, locally comprising as much as 80 percent of the tuff. The X-ray analyses shown in table 4 suggest zeolites, mainly in the form of clinoptilolite, generally comprise about 30 to more than 50 percent of the rock in the ash-fall tuffs in the zone of zeolitization. The minerals other than montmorillonite and clinoptilolite listed in table 5 have not been found in abundance in Rainier Mesa to date, and only opaline silica and mordenite have been reported in amounts exceeding 10 percent. Mica in excess of 10 percent may be found in isolated zones in some pre-Tertiary quartzites.

The general effect of these minerals on the response of geophysical logs is illustrated on figure 19. The matrix material of the rock shown on figure 19 is inert both electrically and with regard to neutron response, i.e., it behaves as an electrical insulator and approximates the standard limestone or sandstone matrix response. The clay surface contains chemically bound unsatisfied charges, chiefly hydroxyls, which attract charges of opposite polarity from the water saturating the pores resulting in the excess of ions in the fluid adjacent to the clay surface. Unsatisfied charges may also exist along broken bonds. This results in the electrochemically bound water shown on the figure. The electrochemically bound water layer, also called the double layer, is the source of the excess conductivity, X , in equation 11, creating a low resistivity path in parallel with the pore water. The double layer is held to the clay surface by strong Coulomb forces and cannot be moved by the capillary differentials existing in the formation or by pressure differentials created by injection (Juhász, 1979). The conductivity of this layer can exceed that of the free pore water by an order of magnitude in fresh water formations. The free water is chemically similar to water produced from the pores, such as the 35 ohm meter water obtained from the samples in t#3. This water is contained in the effective porosity of the rock (ϕ_e).

In a lithologic environment with no hydrated minerals, the neutron log measures porosity because it is sensitive to the hydrogen content of the pore water. Because of the hydrogen contained on the clay surface, the neutron log also "sees" a porosity for the dry material. This is the hydrogen index (HI) listed in table 5. The sum of the producible water or effective porosity (ϕ_e), and the double layer water is the total porosity. The total porosity (ϕ_t) may be obtained by standard laboratory techniques, or may be found in situ from a density log in the saturated formation coupled with a knowledge of

⁹The hydrogen index listed in table 5 is for dry minerals, i.e., those minerals which have been dried to 105 °C. It is approximately the apparent fractional volume water that would be indicated by the neutron log because of the hydrogen contained in the chemistry of the "dry" rock. This dry "water content" is not only dependent upon the mineral but the type of neutron logging tool employed (Edmundson and Raymer, 1979).

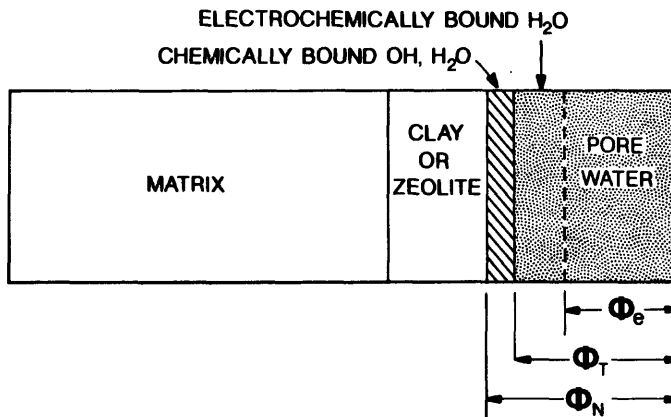


Figure 19.--Rock constituents affecting electric and neutron logs. Productible or effective porosity (ϕ_e) plus electrochemically bound, or double layer, water are what are normally measured as standard laboratory porosity (ϕ_t). The additional chemical-bound hydrogen is what is included in neutron porosity (ϕ_n). (Modified from Hill and others, 1979)

the grain density. Differences between total porosity and neutron porosity (which don't exist in unaltered sands) form the basis for techniques utilizing the density and neutron logs to define clay zones in oil field logging. A discussion of the nature of the bound water in various clays and its relationship to CEC has been reported by Johnson and Linke (1977).

The model on figure 19 may also serve for the zeolitic minerals present in the Rainier Mesa area tuffs. The effects of zeolitic properties on geophysical logs have not received much study, and there are peculiarities in the electrical behavior of these minerals. Zeolites are hydrated aluminosilicates capable of exchanging cations without major changes in structure (Mumpton, 1977). Mumpton attributes the exchange capacity to the replacement of quadrivalent silicon by trivalent aluminum resulting in a deficiency of positive charge. Thus, unlike clays, where the hydroxyls on the exchange sites also contribute a solid hydrogen component to the neutron porosity, a similar analogy cannot be made for zeolites. The chemically bound hydrogen layer on figure 19 is, however, analogous for neutron logs obtained in zeolitic tuffs if we consider the water retained by the zeolites after drying to 105°C as chemical bound water or hydrogen contained in the solid phase.

Bound water in zeolites is not totally driven off at 105°C (nor is it, strictly speaking, in clays). In zeolites part, or all, of the bound water is given off continuously and reversibly from room temperature to 350°C (Mumpton, 1977). Clinoptilolite is stable in air under dehydration to 700°C. Data concerning this phenomenon in NTS tuffs has been reported by Knowlton and McKague (1976) and Pawloski (1981). In keeping with the standard for physical property comparisons, i.e., core tests where water is driven off at 105°C, the bound water in zeolites remaining at 105°C may be conceived of as part of the matrix on figure 19, similar to the OH layer in montmorillonite with regard to "dry" neutron porosity.

Because of the extremely high cation exchange capacity of zeolites (table 5), one also expects an electrochemically bound layer in these minerals similar in a resistivity sense to that shown on figure 19 for clay. However, the behavior of the double layer in zeolites with regard to electrical conduction is the subject of much speculation. This will be addressed shortly. For the present, however, figure 19 will serve to conceptually describe the behavior of zeolites or clay for purposes of electric or neutron logging. The hydroxyl content of the dry clay which presents additional hydrogen to the neutron log may be considered analogous to the water retained by zeolites after dried to the standard temperatures for laboratory measurements of porosity. The double layer exhibited by wet clay due to surface charges is well behaved and documented. It may be considered analogous to a similar layer in zeolites, postulated to exist because of the nature of their exchange capacities, but whose magnitude is as yet incompletely understood for the purposes of electric logging.

We shall neglect zeolites for the moment and address the general electrical behavior of clays. We do this for two reasons: (1) clayey rocks have been extensively modeled and tested in connection with electrical logging in petroleum reservoirs and thus their influence on electrical resistivity can be predicted, and (2) empirical observations on electric logs by the author over several years at NTS have led to the conclusion that, all things being equal, clays appear to provide a considerably greater contribution to lowering electrical resistivity than zeolites.

Evidence for the latter conclusion may be found in examining the surface area of clays and zeolites. The surface area of montmorillonites is the largest known of any group of minerals (Almon, 1979). Figure 20 is a plot of the surface area of the standard API clays, selected tuffs, and clayey sedimentary rocks as a function of CEC. The fact that the clayey samples from various sedimentary environments yield a good relationship between CEC and surface area, as opposed to the tuffs, suggests difficulties in attempting to explain the electrical resistivity of zeolites using clay models.

Effect of Clay on Electrical Resistivity

Here we make another assumption concerning the electrical behavior of the tuffs in Rainier Mesa. Namely, that the electrical resistivity model of the clays contained within the tuffs is similar to that observed in sandstones. We temporarily ignore the contribution of the zeolites and assume that the clay distributed in the pores will behave electrically in a manner similar to that of sandstones containing clay. The zeolites are assumed to yield a separate contribution to the tuff resistivity independent of the clay, and are considered an additional component of conductivity summing with that of the clay-bound water and pore-water components. This approach is required because there are no models for the electrical resistivity of cation exchange minerals other than those developed for clays. Thus quantifying the magnitude of clay effects is considered the initial step in understanding resistivity observed on electric logs in Rainier Mesa. This further assumes that the electrical behavior of Na montmorillonites (the clay type addressed in existing oil-field models of electrical resistivity) is not grossly different from those in Rainier Mesa.

Several solutions have been offered for equation 11. Many employ empirical relationships obtainable from logging tools to take into account the clay conductivity term, X . A number of models have been developed to provide solutions specific to a region and frequently involve other logs, such as gamma ray or neutron, to obtain an estimate of the clay volume for inclusion in the X term. An extensive review of these formulations has been given by Worthington (1985). Only a few attempts have been made to describe X in purely electrical terms based on laboratory observations. The most prominent of these is the model developed by Waxman and Smits (1968) and further extended by Waxman and Thomas (1974). In the Waxman-Smits (WS) model extensive laboratory measurements were employed to demonstrate that the conductivity of the double layer could be related to the CEC of the clay and the concentration of the counterions in the double layer. This results in a direct determination of the X term in equation 11 which adds to the normal pore-water conductivity. The sum of this double-layer conductivity and the

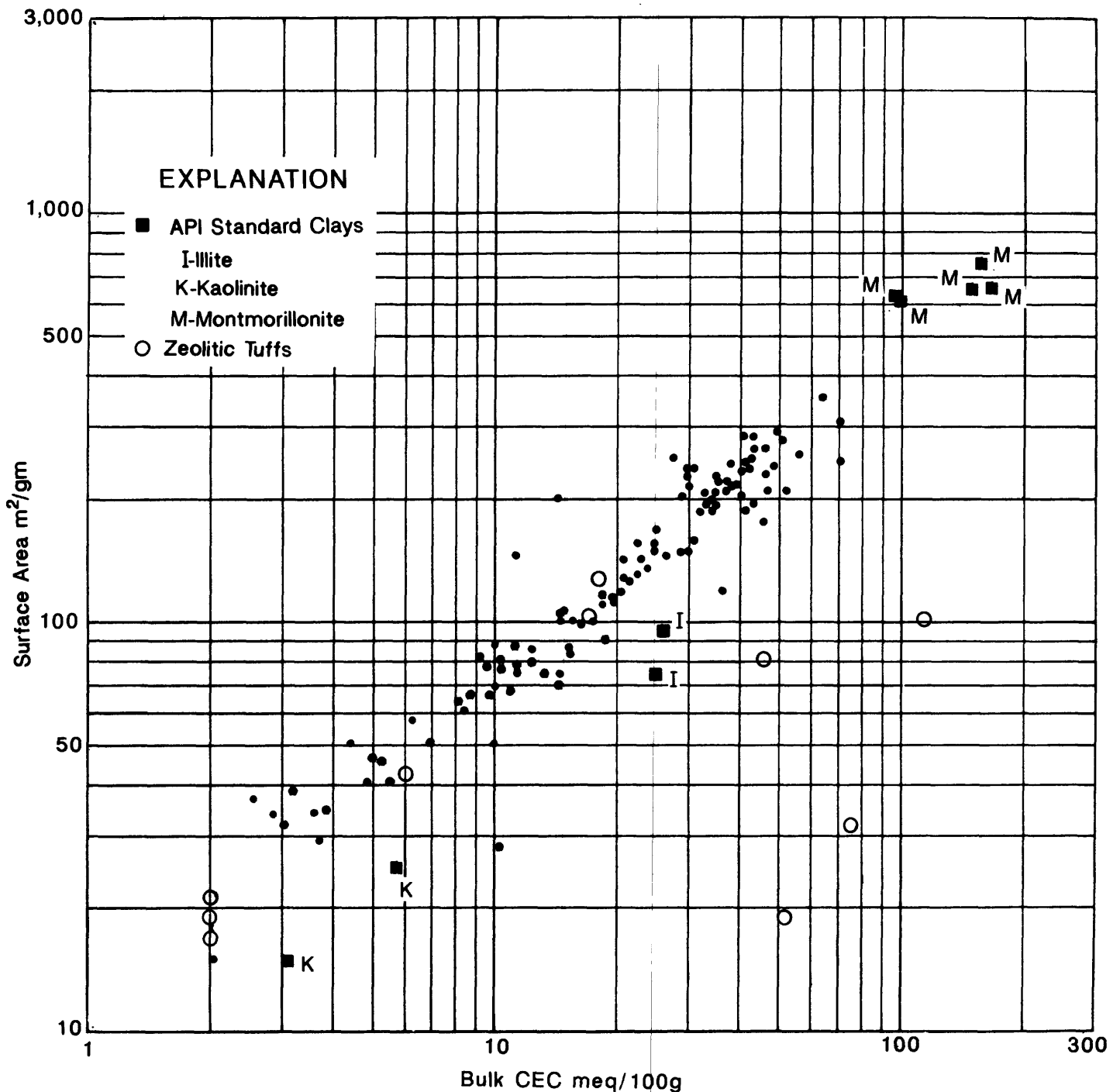


Figure 20.--Surface area versus cation exchange capacity for several rock types. Symbols not identified represent clay sands from California, Oklahoma, Louisiana, and Wyoming. Data on clays after Patchett (1975). Data on zeolitic tuffs from Cs exchange capacities and surface areas reported by Daniels and others (1982).

effective pore-water conductivity is the water conductivity which now relates to rock conductivity through Archie's Law. At pore-water conductivities greater than C_1 in figure 17, the relationship is essentially linear and the slope of the plot is $1/F^*$. F^* is a formation factor similar to F in equation 2 except that the pore-water conductivity is now comprised of the sum of a free and bound-water component. F^* is used to denote this modification.

The Waxman-Smits (WS) formulation for a saturated rock is,

$$C_o = 1/F^* (C_w + BQ_v) \quad (13)$$

where X in equation 11 is now BQ_v/F^* . The concentration of counterions, a function of pore-water resistivity, is the variable which describes the entire range of the C_o - C_w plot in figure 17, including the curvature below C_1 , and is given as,

$$B = (1 - 0.83 \exp(-0.5/R_w))(3.83) \quad (14)$$

where R_w is the resistivity of the water saturating the pores.¹⁰ F^* is the reciprocal of the straight line portion of the C_o - C_w plot as shown on figure 17. The X -axis intercept, C_x , is equivalent to $3.83 Q_v$. Thus, one may theoretically define the conductivity behavior of a core at all saturants with a laboratory measurement at only two points above C_1 . The value of F^* is defined from the slope and the CEC related term Q_v may be calculated from C_x . In practice four or more points are generally obtained for the C_o - C_w plot and the CEC is often measured independently. The value of B at our postulated 35 ohm-meter Rainier Mesa pore water is 0.696. However, the experimental data of WS did not extend above about $R_w = 5$ ohm-meters and we assume extension of the model to our range is valid. We found no data in the literature examining the WS formulation in our range of R_w .

Because current conduction is through the rock pores, CEC is normalized to pore volume rather than used in units of meq/100 g of dry rock, the units normally reported in many geotechnical applications. This relationship is given by,

$$Q_v = CEC (1-\phi) D_g/\phi \quad (15)$$

where CEC is in meq/g, ϕ is porosity, and D_g is grain density. The units of Q_v are meq/cc.

¹⁰Equation 14 is applicable at 25 °C and we will not be concerned with its temperature dependence because of the proximity of this temperature to that at working depths in the Rainier Mesa drill holes. Temperature dependence of resistivity in rock containing double-layer counterions differs from that in a clean rock such that the formation factor F^* is not constant with temperature. Thus, one cannot correct R_w for temperature at a depth of interest and divide it into the R_o observed on the electric log and obtain a constant as is the case in clean sands. Techniques for this correction are discussed by Waxman and Thomas (1974) and Clavier and others (1984).

Here we come to an important, but often overlooked, fact. Resistivity is related to the pore volume distribution of clay, and not to the clay content of the rock per se. Consequently, two rocks exhibiting the same CEC (clay content) may differ appreciably in Q_v and, consequently, resistivity if the porosity difference is large and the pore waters are relatively fresh. Resistivities of porous rock with the same clay content can easily differ by greater than two to one because of porosity differences. All other things being equal, it is apparent that the lower porosity rocks would tend to contribute considerably more to the bound-water component, BQ_v , than high porosity rocks. This difference is not sufficient, however, to violate the trend of decreasing resistivity with increasing porosity predicted by equation 1 for unaltered rocks. Thus, for two tuffs with equivalent CEC the higher porosity tuff will always exhibit the lower resistivity.

Because Q_v is not a familiar term at this stage of logging experience in the Rainier Mesa area, it is appropriate to get some feel for the magnitude of values of Q_v encountered in clayey sedimentary rocks. The Q_v of the entire suite of shaly sands used to develop the WS relationship are shown in histogram fashion on figure 21 along with the range in CEC and porosities reported. This suite of data has been used to test most models of double-layer conductivity. The CECs are generally considerably less than might be expected for zeolitic tuff samples or tuff samples with appreciable amounts of clay. The object of the Waxman-Smits investigations, however, was to develop useful relationships in shaly sands capable of oil production. Loss of permeability at high clay contents excludes sands of high clay content from this category. Waxman and Smits note that a limiting permeability for oil production in shaly sands occurs at a Q_v of about 0.5.

Figure 22 shows other relationships within this suite of data (which consists of samples from several geographic locales and geologic ages) that are of interest. It is noteworthy that figure 22 does not indicate any relationship between Q_v and porosity. However, well behaved relationships between these two parameters exist in some sedimentary rocks. Where true, this is obviously a potent relationship because of the many porosity tools available in logging. A weakness in the WS approach is the need for laboratory tests on core, however a universally applicable method of determining Q_v in clay sands using only downhole parameters derived from logging tools has not yet been found.

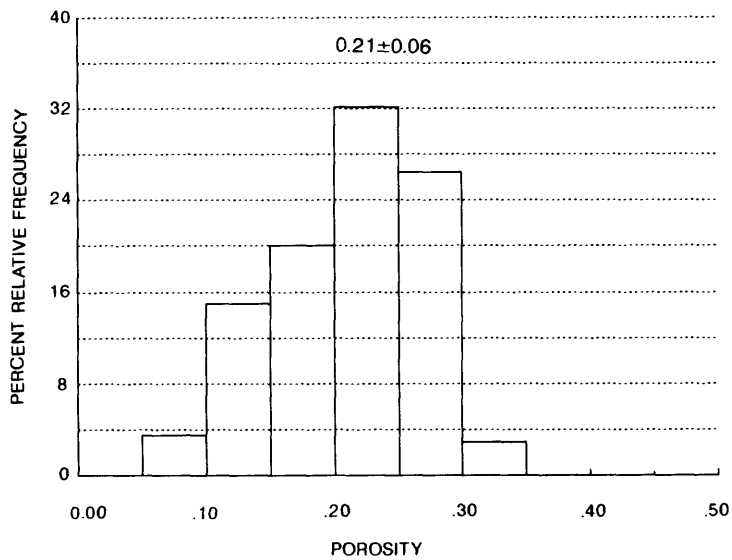
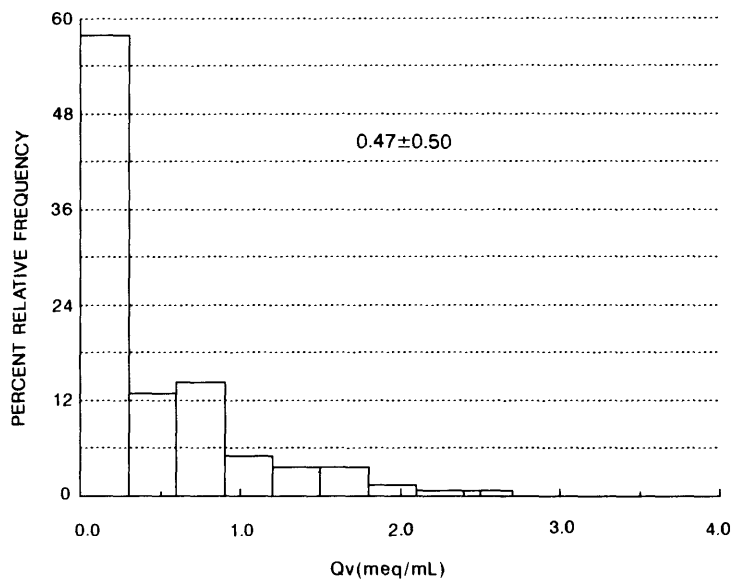
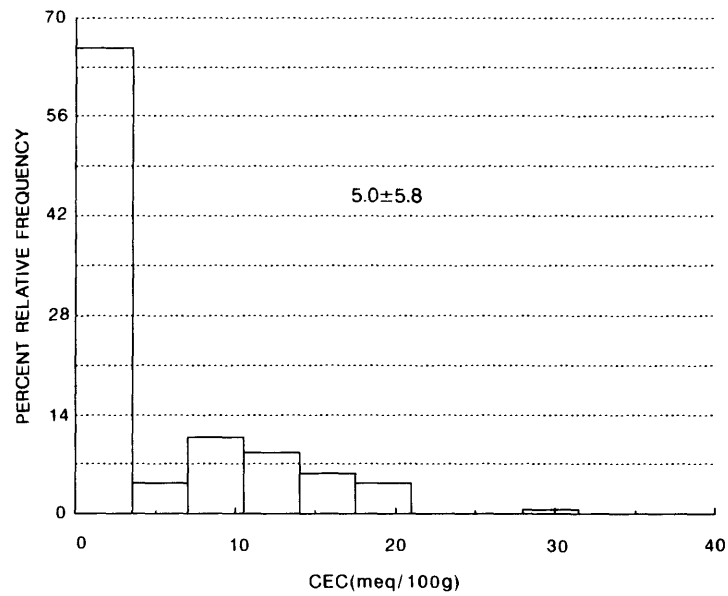


Figure 21.--CEC, Qv, and porosity distribution for 140 clayey sandstones used to derive WS model. Grain density assumed 2.65 g/cc. Data taken from Clavier and others (1977).

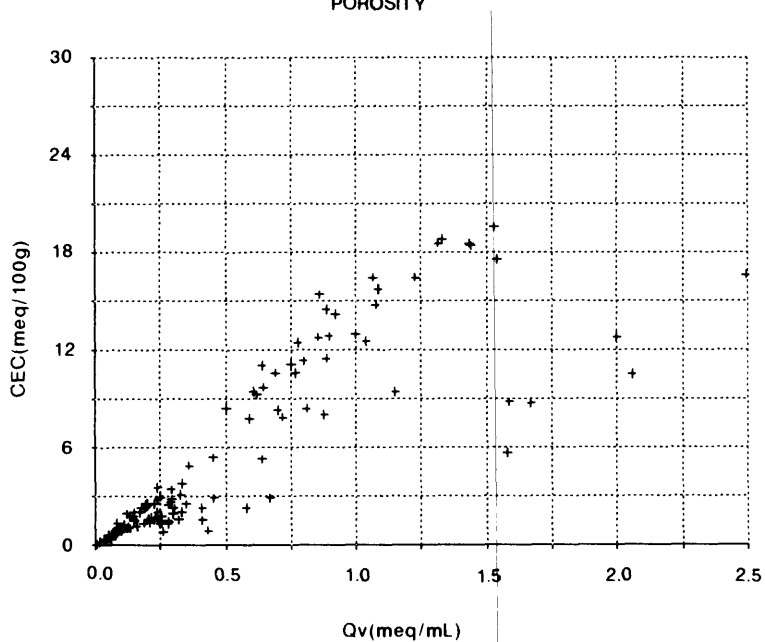
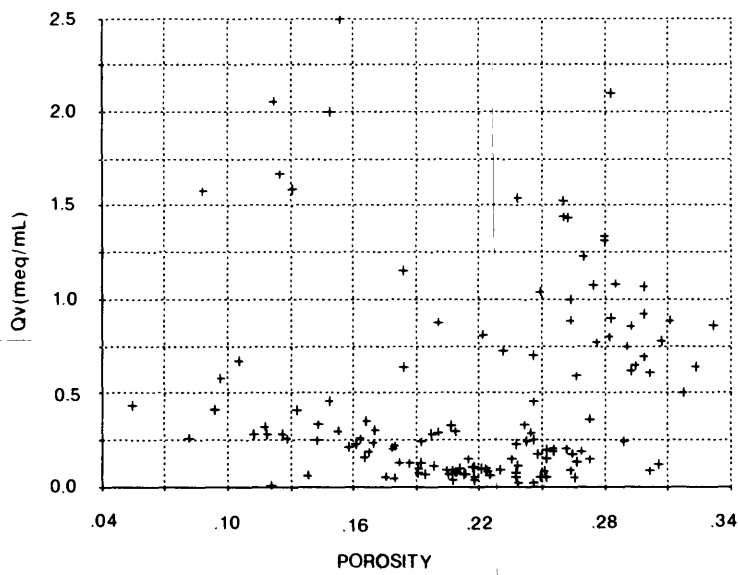
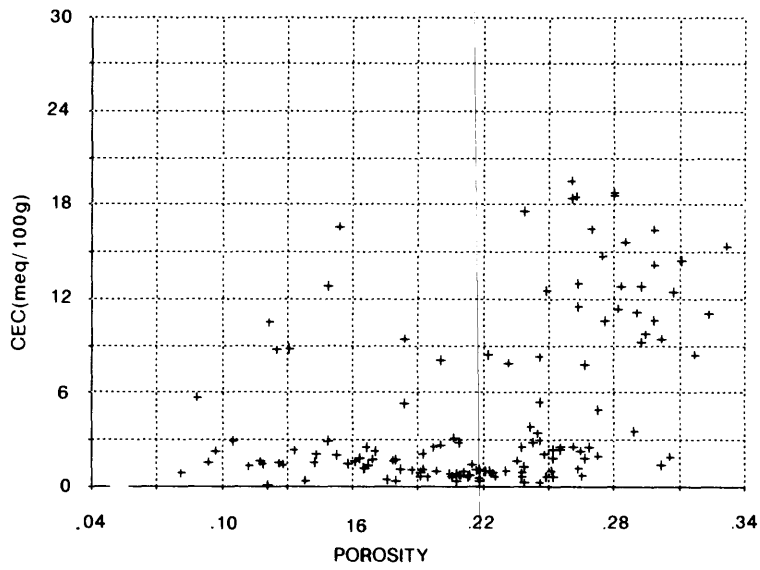


Figure 22.--Relationships among Q_v , CEC, and porosity for 140 clayey sandstones used to derive WS model. Grain density assumed 2.65 g/cc. Data taken from Clavier and others (1977).

We now proceed to examine the applications of these relationships with regard to the resistivities observed on Rainier Mesa logs. One additional assumption required is a value for the CEC of the clay found in the tuffs. The average CEC of montmorillonite is reported by Johnson and Linke (1977) as 1 meq/g. For this value, the percentage clay is equivalent to the CEC and may be used for CEC in equation 15. Our approach at this stage is not to be extremely precise, but to obtain some idea of the reality of the WS approach with regard to the magnitude of resistivities and clay contents observed in the tuffs of Rainier Mesa.

Figure 23 reproduces the electric and density logs obtained in the zeolitized tuffs in the section of e#3 covering tunnel beds 3 and 4. As mentioned earlier, these rocks may be considered saturated. The electrical resistivity on these logs is typical of the range seen in the tuffs in the zone of zeolitization. The agreement of the 16- and 64-in. normal log resistivities on the original log throughout most of the interval shown suggests that these logs are measuring true formation resistivity. Only the 16-in. normal log is shown on the figure.

On the figure are also plotted the resistivity log expected if only unaltered tuff were present and saturated with 10 (ELOG10) and 35 (ELOG35) ohm-meter pore water. These data were obtained from the Archie equation with "m" assumed 2.¹¹ The porosity may be approximated from the density log by assuming a grain density of 2.5 g/cc (Carroll, 1989). Note that for a 10 ohm-meter pore water, Archie's equation for unaltered tuff can explain the observed resistivity in several locations without the requirement of any double-layer material. This again serves to emphasize the critical importance of a correct knowledge of R_w in these rocks. The approximate variation of R_w needed in the pore water to completely explain the resistivity on the basis of Archie's Law for clean rocks is also plotted on the figure (RWA). It is noteworthy that Keller's (1962) value of 1.6 ohm-meter derived for R_w would be difficult to fit in any of these formulations.

¹¹Some debate exists as to the range of the cementation exponent in clayey sands. Waxman and Smits (1968) indicate it to be an approximately increasing function of clay content approaching 3 at high clay contents, whereas in the "dual-water" model of Clavier and others (1984) the value is more uniformly 2 regardless of clay content. The data on figure 18 suggest a somewhat higher value than 2 for the tuffs. An interesting evaluation of the variation of "m" in clean rocks has been published by Gomez-Rivero (1976).

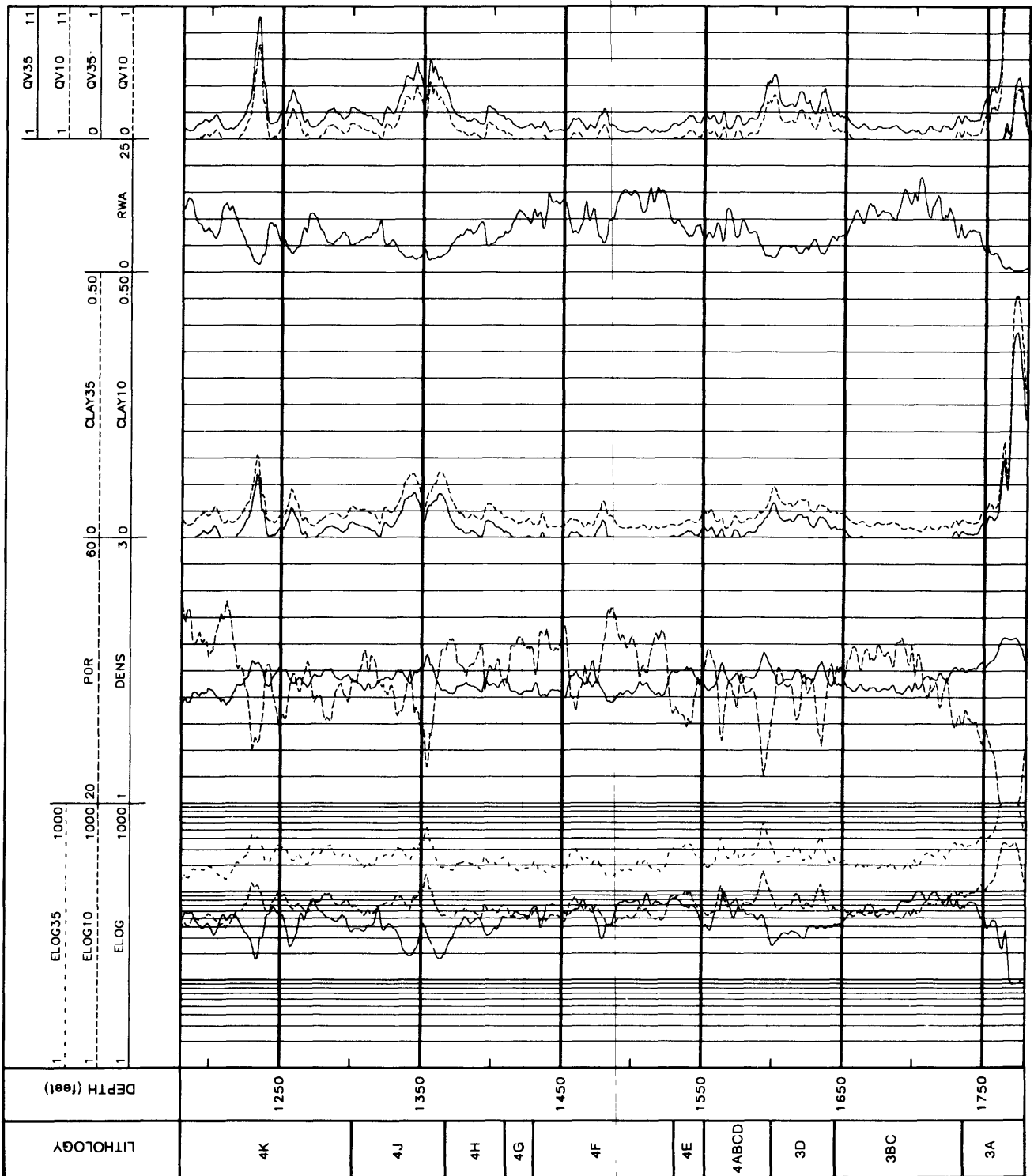


Figure 23.--Electric (ELOG) and density (DENS) logs obtained in tunnel beds in e#3 hole. Porosity (POR) calculated from density log assuming 2.5 g/cc grain density. Other parameters calculated from Archie's equation or WS equation assuming 10 and 35 ohm meter pore water.

The percentage clay that would be required in the tuff to explain the observed resistivities using the WS equation is shown for both 35 and 10 ohm-meter pore water. This is obtained by rearranging equations 13 and 15 with the above mentioned parameters to obtain the unknowns,

$$Q_v = (C_o F - C_w)/B = (C_o/\phi^2 - C_w)/0.696 \quad (16)$$

and

$$Cl = (Q_v \phi)/((1-\phi) 2.5) \quad (17)$$

where Cl = fractional percent clay. The value of Q_v resulting in these percentages of clay is also shown for the two pore-water resistivities. The percentage of clay becomes zero or less for those values of resistivity where Archie's equation is satisfied without recourse to double-layer material. At 35 ohm-meter pore water the observed resistivity is only satisfied where clay is ubiquitously present in the tuff.

What is noteworthy in these approximations is that clay is generally required in only minor amounts to explain the resistivity observed, amounts that are typically observed in the samples obtained to date. The low resistivity markers mentioned earlier, subunits 4J and 3D, require clay in amounts of about 10 percent, not unreasonable values. The 3A/Tbt contact, which is a consistently low-resistivity marker throughout the Rainier Mesa area, is indicated to require relatively large amounts of clay to support the model. Clay has been reported in excess of 30 percent in tunnel bed subunit 3A (table 4) but not in all samples, although to sufficiently address the clay content, a systematic study of the distribution of clay at this contact is needed.

The clay content data shown on figure 23 are conservative because lower values of R_w would tend to lower apparent clay content. The clay contents are generally in a range which appear to be typical of the tuff. The CEC could arguably be considered overly optimistic for the clay, although data presented in the laboratory section of this report tend to support a value of 1 meq/g. If the CEC of the clay was decreased, the additional counterions needed in the form of a double-layer contribution from the zeolites would be trivial. The small amounts of clay resulting from the above calculations leaves in question the contribution of zeolites and their high attendant CEC, a topic which will be further discussed.

Unsaturated Zone

The unsaturated zone should present us with a more unequivocal test of the WS model because limited X-ray analyses (fig. 14, table 4) indicate that these rocks are almost completely deficient in zeolites and that the dominant alteration product present in the rock is clay. This suggests that the zeolites in Rainier Mesa may have formed in an essentially open hydrologic system by meteoric waters moving downward or essentially downward. Systems of this type are discussed in detail by Hay and Sheppard (1981). In addition, the tuffs in the unsaturated zone are often semi-consolidated, suggesting that the tortuosity is more akin to sandstones.

The major drawback in evaluating these rocks is the frequent absence of a fluid column above the top of zeolitization preventing the acquisition of electric logs in these 4-in. holes. Another drawback is lack of knowledge of the extent of invasion. Unlike the zeolitized zone, porosity cannot be directly calculated from the density log because of unknowns concerning the extent of invasion of drilling mud and hence the saturation. Neutron logs obtained in Rainier Mesa indicate that invasion is not sufficient in some holes to present a saturated rock to this tool (Carroll, 1989). The calculations which now follow are, therefore, subject to greater uncertainty than those for the saturated zone.

The standard method of deriving saturation, equation 2, is similarly complicated by the presence of clay. As previously mentioned, it is in the derivation of saturation that the electric log assumes its major importance. In the presence of several inches of invasion, the electric log is about the only geophysical log from which one may derive saturation. Unlike the saturated zone where porosity can be derived from several logging tools, the electric log is often mandatory in the unsaturated zone in order to obtain true rock saturation.

The WS formulation for the unsaturated zone is,

$$C_t = 1/F (S_w^n) (C_w + BQ_v/S_w) \quad (18)$$

which, for the commonly assumed value of $n = 2$ is,

$$C_t = 1/F (S_w^2 C_w + BQ_v S_w) \quad (19)$$

The absence of clay ($Q_v = 0$) reduces these equations to equation 2, the standard saturation equation for a clean rock. As in the case of saturation, the equivalent pore-water conductivity of the clayey sand is considered the sum of the contributions of the producible water and the clay-bound water, and the rock is presumed to behave in a manner similar to a partially saturated clean rock of the same porosity, tortuosity, and formation factor, but with the pore water now composed of two components. In the case of partial saturation, however, WS found that the exchange cations become more concentrated in the pores. This results in the division of the shale term, BQ_v , by S_w in equation 18.

The 16-in. normal and the density log, obtained in the short section in the vitric tuff zone of e#3 between top of fluid and top of zeolitization, are reproduced on figure 24. The porosity calculated from the log assuming a grain density of 2.30 g/cc is also listed (POR230). This low grain density is not unreasonable for some sections in the vitric zone, and is necessary to yield reasonable values of porosity, a possible suggestion that invasion is not total within the radius of investigation of the density tool, which is probably less than 6 inches.

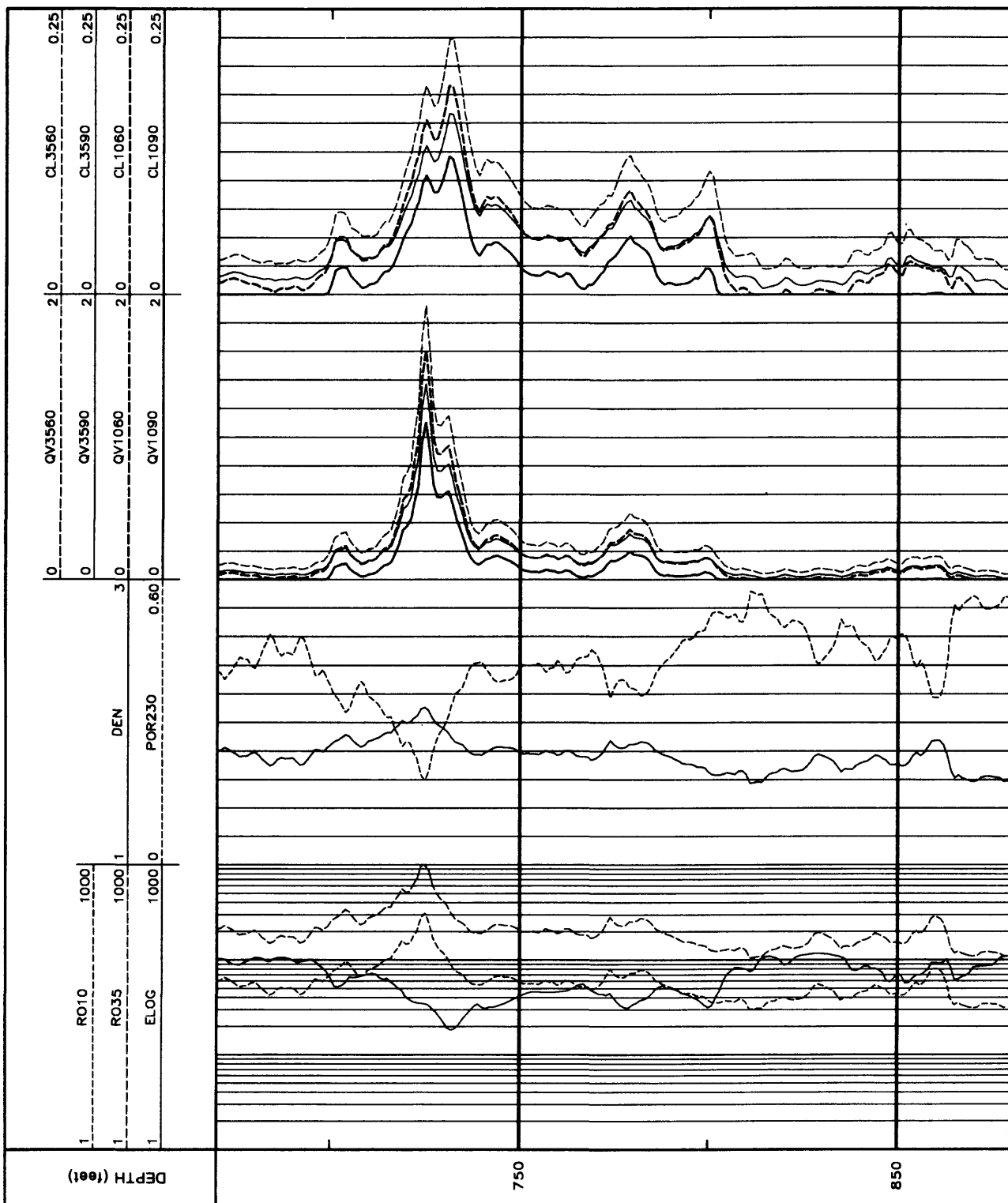


Figure 24.--Electric (ELOG) and density (DEN) logs obtained in unsaturated zone in e#3. Porosity (POR230) calculated from density log assuming 2.3 g/cc grain density. Other parameters calculated from Archie's equation or WS equation assuming 10 and 35 ohm-meter pore water.

If we assume this porosity is saturated, Archie's equation for a clean rock yields the R_o values for tuff resistivity plotted on the figure for a 10 and a 35 ohm-meter pore water. Given the nature of the saturation equation for a clean rock (equation 2), it is evident that only for those regions where R_o is less than the measured resistivity can the saturation be less than total because R_o is always less than R_t under these conditions. This is also true for clayey rocks in spite of the fact that the counterion conductivity increases with decreasing saturation, i.e., the saturated resistivity is always less than that at partial saturation.

Where the values of R_o on figure 24 are less than the measured resistivity the tuff may contain clay. For 35 ohm-meter pore water the observed resistivity does not contradict theory. For the partially saturated tuff containing a 10 ohm-meter pore water, there are a few locations where the tuff resistivity is equivalent to a totally saturated condition (e.g., near 790 ft) and several broad zones where the theoretical saturated resistivity is less than the recorded resistivity (e.g., 800 to 880 ft) indicating our parameters are in error somewhere.

The values of Q_v needed to explain these resistivities in light of the WS model (equation 19) are listed for a 60 and 90 percent saturation of the tuff. In addition, the clay content (CL) equivalent to these values of Q_v is also listed, again derived with the assumption $CEC = 1$ meq/g. The first two numbers on the figure headings refer to the pore-water resistivity and the last two to the percent saturation of pores. Those zones wherein a 10 ohm-meter pore water is assumed, and which exhibit a saturated clean rock resistivity less than the observed resistivity, understandably yield negative clay contents at 90 percent saturation. These zones do, however, reflect clay at 60 percent saturation because the resistivity of a partially saturated clayey rock can exceed that of a clean saturated rock of the same porosity depending on the parameters involved. This again illustrates the importance of knowing precisely the values of the parameters applicable in the WS equations.

The exact saturation of the tuff in the vitric zone is presently a matter of some conjecture. Values in the range of less than 60 percent to in excess of 90 percent have been reported (Carroll, 1989). A number of the samples from which this range was derived were obtained under drilling conditions which subjected the samples to the possibility of drilling fluid contamination. We have chosen 60 and 90 percent saturation to cover the range of uncertainty.

The values for clay content listed on figure 24 are not particularly unreasonable and, as in the saturated zone, can generally be explained again by the ubiquitous presence of small amounts of clay. Thus, even with fairly approximate parameters, the WS formulation appears to yield results comparable with observed resistivities and clay contents in the tuff.

Clay Content Versus Resistivity

Based on electric log resistivity and visually observed clay, an empirical approach has been used over the years to identify clayey tuff zones from electric logs in Rainier Mesa and at NTS. Tuffs exhibiting resistivities less than 20 ohm-meters are considered potentially clayey, and resistivities

of less than 10 ohm-meters are considered possibly indicative of high clay content (Carroll and Cunningham, 1980). Although it has been since recognized that there are other variables which may reduce resistivity, these guidelines are still considered valid. Because this observation is based somewhat on the quantity of clay affecting resistivity rather than the clay distributed within the available pore space as in the WS model, it is of interest to examine the theoretical range in resistivity predicted by the WS model, i.e., the extent to which clay content per se is reflected in electrical resistivity.

Figures 25 and 26 are plots bracketing the range of theoretical resistivity predicted by the WS model as a function of clay content where the clay exhibits CECs of 1 meq/g and 0.5 meq/g. Figure 25 represents the saturated tuff in the zeolitized zone. The extremes on the plot were calculated using porosities of 25 and 45 percent, cementation exponents of 2.0 and 2.4, and water resistivities of 10 and 35 ohm-meters in equation 13. The lower plot in the figure is an expanded version for theoretical clay content above 20 percent.

Figure 26 is the same theoretical representation for the vitric tuff with saturation values of 60 and 90 percent, water resistivities of 10 and 35 ohm-meters, and cementation factors of 2.0 used to bound the ranges shown. Because of the often friable nature of the unsaturated tuff, a saturation exponent of 1.8 was assumed in equation 18. In addition, the upper limit of porosity was extended to 50 percent for the vitric tuff. Grain densities of 2.5 g/cc and 2.4 g/cc were used for the saturated (zeolitized) and partially saturated (vitric) tuff, respectively. The extremes in resistivity obtained for the two values of CEC using these combinations of parameters are shown on the figures. The differences in the parameters assumed for the two rock types result in almost the same range in resistivity for the two conditions. If the same parameters were used, a relatively larger range in resistivity would obviously result for the partially saturated case.

The plots on figures 25 and 26 indicate that clay content per se bears no direct relationship to resistivity.¹² As previously observed the volume distribution of clay in the porosity is the major factor affecting resistivity, not clay content or CEC. At low clay contents the range in resistivity is seen to be fairly large. At the higher clay contents the sensitivity of resistivity to clay content is rather small. In connection with the latter, note that the WS model indicates resistivity tends to approach a fairly constant value at high clay contents. Limiting values of resistivity have also been reported for shales by other investigators (Patchett, 1975). Based upon empirical evidence from electric logs obtained in Rainier Mesa this limit appears to be around 2 to 8 ohm-meters, and these values appear to occur at clay contents of 50 percent or less.

¹²This assumes a purely random distribution of clay in nature. As previously mentioned, in some sedimentary rocks Q_v has been found to be porosity dependent, thus, a relationship between clay content and resistivity can exist (Juhász, 1981).

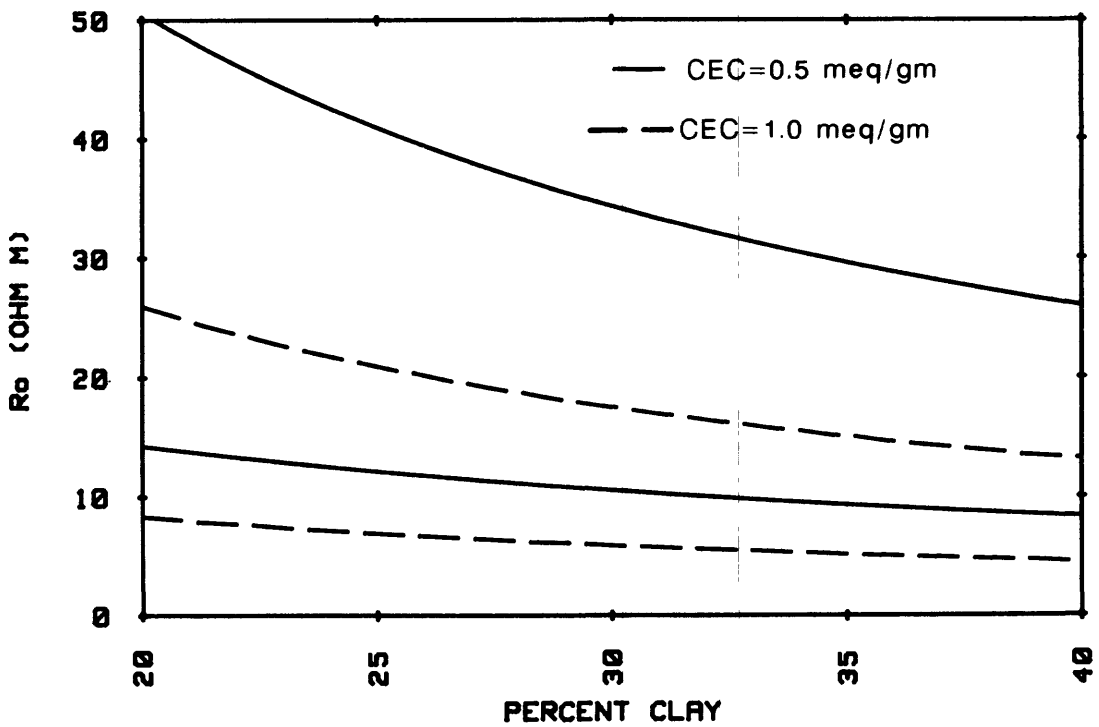
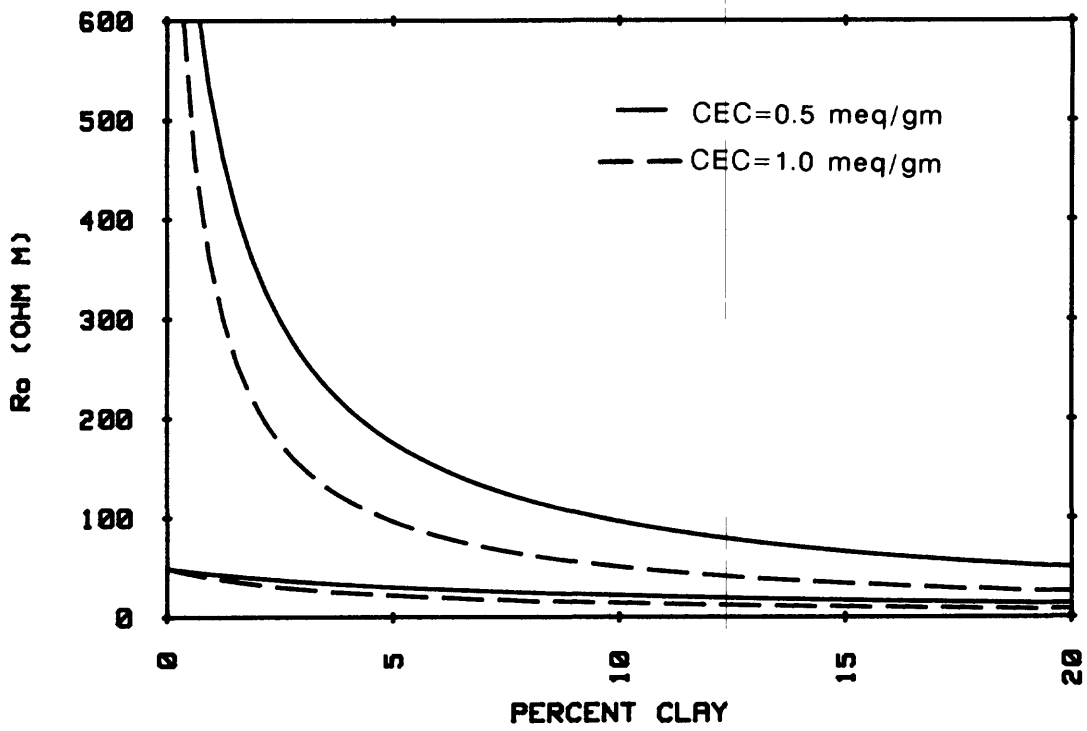


Figure 25.--Range of resistivities as a function of clay content predicted by WS model for tuffs in the saturated tunnel beds. Clay CECs of 0.5 and 1 meq/g are assumed.

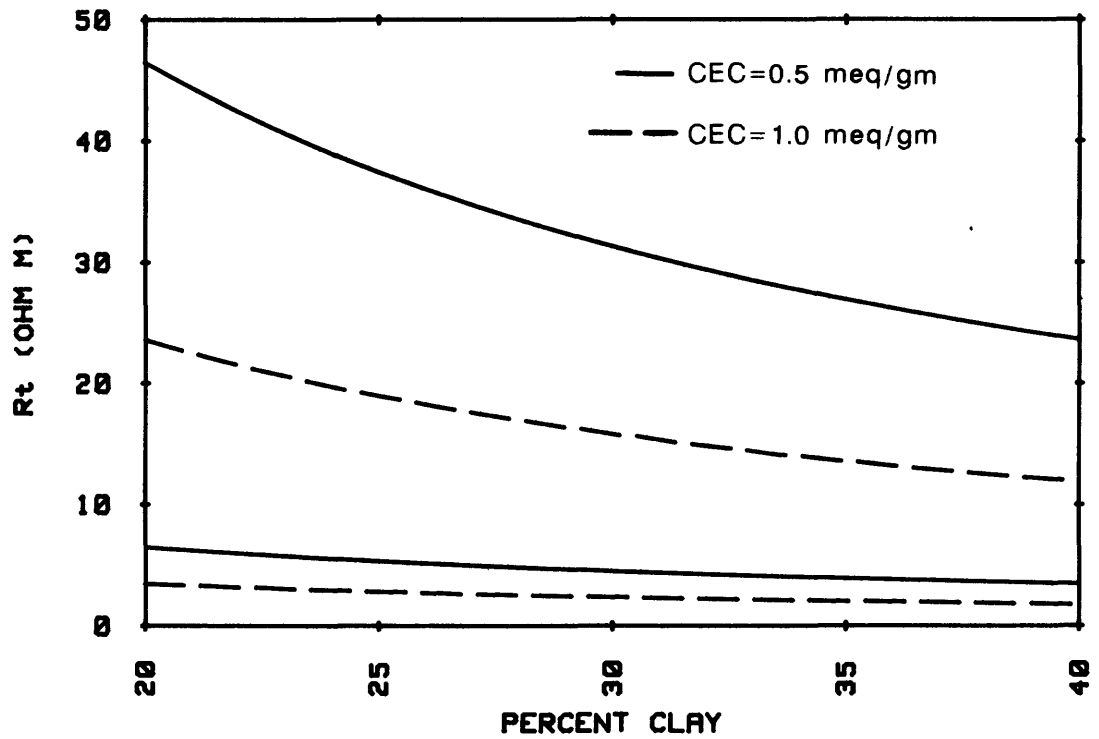
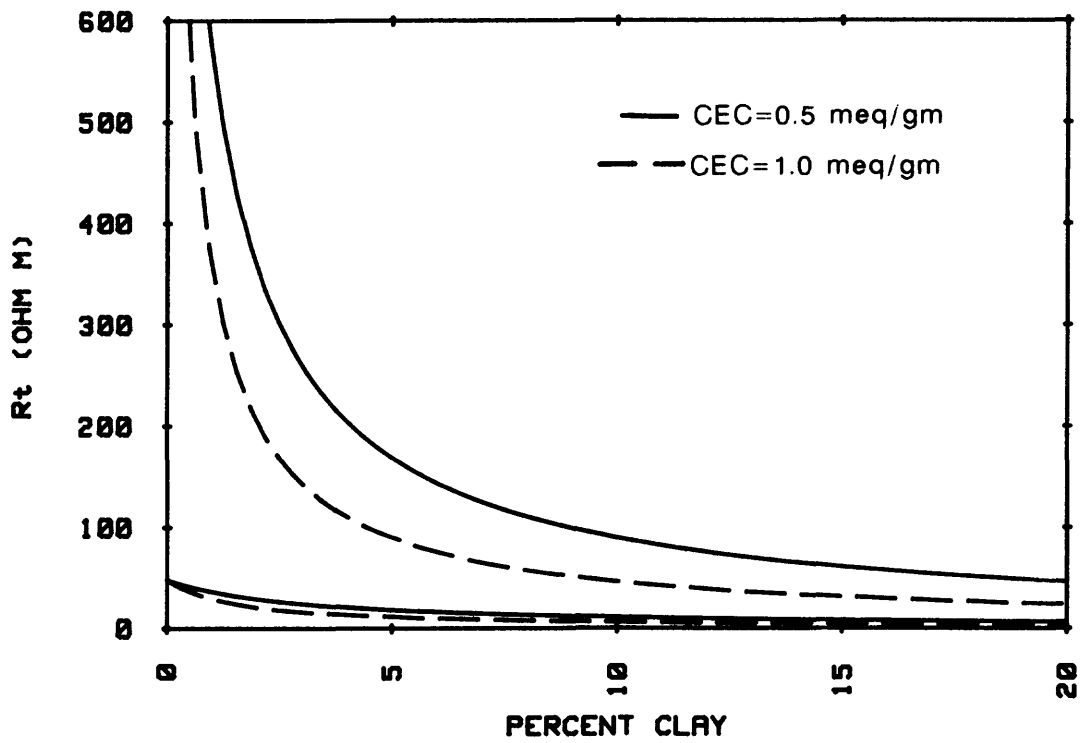


Figure 26.--Range of resistivities as a function of clay content predicted by WS model for tuffs in the unsaturated zone. Clay CECs of 0.5 and 1 meq/g are assumed. Cementation factor of $m = 2$ assumed in both cases.

With regard to the rule-of-thumb of a value of less than 20 ohm-meters suggesting the possibility of clay in relatively large amounts, and less than 10 ohm-meters suggesting one should have a definite concern with regard to the presence of clay, the data suggest that theoretical conditions exist where these guidelines are violated. However, the author has never observed the presence of large amounts of clay alteration over large volumes of rock in Rainier Mesa, or elsewhere at the NTS for that matter, where this rule of thumb is violated. This applies to wet clay and may suggest restrictions on the ranges shown on figures 25 and 26.

The oil-field approach to the saturation equations in clayey sands is based on a geologic model where oil has displaced water in the rock to some degree. In our analogy this oil is air, and this leads to some unanswered questions. Do tuffs with relatively high clay contents actually exist at the low end of our porosity range, or does the physical mechanism of extensive alteration require higher porosities? At what lower limit of clay content can the tuffs sustain partial saturation? The very nature of the adsorbing properties of clay suggests that at shallow depths of burial they must be saturated, even in the unsaturated zone, if clay contents reach certain limits. Consequently, the range in the resistivity possible on figures 25 and 26 may be optimistic.

Effect of Zeolites on Electrical Resistivity

The data in the foregoing sections leads to the conclusion that the resistivity in the tuffs within Rainier Mesa can almost totally be explained by the presence of ubiquitous amounts of clay, generally present in quantities less than 5 percent. If true, then one is concerned with the contribution of zeolites to resistivity given their high CEC (higher than any of the clays in table 4) and their large volume in the rock. Zeolites exhibit some of the highest CEC values of any group of minerals. Amphlett (1964, p. 44) reports the CEC of the feldspathoid cancrinite as over 10 meq/g, with other zeolites ranging from 2.3 to 9.2 meq/g. The zeolite of specific interest in Rainier Mesa, as may be seen in table 5, is clinoptilolite. The CEC of clinoptilolite is in the range of 1.7 to 2.3 meq/g and thus, theoretically, should dominate in the WS model in the tuffs.

Specific data concerning the CEC of zeolitic tuff samples obtained directly from Rainier Mesa were studied by J.W. Hasler and A.O Shepard (USGS, written commun., 1963). In an investigation of the possibility of utilizing waste rock from Rainier Mesa tunnels as a base material for encasing radioactive waste, they measured the CEC on a total of 27 tuff samples from the U12g and U12e tunnel dumps. The clinoptilolite content of these samples ranged from 25 to 50 percent. (Traces of clay were found in all the samples.) The average CEC determined for these samples was 80 meq/100 g with a range of 46 to 113 meq/100 g.

The use of this average CEC in the WS formulation results in predicted resistivities in the zeolitized tuff as shown on figure 27. These results were calculated from the same resistivity and density logs shown on figure 23. In addition to the resistivities that would be derived from the WS model for a 10 ohm-meter and a 35 ohm-meter pore water, the Q_v for the calculated porosities is also listed on the figure. A value of 2.0 was assumed for the cementation exponent.

The data indicate theoretical resistivities an order of magnitude lower than generally seen in the zeolitized zone in Rainier Mesa. Because errors in our estimations of R_w would be on the high side, the conclusion is that, unlike clay, the WS formulation does not yield even reasonable estimates of resistivity in this environment. The exchange capacity of these rocks is apparently not very accessible for electrical conduction in these fresh water environments.

This odd electrical resistivity behavior of zeolites has been observed by other investigators. Figure 28 is a summary of the results of several investigators in deriving WS-type plots for zeolites. Measurements of the conductivity of chabazite and mordenite (CEC of 89 meq/100 g and 69 meq/100 g; Q_v of 2.0 meq/cc and 2.3 meq/cc, respectively) by Wiley and Snoddy (1986) resulted in the conclusion that the effect of the CEC was considerably reduced from that predicted using a WS model. Both of their samples contained 4 to 5 percent illite and smectite in addition to the zeolite minerals. The latter were reported to comprise 86 to 90 percent of the samples tested.

Clavier and others (1977) report an even more surprising result for a sample of clinoptilolite. Their plot, also reproduced on figure 28, indicates the total absence of any additional ion contribution to rock conductivity over that normally predicted for an unaltered rock. This sample exhibited a CEC of 2.03 meq/g and Q_v of 2.8 meq/cc. They concluded that the compensating ions of this mineral have no mobility at room temperature.

Poor ion mobility within zeolites may also be inferred from the work of Starkey (1964), who measured the CEC of an NTS tuff sample. Using a sample containing one-third clinoptilolite crushed to 60 mesh, Starkey estimated it would take up to 4 years before the exchange capacity would reach a constant value, whereas, heating the sample reduced this to reasonable times. Soil containing montmorillonite reached a constant CEC value almost instantaneously.

Additional evidence for the relatively trivial contribution of clinoptilolite to surface conduction in fresh-water environments has been reported by Olhoeft (1986). Measuring the complex resistivity of clinoptilolite saturated with both distilled water and brine, he concluded that clinoptilolite saturated with distilled water chiefly exhibits volume conduction through the pores with little or no double-layer contribution. The brine saturated material, on the other hand, contributed a considerable ion-exchange component to the electrical conduction. The exchange capacity of

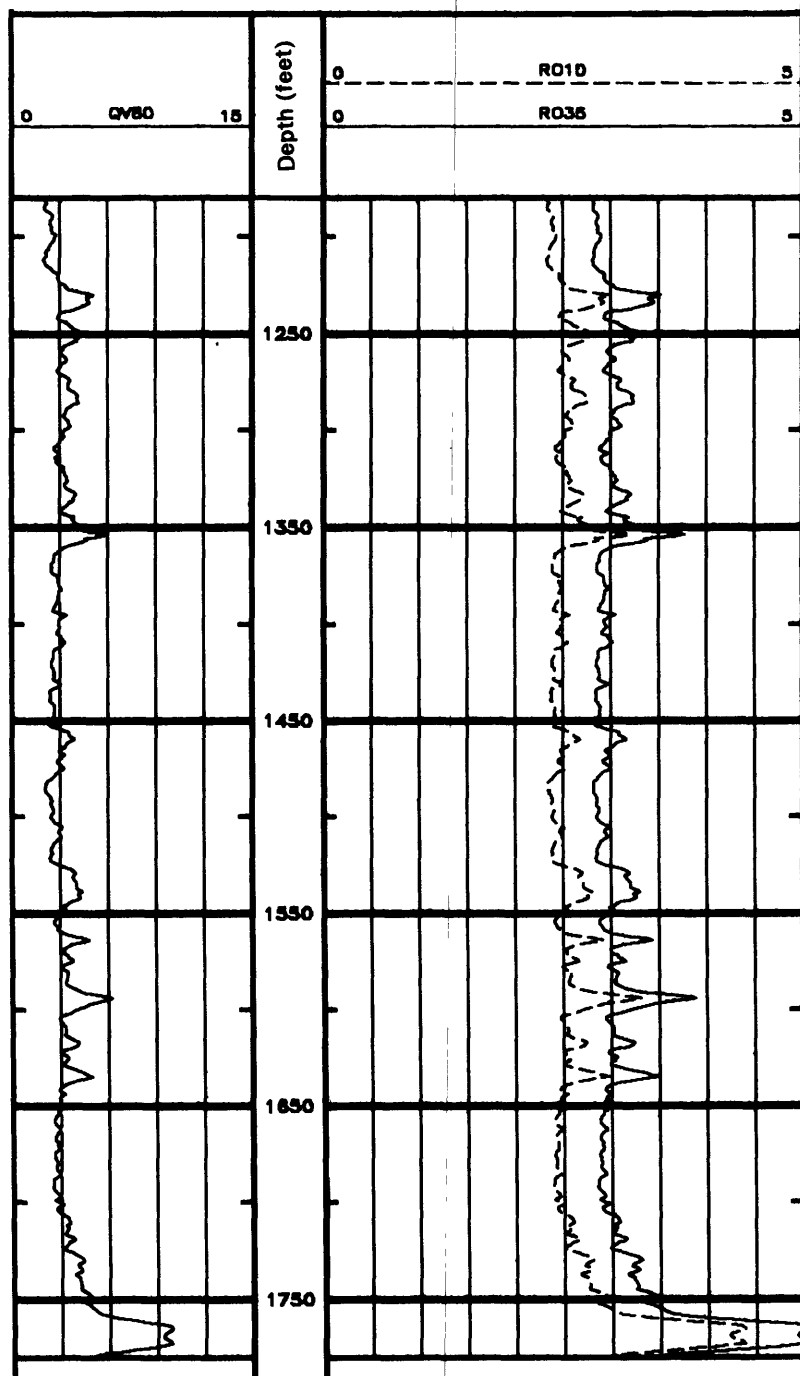


Figure 27.--Theoretical electric log resistivities and Qv which would be observed in the tunnel beds in e#3 for an average tuff CEC of 80 meq/100 g.

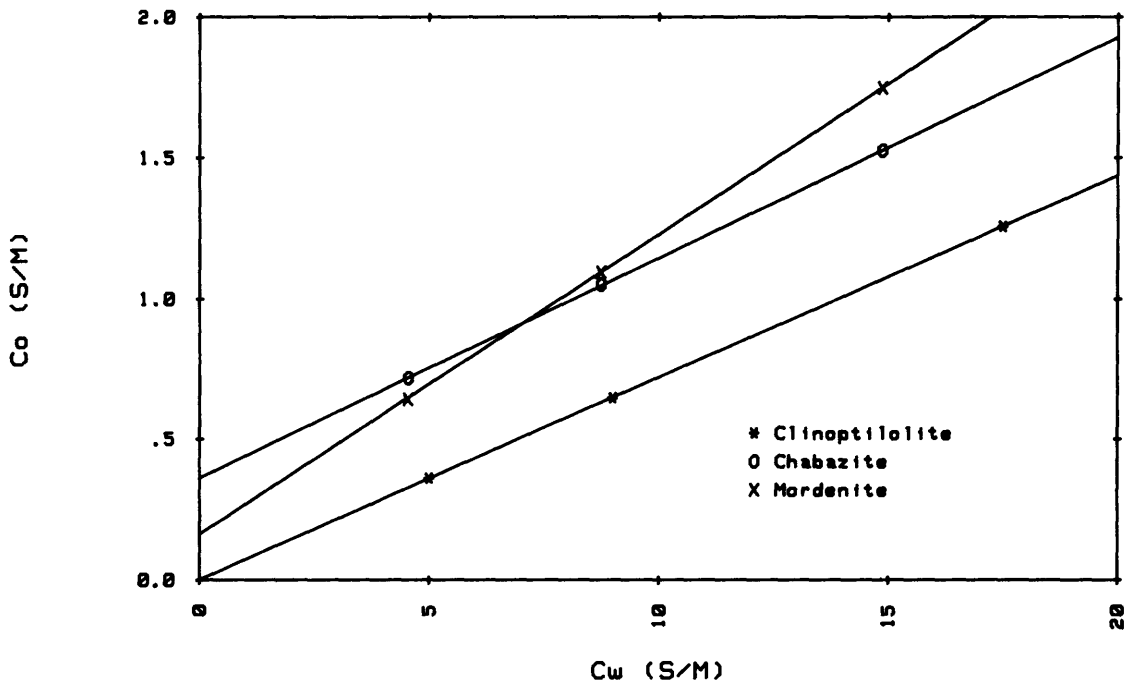


Figure 28.--Waxman-Smiths plots of conductivity of core versus saturant reported for three zeolites. Data modified from Wiley and Snoddy (1986), and Clavier and others (1977).

water saturated clinoptilolite was found to increase not only as a function of pore-water salinity, but also with temperature. Olhoeft estimated an order of magnitude increase in CEC in clinoptilolite saturated with distilled water from 23°C to 103°C. This observed increase in exchange capacity with temperature raises questions as to what mechanism Starkey was observing. More importantly, it suggests that a deep borehole in volcanic rocks saturated with fresh water might require a considerably different approach to electric log interpretation in zeolites of similar mineralogy near the top and bottom of the hole due to possible temperature effects on zeolite exchange capacity.

Citing the work of van Olphen (1977), Olhoeft concluded zeolites contain surfaces of constant potential, where an increase of ions in solution increases the ion-exchange capacity of the material. This is in opposition to montmorillonites which have surfaces of constant charge and exhibit CEC generally independent of pore-water salinity. These data confirm the complexity of the electrical behavior of zeolites, particularly if one is seeking a WS-type solution over a wide range of temperature and pore-water salinities.

These observed small contributions of zeolites to double-layer conductivity at low temperatures in relatively fresh water environments in comparison with their high exchange capacities appear to be supported by the resistivities observed on electric logs in Rainier Mesa. Thus, tuffs of high zeolite content appear to contribute little to double-layer conductivity in the temperature-water chemistry environment of Rainier Mesa. This contribution, at best, may be equivalent to trace amounts of clay (probably 5 percent or less). In the zeolitized zone this contribution would render the plots on figure 25 somewhat optimistic regarding clay content.

LABORATORY MEASUREMENTS

In order to directly examine the effect of mineralogy on tuff resistivity, a suite of 26 samples was selected consisting of vitric, clayey, and zeolitized tuff. The zeolitized tuffs were visually selected with the hope that clays in these samples would be minimal. The expense of attempting to obtain zeolitic samples with no clay (if, in fact, such a condition holds in the Rainier Mesa tuffs) by numerous X-ray diffraction studies was not considered economical. Two-terminal resistivity measurements were made of electrical resistivity at 1 kHz, using salt-saturated blotters and saturating the cores with fresh water. The measurement system has been described by Carroll and Muller (1973). The resistivity of the saturant was estimated at 20 ohm-meters. Because of the wide range in sample mineralogy the object of the study was to examine gross relationships between cation exchangeable minerals and observed resistivity at saturants near natural state in Rainier Mesa. The resistivity measurements are considered accurate to no better than 10 percent.

The results of X-ray analyses of these samples are listed in table 6. CEC, resistivity, and other pertinent physical properties are listed in table 7. The samples were ground to 200 mesh for the measurement of CEC.¹³ Adjacent samples cut from the same core were used for CEC and resistivity measurements. It is noteworthy that for those samples in table 7 which contain clay with only minor amounts of zeolite, the percent clay is approximately equivalent to the CEC, somewhat justifying the assumption of CEC = 1 meq/g used in the calculations concerning electric logs. We also note the presence of smectite in almost all these samples, as well as the high zeolite content in several of the samples. The samples with high clay content were purposely selected from locations known to be highly argillized.

Figure 29 depicts plots of the saturated electrical conductivity versus total clay content and the electrical conductivity versus total zeolite content. The zeolitic content indicates no relationship to conductivity and, in fact, tends to suggest a trend of higher conductivity with lower zeolite (CEC) content. The clay, on the other hand, indicates a distinct trend of increasing clay content with resistivity. As remarked previously, the WS formulation indicates that the clay content per se should bear no relationship to conductivity for a purely random distribution of clay content and porosity. However, because of the limited porosity range in these samples, such a relationship occurs. A plot of Q_v versus CEC (not shown) is also fairly linear as would be expected from equation 15 for these conditions.

¹³Sample grinding increases the measured exchange capacity, as demonstrated in clays by Campos and Hilchie (1980). Crushing is necessary because of low permeability. In low-porosity welded tuffs, this may be highly misleading because of the creation of excessive broken bonds. The general procedure is to crush cores for WS CEC measurements, although the initial investigations of Hill and Milburn (1950) relating CEC to resistivity utilized the full core sample, a technique which is not possible with high clay contents. Discrepancies have often been reported between Q_v obtained from CEC measurements and Q_v determined electrically from the C_x intercept of figure 17. Clavier and others (1984) attribute such discrepancies to charges fixed on desiccated surfaces and grain contacts yielding no electrical effect but appearing in CEC determinations. They prefer the use of electrically determined Q_v . In the presence of zeolites this approach may be the only one viable, if in fact, a WS formulation can be simply derived.

One should also be aware that montmorillonite is rather robust with regard to CEC determination, yielding approximately equivalent results for several techniques. Because processes and surface behavior are different, some of these techniques will not work with clinoptilolite, producing erroneously low CEC values. CEC and its determination in clinoptilolite have been reported by Ming and Dixon (1987), and Ming and Mumpton (1989). An updated technique for determination of clinoptilolite CEC is being published by Ming (D.W. Ming, NASA, written commun., 1989).

Table 6.--Results of X-ray diffraction analyses of tuff samples on which electrical resistivity measurements were made

[Analyses performed by S.J. Chipera, Los Alamos National Laboratory. Tr. = trace; leaders (--) indicate quantity not measured; see figure 2 for explanation of lithologic symbols]

Sample no.	Lithology	Hole and sample depth	Smectite	Mica	Hornblende	Quartz	Tridymite	Cristobalite	Clinoptilolite	Mordenite	Calcite	Opal	Feldspar	Glass	Hematite	Kaolinite
1	Densely welded tuff, Tm	e#3-232	--	Tr.	--	23	--	14	--	--	--	--	63	--	--	--
2	Densely welded tuff, Tmr	g.10#1-1345	Tr.	--	--	22	--	--	--	--	--	--	83	--	--	--
3	Zeolitized tuff, Tt4k	e#3-1230	7	--	--	Tr.	--	--	75	--	--	4	9	--	--	--
4	Zeolitized tuff, Tt4k	-1246	Tr.	Tr.	--	Tr.	--	--	80	--	--	15	10	--	--	--
5	Zeolitized tuff, Tt4k	-1247	2	--	--	Tr.	--	--	66	--	--	18	20	--	--	--
6	Zeolitized tuff, Tt4k	-1289	5	6	Tr.	3	--	7	32	--	--	--	50	--	--	--
7	Zeolitized tuff, Tt4j	-1339	10	--	--	5	--	--	39	--	--	15	27	--	--	--
8	Zeolitized tuff, Tt4j	-1360	11	Tr.	--	13	--	--	34	--	--	12	35	--	--	--
9	Zeolitized tuff, Tt4f	-1449	1	--	--	6	--	--	74	--	--	8	12	--	--	--
10	Zeolitized tuff, Tt4f	-1525	1	--	--	2	--	--	56	11	--	22	13	--	--	--
11	Zeolitized tuff, Tt3bc	-1684	Tr.	Tr.	--	3	--	--	67	15	--	10	10	--	--	--
12	Zeolitized tuff, Tt3bc	-1704	1	--	--	23	--	--	53	12	--	--	20	--	--	--
13	Clayey tuff, Tt3a	-1773	35	1	--	19	--	--	--	--	--	--	42	--	1	--
14	Zeolitized tuff, Tt3a	-1779	19	Tr.	--	21	--	2	29	--	--	--	25	--	--	5
15	Zeolitized tuff, Tt3bc	-1743	4	Tr.	--	36	--	--	10	--	--	--	56	--	--	--
18	Vitric tuff, Tp	e#1-471	6	--	--	--	--	--	--	--	--	--	5	89	--	--
19	Vitric tuff, Tp	-545	11	--	--	4	Tr.	Tr.	--	--	--	--	5	80	--	--
20	Vitric tuff, Tp	e#3-525	5	--	--	--	--	--	--	--	--	--	7	88	--	--
21	Vitric tuff, Tp	-543	7	--	--	--	--	--	--	--	--	--	8	85	--	--
22	Vitric tuff, Tp	-567	4	--	--	Tr.	--	--	--	--	--	--	7	87	--	--
23	Vitric tuff, Tp	t#2-582	29	--	--	1	--	--	--	--	--	--	41	21	Tr.	--
24	Clayey tuff, Tt4k	1no3ug7-40	64	Tr.	Tr.	Tr.	--	--	4	--	Tr.	6	22	--	--	--
25	Clayey tuff, Tt4k	1-82	33	1	Tr.	Tr.	--	--	21	--	1	18	28	--	--	--
16	Clayey tuff, Tt4k	1no5ex2-1211	22	Tr.	--	--	--	--	35	--	--	27	13	--	--	--
17	Clayey tuff, Tt4k	1no5ug8-140	53	1	--	Tr.	--	4	7	--	1	--	29	--	--	--
26	Clayey tuff, Tt4k	1-141	66	1	--	--	--	--	--	--	1	13	24	--	--	--

¹Horizontal drill hole, not shown on figure 1.

Table 7.--Physical properties, electrical resistivity, and cation exchange capacity of selected tuff samples

[Physical properties measured by G.L. Erickson, USGS; cation exchange capacities measured by Colorado State University Soil Testing Laboratory; leaders (--) indicate no measurement; see figure 2 for explanation of lithologic symbols]

Sample no.	Lithology	Location	Saturated density (g/cc)	Grain density (g/cc)	Porosity (g/cc)	Ro (ohm meters)	CEC (meq/100 g)	C/Z ¹	Qv
1	Densely welded tuff, Tma	e#3-232	2.43	2.56	8	331	2.7	0/0	0.79
2	Densely welded tuff, Tmr	9.10#1-1345	2.36	2.62	16	575	4.8	Tr/0	.66
3	Zeolitized tuff, Tt4k	e#3-1230	1.91	2.42	36	25	124.9	7/75	5.37
4	Zeolitized tuff, Tt4k	-1246	1.86	2.33	36	55	118.0	Tr/80	4.89
5	Zeolitized tuff, Tt4k	-1247	1.87	2.34	35	57	106.8	2/66	4.64
6	Zeolitized tuff, Tt4k	-1289	2.03	2.58	35	38	48.2	5/32	2.31
7	Zeolitized tuff, Tt4j	-1339	1.99	2.53	35	17	77.2	10/39	3.63
8	Zeolitized tuff, Tt4j	-1360	2.06	2.58	33	14	63.1	11/34	3.31
9	Zeolitized tuff, Tt4f	-1449	1.90	2.41	36	51	115.4	1/74	4.94
10	Zeolitized tuff, Tt4f	-1525	1.76	2.38	45	32	121.3	2 ¹ /56+11	3.53
11	Zeolitized tuff, Tt3bc	-1684	1.88	2.38	36	50	140.1	2 ¹ Tr/67+15	5.93
12	Zeolitized tuff, Tt3bc	-1704	1.93	2.46	36	95	110.4	2 ¹ /53+12	4.83
13	Clayey tuff, Tt3a	-1773	2.02	3 ² .73	41	7	36.6	35/0	1.44
14	Zeolitized tuff, Tt3a	-1779	2.25	2.53	18	13	66.0	4 ¹ 9/29	7.61
15	Zeolitized tuff, Tt3bc	-1743	2.07	2.52	29	67	27.3	4/10	1.68
18	Vitric tuff, Tp	e#1-471	1.65	2.27	49	81	6.8	6/0	.16
19	Vitric tuff, Tp	-545	1.92	2.41	34	30	13.4	11/0	.63
20	Vitric tuff, Tp	e#3-525	1.75	2.25	40	103	6.0	5/0	.20
21	Vitric tuff, Tp	-543	1.70	2.28	45	33	8.5	7/0	.24
22	Vitric tuff, Tp	-567	1.86	2.37	37	69	7.9	4/0	.31
23	Vitric tuff, Tp	t#2-582	1.81	2.57	48	27	25.4	29/0	.71
24	Clayey tuff, Tt4k	5 _{no3} ug7-40	--	--	--	64	64.9	64/4	--
25	Clayey tuff, Tt4k	5-82	1.93	2.64	43	5	55.8	33/21	1.95
16	Clayey tuff, Tt4k	5 _{no5} ex2-1211	1.94	2.52	38	7	60.7	22/35	2.50
17	Clayey tuff, Tt4k	5 _{no5} ug8-140	2.00	2.62	39	5	51.7	53/7	2.12
26	Clayey tuff, Tt4k	5-141	1.97	2.72	44	2	66.0	66/0	2.28

¹C=clay (smectite), Z=zeolite (clinoptilolite) as listed in Table 6.

²Zeolites=clinoptilolite plus mordenite.

³Sample disaggregated on saturation. Grain density determined by powder grain method.

⁴Five percent kaolinite not included with clay.

⁵Horizontal hole, not shown on figure 1.

⁶Sample disaggregated on saturation. Resistivity measured on paste created by grinding sample with mortar and pestle.

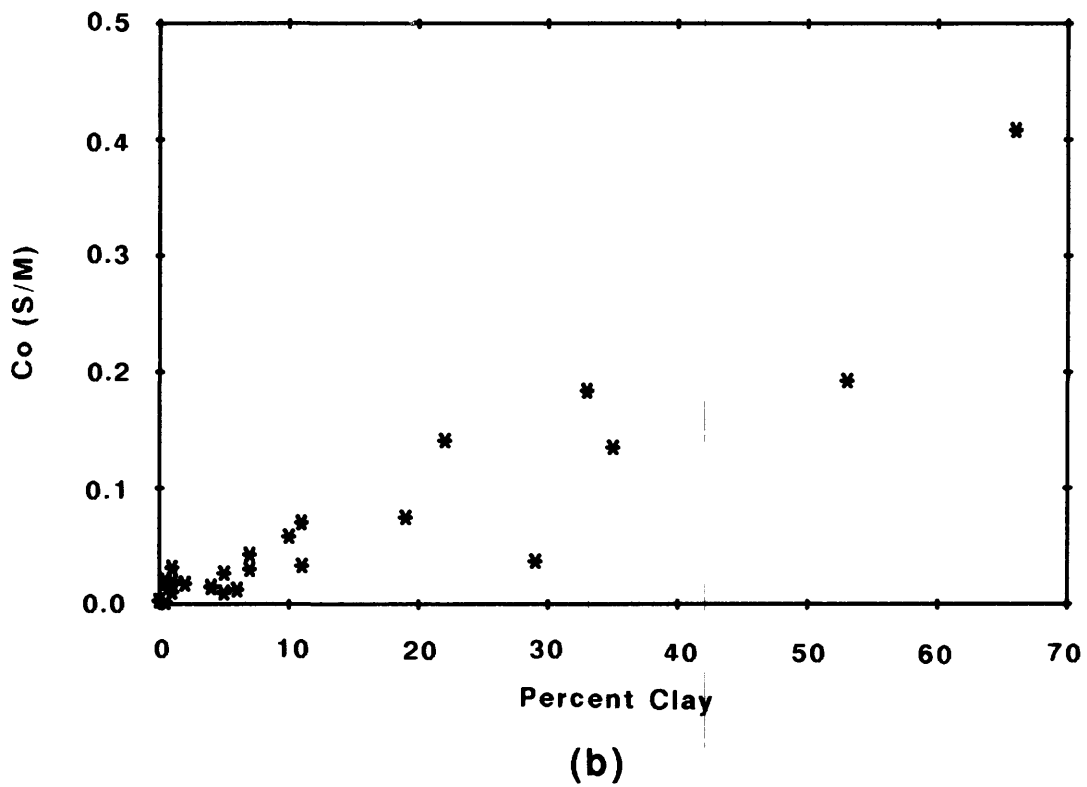
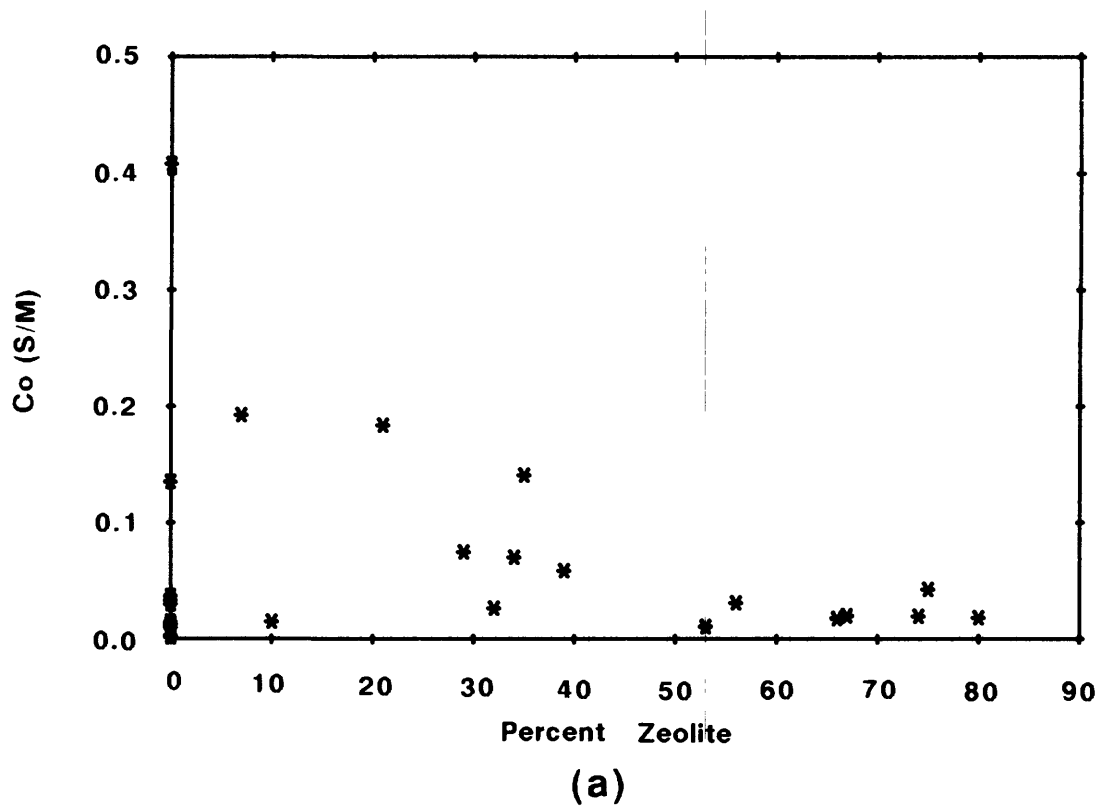


Figure 29.--Conductivity of selected tuff samples from Rainier Mesa area versus (a) zeolite content and (b) clay content.

As a final exercise, the conductivities of all the samples were plotted against the conductivities that would be predicted by the WS equation. The Q_v listed in table 7 was used along with a value of R_w of 20 ohm-meters and a cementation exponent of two. These data are shown on figure 30a. This plot obviously indicates no relationship between theoretical and measured values. On figure 30b only the percent clay in all the samples was used in the WS equation assuming a CEC of 1 meq/g for the clay. This plot shows a considerably improved agreement with the WS model.

The foregoing again lead to the conclusion that the dominant mechanism controlling surface conductivity in the Rainier Mesa tuffs is the clay component of the mineralogy. The high CEC of the zeolites appears to contribute little to conductivity in the Rainier Mesa environment. The exact contribution of zeolites in large concentration in the tuffs, if any, needs to be further investigated.

In closing this section, note should be taken that there are several mechanisms which we have not addressed concerning conductivity in these zeolitic rocks, chiefly because of lack of knowledge. The pore size distribution is obviously of importance, particularly the manner in which the clay is distributed and whether in trace amounts the counterions in the clay are freely mobile under an electric field. In volcanic glass, both clay minerals and zeolites can form depending on constituents and activities of the pore water. What results with regard to ionic mobility within pore channels, when the clay is formed in small amounts within large zeolitic masses, is unknown. Clay also appears to form either uniformly in the matrix or in isolated zones as altered pumice thus offering different distributions for electrical conduction. The accessibility of ions for electrical conduction within zeolitized pore channels and the variation of these pore channel openings is also an unknown factor. The large exchange capacities of the zeolites may differ in their contribution, however small, to double-layer effects depending on the compaction and alteration history. In the presence of moderate amounts of wet clay, i.e., greater than about 10 to 20 percent, these appear to be second order effects. To what extent they are second order effects in the presence of trace amounts of clay in the zeolitized zone needs further investigation.

OTHER ELECTRICAL PROPERTIES OBTAINED IN LOGGING

There are several additional electrical properties other than resistivity obtainable from geophysical logging tools. These logs have not been utilized or studied in detail in Rainier Mesa, and the properties affecting their behavior in the volcanic rocks are not well understood. As in the case of electric logs in general, the key to understanding the utility of most of these logs lies in laboratory study of core mineralogy and properties. These logs are magnetic susceptibility, induced polarization, spontaneous potential and dielectric constant. Logs recorded by the USGS measuring two of these properties, induced polarization and magnetic susceptibility, are shown on

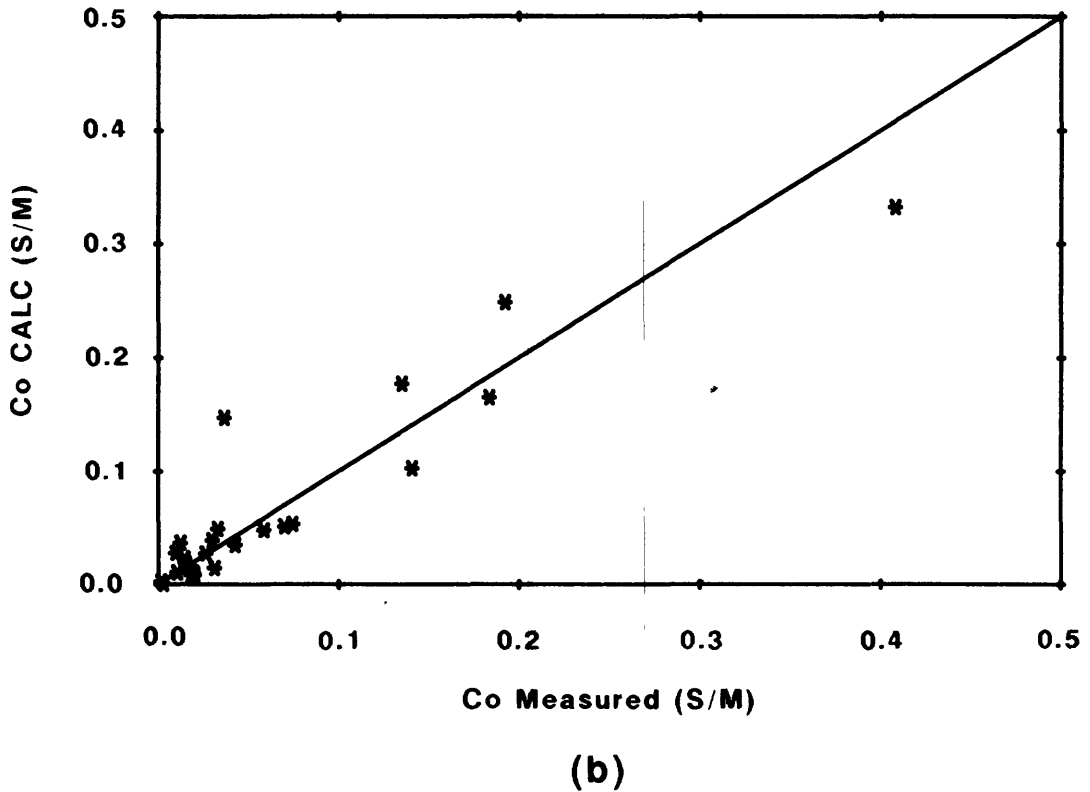
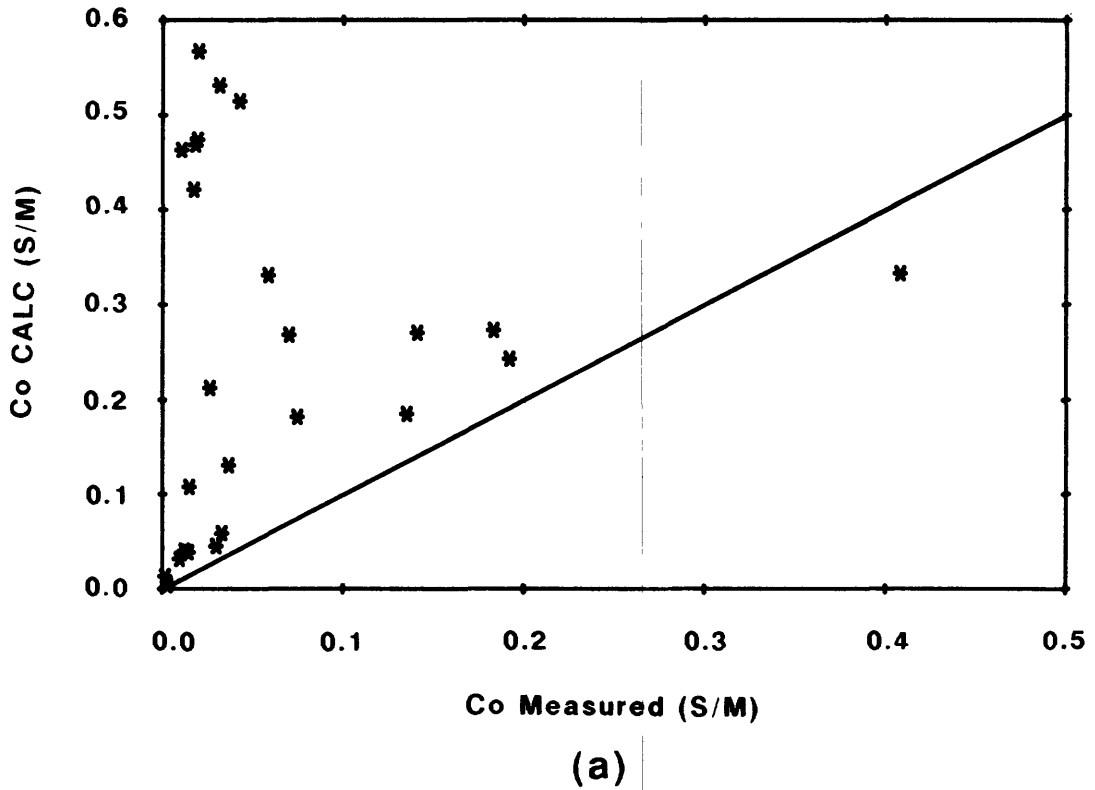


Figure 30.--Calculated WS conductivity of selected tuff samples from Rainier Mesa area versus measured conductivity for (a) all samples using measured Q_v and (b) samples using only the clay component with assumed CEC = 1 meq/g.

figure 31 (in pocket). A 4-in. normal log is also shown for comparison with the 16-in. normal usually recorded. The 4-in. normal does not indicate that any dramatic increase in bed resolution is obtained with the smaller spacing.

Magnetic Susceptibility

The USGS ran an experimental magnetic susceptibility log in the e#3 hole in 1974 (fig. 31). The log was run to determine its utility as a correlation tool and to examine the possibility of differentiating reworked ash-fall tuffs from ash-fall tuffs. The log depth was limited by the available cable on the logging truck.

Magnetic susceptibility logs historically evolved as tools for mineral exploration and have only a secondary role as correlation devices. They have received little use in petroleum exploration due to the general absence of magnetic materials in sedimentary environments of interest to oil exploration. In igneous, metamorphic, or volcanic environments their utility as correlation logs is probably greater than other tools at some horizons. The anomaly centered at 730 ft on figure 31 is one such example. The relatively higher response in this zone is due to a biotite-rich zone in the Paintbrush Tuff which is also found on magnetometer logs obtained in Yucca Flat. This horizon is not particularly notable on other logs. Other anomalous zones appear to be present, notably in the vicinity of the welded Grouse Canyon Tuff. The magnetic susceptibility does not appear to relate to the top of zeolitization.

The continuity and cause of the several anomalies remain to be investigated as does the general utility of this log. The limited data suggest it would be worthwhile to obtain this log in several boreholes throughout the complete depth of the volcanic section in Rainier Mesa.

The log depicted in figure 31 was obtained with a Simplec tool containing the coil, inductance bridge, driver oscillator, and detector all mounted within the probe. The probe also contained a heating unit to reduce thermal effects in addition to a relative calibration unit. A more sophisticated version of this unit, with a sensitivity of the order of 10^{-6} cgs units, has been reported by Scott and others (1981).

Some attempts are presently underway to combine magnetic susceptibility and magnetometer logs to roughly define the magnitude and direction of the remanent vector as well as the total field in connection with investigations on Yucca Mountain at the NTS. Such an attempt, if successful, could add valuable additional data concerning structure and stratigraphy in the volcanic section from downhole measurements. A combination total magnetic field-susceptibility log for use in slim holes has been reported by Balch and others (1987). Slim-hole induction logs capable of measuring susceptibility have been reported from several sources (Bristow, 1987).

The magnitude of susceptibility in the volcanic rocks is of interest with regard to the application of other geophysical logs such as dielectric constant and nuclear magnetic resonance. Available data indicate that the susceptibility of the volcanic section generally contributes less than 1 percent to increasing the overall magnetic permeability of the tuff above the free space value. A 1 percent increase in magnetic permeability would require

magnetic susceptibilities on the order of 8×10^{-4} cgs units. Emerick compiled ranges of susceptibility measured on samples from various lithologic units in Rainier Mesa (W.L. Emerick, USGS, written commun., 1966) These data are reproduced in table 8. Additional data concerning magnetic properties of NTS rocks have been reported by Bath (1968).

Table 8.--Magnetic susceptibility of samples from units in Rainier Mesa

Lithology ¹	Number of samples	Range (cgs x 10 ⁻⁴)	Mean (cgs x 10 ⁻⁴)
Tmr (welded)	20	2.04-11.26	4.69
(nonwelded)	13	0.75- 5.91	2.38
Tp (vitric)	55	0.36-10.02	1.71
Tp (zeolitized)	20	-0.03-27.47	2.68
Tbg (welded)	12	0.33-24.11	7.61
Tt5 (vitric)	7	0.22- 6.53	2.37
Tt4 (zeolitized)	65	0.04-18.73	3.56
Tt3 (zeolitized)	25	0.37- 5.68	1.90
Tt2 (zeolitized)	33	0.06- 3.99	1.49
Welded tuff	32	0.22-24.11	5.79
Vitric tuff	75	0.36-10.02	1.89
Zeolitized tuff	143	-0.03-27.47	2.67

¹See figure 2 for explanation of symbols.

Induced Polarization

Induced polarization (IP) logs were run experimentally by the USGS in n#6 and e#3. The log from e#3 is reproduced on figure 31. Induced polarization results from capacitive effects in rocks due to either metallic minerals or clays and other minerals exhibiting cation exchange capacity. Metallic minerals capable of producing IP effects have not been reported in the rocks at Rainier Mesa, however, metallic minerals such as disseminated pyrite have been found elsewhere at NTS. The utility of this measurement in Rainier Mesa probably lies in the extent to which it may be a correlation tool yielding lithologic data not available from other logs, and the extent to which it can provide quantitative or semi-quantitative information on clay and zeolite content.

IP measurement techniques utilize either an observed change in resistivity at two frequencies, an observed voltage decay of a square wave induced in the formation, or a phase shift between current and voltage. Principles for the various measurement techniques may be found in Sumner (1976). The log on figure 31 was obtained using a constant-current source (maximum current 25 ma) consisting of a 10 Hz modified square wave. The integrated voltage obtained over a 9 ms interval, 5 ms after current shutoff, was used to obtain the IP response.

The log shown on figure 31, like the magnetic susceptibility log, requires considerably more application in holes in Rainier Mesa, or more detailed mineralogic and laboratory tests on samples, before its utility can be established. The IP log, like all resistivity logs, also requires corrections for the borehole mud resistivity. Departure curves for this type of correction have been discussed by Tripp and Klein (1988) and Freedman and Vogiatzis (1986).

The induced polarization log, at one time almost entirely within the province of mineral exploration, has gained increasing interest in petroleum environments because of its relationship to Q_v in shaly sands. Vinegar and Waxman (1984) measured the IP response of several shaly sands ($Q_v = .07$ to $.95$) and found a linear relationship between the quadrature conductivity and Q_v , with quadrature conductivities and phase angles nearly independent of frequency. They also develop the interesting theory that at high salinities, or in clean sands where BQ_v in the WS equation is not significant, saturation is a function of the ratio of the phase angles at saturation and partial saturation. The phase angles measured by Vinegar and Waxman were quite small, typically less than 10 mrad, but approaching 20 mrad at lower salinities (0.01M), an advantage in the fresh water environment of Rainier Mesa. By contrast, phase shifts in metallic ore samples as high as 350 mrad have been measured (Zonge and others, 1972).

It is possible that a systematic study of IP may provide additional techniques to quantify the electrical model in the tuffs. IP in clayey tuffs, however, has limitations with regard to resolving clay content. When clay becomes too concentrated in the rock, the IP response becomes negligible. This has been observed by several investigators and is attributed to the need for clay-free zones in the pores sufficient to develop electric gradients or sufficiently long relaxation times. Where this limit of clay content exists is not precisely defined, however, Vinegar and Waxman report quantifiable IP effects for their data for Q_v less than 1.0 meq/cc and porosities less than 12 percent. This is somewhat analogous to a similar lack of sensitivity of electrical resistivity at high clay contents.

The extent to which the IP effects recorded on figure 31 are due to the presence of zeolites in the tuff is unknown. Nelson and others (1982) report phase shifts of 7 to 18 mrad for conglomerate samples containing thin coatings of heulandite and clinoptilolite. The CEC of these samples was over an order of magnitude lower than the zeolites in the tunnel beds in Rainier Mesa, being less than 5 meq/100 g. Their samples also contained montmorillonite, and the authors were unable to separate the relative effects of the two minerals on the IP response. They believed, however, that more than half of the IP response of 20 mrad observed in surface measurements was due to the zeolites. Wiley and Snoddy (1986), in their studies of the complex resistivities of mordenite and chabazite, recorded small phase shifts at 30 Hz similar to those measured by Vinegar and Waxman on clayey sands. As previously noted, the Wiley-Snoddy zeolite samples also contained 4 to 5 percent clay. The data reported by Olhoeft (1986) for pure clinoptilolite saturated with distilled water, although not indicating any significant contribution due to exchange capacity to the resistivity model, does indicate phase shifts near 20 mrad at 30 Hz. These data again point to significant gaps in our knowledge of the electrical behavior of zeolites.

Spontaneous Potential

In petroleum logging the spontaneous potential or SP log is used to determine the resistivity of saline pore water. SP log interpretation in drill holes at NTS is complicated by many factors. Logs are not obtained over much of the geologic section chiefly because lost circulation does not allow a mud column to be maintained at high levels in the hole. Most drilling techniques elsewhere at NTS also do not result in a mud column over any significant length of the hole. Where lost circulation results, as it does in much of the Rainier Mesa drilling, control of the mud chemistry is also difficult. Thus, if the SP were amenable to interpretation in a controlled laboratory environment, the results might be difficult to implement in a real drilling environment. A further complication is the chemistry of the pore water (table 2). Most models relating SP response to rock and pore-water characteristics involve the use of NaCl solutions, generally at large concentrations. The presence of fresh water with Ca and Mg ions complicates the reduction of the data. The extremely low interstitial permeability in portions of the zeolitized tuff may also be a complicating factor.

The SP has several potential capabilities that render it possibly worthy of further investigation. Aside from the theoretical possibility of providing R_w , a highly significant and elusive parameter in the zeolitized tuffs, it has been found to be a measure of clay (Q_v) in shaly sands (Smits, 1968). Thomas (1976) also related Q_v to SP and fielded a system to measure membrane potential on cores at the well site in order to determine Q_v directly without CEC measurements.

The interpretation of the SP in a normal saline environment can be quite involved. Details have been reported by Doll (1949) and Gondouin and others (1957). In order to address the possible applicability to the Rainier Mesa area, a simplified version of the normal oil-field response is shown on figure 32. The response (mv) of the SP at 25 °C is obtained from,

$$SP = -71 \log A_1/A_2 \quad (20)$$

where A_1 is a function of the ion content of the borehole mud filtrate and A_2 is a function of the ion content of the formation water. This equation is derived assuming that one part of the observed potential is developed between the mud filtrate and the formation waters as ions migrate across the formation boundary of a clean sandstone in an attempt to equalize concentration differences. This liquid junction potential is shown on figure 32 for formation waters more saline than the mud filtrate, the normal condition in petroleum logging. A second potential arises across the junction of an adjacent shale and the mud filtrate. The shale is assumed to be a perfect clay, acting as an ion selective membrane yielding zero anion mobility. Thus, only the cations carry charge across the formation-mud column boundary. For salt concentrations less than 1N, activities, concentrations, or resistivities may be used for the right side of equation 20. Thus, ideally the deflection opposite the clean sand coupled with knowledge of mud filtrate resistivity allows R_w to be calculated.

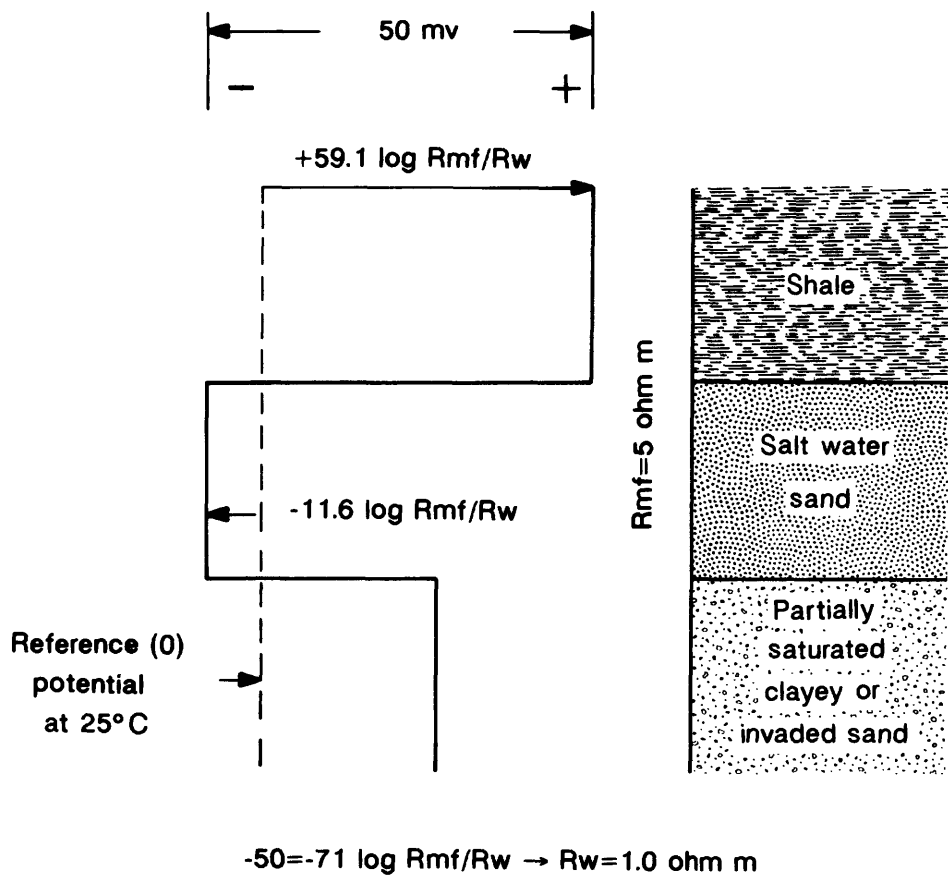


Figure 32.--Ideal SP response in sand-clay sequence.

Sands which are clayey, i.e., which are not perfect shales, yield SP deflections which are understandably somewhere between the two extremes. As previously mentioned, SP deflections in this case have been related to volume clay content, Q_v . However, partially saturated clean sands also show SP behavior similar to clayey sands with a reduction in SP from saturated values (Ortiz and others, 1972). Invasion also reduces the SP effect (Doll, 1949).

Figure 33 illustrates an SP log somewhat typical of those obtained in Rainier Mesa when bentonite drilling muds are used. The log indicates generally little activity in the unsaturated zone above the top of zeolitization (when a mud column can be maintained at that height) with increasing activity in the zone of zeolitization. Positive deflections occur opposite low resistivity zones believed to be clay bearing. These are the Tbt/3A boundary, Tt3d, and opposite the clay alteration at the tuff/quartzite boundary. The Tbt/3A horizon is almost universally a shale baseline of a sort on the Rainier Mesa logs, however, this baseline tends to drift toward more positive values deeper in the section.

Keller (1959b) measured the SP on 156 cores from this hole using the core as a membrane to separate salt concentrations of ten to one. The cores were from tunnel beds 3, 4, and 5, and the Paintbrush Tuff. All the core exhibited some degree of ion selectivity, passing cations but not anions.

One apparently contradictory note is the positive SP deflections on figure 33, similar to those on figure 32, opposite what we take to be clay zones. Figure 32, however, is based on the premise of saline formation waters less resistive than the mud filtrate. If our derived resistivity of 35 ohm-meters is representative of the tuff pore water it is difficult to see how mud resistivities greater than this can be maintained in drilling, and thus the SP should be reversed from that shown. This contradiction may be due to the chemistry of the Rainier Mesa pore waters. In fresh waters, the presence of Ca and Mg ions have a large effect on SP (Gondouin and others, 1957; Alger, 1966; Alger and Harrison, 1987). The effective activities of Ca and Mg on the SP response can exceed that of Na by over an order of magnitude at low concentrations. The term in equation 20 representing formation waters must be modified to take this into account. It is often assumed that the mud filtrate resistivity may be taken to be chiefly NaCl, the clay in the mud adsorbing the divalent cations. In this case the activities are used in the right-hand term of equation 20, and the equation becomes,

$$SP = -71 \log A_w/A_{mf} \quad (21)$$

where A_w is the activity of the pore water and is given by the sum of the activity of Na and the square root of the sum of the activities of Mg and Ca. The activity of the mud filtrate, A_{mf} , is the activity of the Na in the mud. Charts are available to convert activity to resistivity for Na, and parts per million to activity for Na, Ca, and Mg (Gondouin and others, 1957;

Alger, 1966). We are interested in what values of mud resistivity are required to make the ratio of activities in equation 21 positive (and thus give the negative SP deflections opposite less clayey zones as in fig. 32) and whether these values are reasonable. Averaging the Na, Ca, and Mg cations listed in table 2 for the pore water in t#3, yields approximately 40, 11, and 3 ppm, respectively. Using charts provided by Alger (1966) the activities of Na (0.0017 g-ion/L) and the effective activities of Ca and Mg (0.017 g-ion/L) yields,

$$SP = -71 \log 0.019/A_{mf} \quad (22)$$

Charts relating the resistivity of NaCl to activity indicate a value for R_{mf} of about 3.5 ohm-meters (3.9 ohm-meters at tunnel-level temperature of 20 °C) is equivalent to an activity of 0.019 g-ion/L. Thus, a mud filtrate resistivity of greater than 3.5 ohm-meters would be sufficient to yield positive SP deflections opposite clay zones similar to polarities normally observed in logging practice. As previously mentioned, the mud resistivity recorded on logs from Rainier Mesa ranges from 1.4 to 29 ohm-meters (20 °C). A histogram of mud resistivity distribution is shown on figure 34. Because these samples were all obtained from the mud tank rather than the hole, their applicability is uncertain, but the general presence of mud filtrate resistivities in excess of 3.5 ohm-meters is not difficult to envision.

On rare occasions (e#3) reversed SP has been noted on SP logs obtained in Rainier Mesa. Insufficient data on mud properties do not allow conclusions to be drawn as to cause. It should also be noted that the presence of clean tuff and an adjacent clay layer which behaves as a nearly perfect ion selective membrane, such as depicted on figure 32, does not exist in the volcanic rocks. If quantitative interpretation of the SP log is to be attempted, the use of some marker horizon such as the Tbt/3A contact may be suitable. If sufficient pore-water samples could be obtained, an approach such as used by Evers and Iyer (1975) might be attempted. Neglecting equation 21, the solution of which actually requires a prior knowledge of water chemistry in the presence of divalent cations, Evers and Iyer developed relationships between R_w calculated from SP data, and true R_w from water samples for various lithologies in Wyoming oil basins. These relationships were then used to predict R_w from the SP log in other holes.

Dielectric Constant

No dielectric constant logs have been run in the Rainier Mesa area because the 4-in. hole sizes generally used in the exploration program are not compatible with sonde diameters. The dielectric constant, or electromagnetic propagation tool, is theoretically a water-content tool and ideally yields total-water content as do neutron tools. The extent that it may be superior in this regard compared to the use of other tools in the volcanic rocks has yet to be demonstrated. Dielectric constant tools, unlike the electric log, are relatively high-frequency devices, ranging from 10 MHz to gigahertz frequencies. These high frequencies are required in order to obtain a sufficient phase shift to measure the in-phase and quadrature components of the electric field needed to derive the dielectric constant. The log is presented as both a resistivity and a dielectric constant, and the basis for

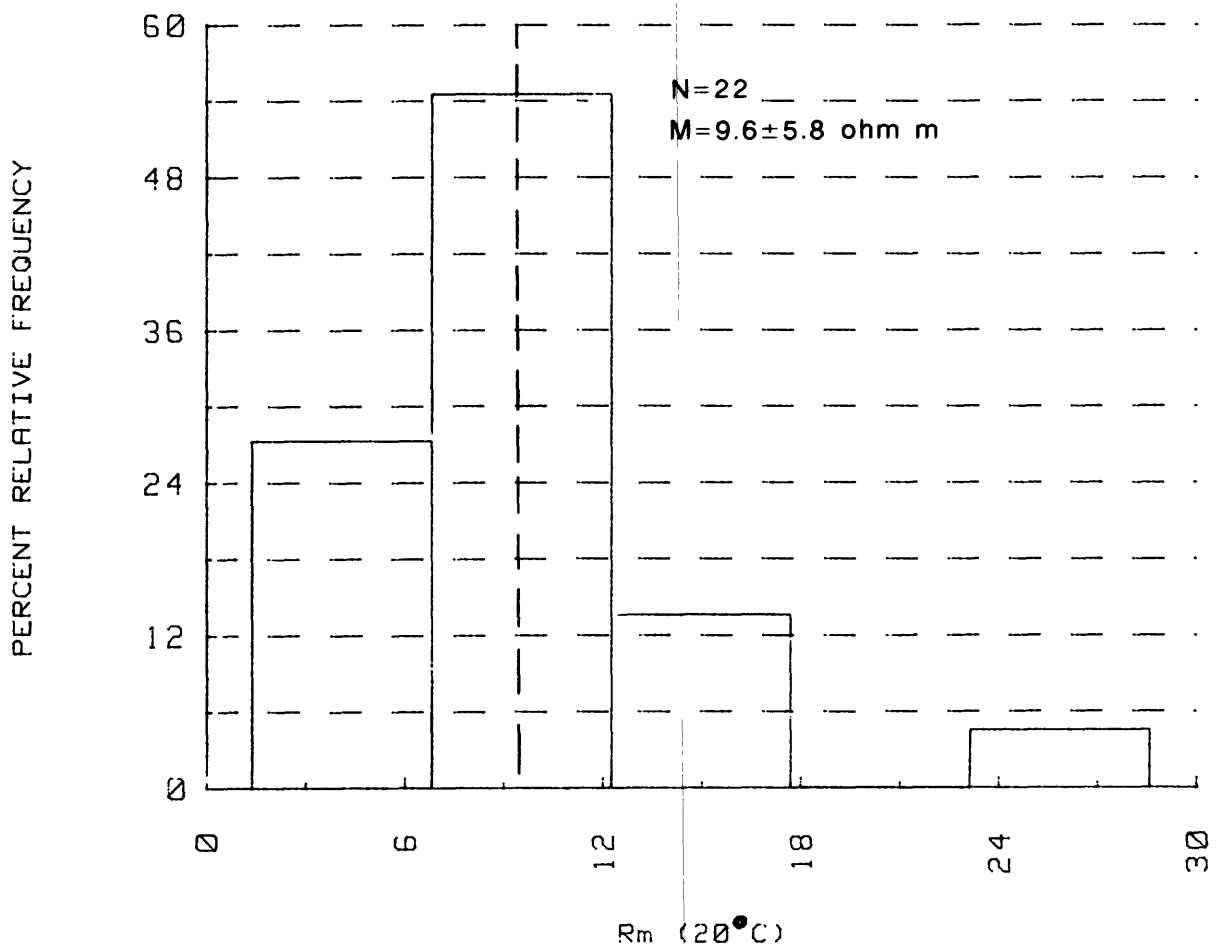


Figure 34.--Mud resistivities recorded from pit or tank samples obtained on Rainier Mesa. Number of samples (N), mean (M), and one standard deviation are listed.

interpretation is the large difference between the relative dielectric constant of water (close to 80 for the Rainier Mesa environment) and the small dielectric constant of the matrix of most lithologies (less than 10). The dielectric constant tool's application as a porosity or water-content device utilizes some type of mixing formula which, in its simplest form, is similar to the Wylie time-average formula relating sonic travel time and porosity. In this form the saturated porosity is obtained from

$$t_{po} = (1-\phi) t_{pm} + (\phi) t_{pw} \quad (23)$$

where ϕ is porosity, t_{po} is observed reciprocal propagation velocity or propagation time (in ns/m), t_{pm} is matrix travel time, and t_{pw} is the travel time in the fluid. Propagation time in fresh water is about 30 ns/m and for sandstone about 7 ns/m. The use of relative dielectric constant (k) in equation 22 arises from the equation of propagation time of a lossless electromagnetic wave in a material as $\sqrt{\mu\epsilon}$. The relative dielectric constant, k , is the ratio of the permittivity of a material to that of free space, ϵ/ϵ_0 . Because the magnetic permeability (μ) of the rocks in the Rainier Mesa area generally differs from the free space value by less than 1 percent, the values for respective propagation times in equation 22 can be replaced by the square root of the relative dielectric constants of rock matrix and water. The relative dielectric constant of fresh water is about 78, and that of sandstone (which can often be taken as a first approximation to volcanic rock) is about 5. Thus, the theoretical sensitivity of this tool to water content should be good. The ratio of matrix to water constants of about 4 to 1 is nearly the same as the matrix travel-time terms in the Wylie time-average equation for determining water content from the sonic log. The dielectric constant approach, however, is theoretically not subject to the formation restraints on saturation, overburden pressure, and mineralogy in its application as is the sonic log.

Some forms of the dielectric constant sonde can be run in a dry hole. Thus, another possible advantage of this tool is the ability to obtain rock resistivity at the higher ranges in the unsaturated zone where the induction log is not useful. At the higher resistivities seen in Rainier Mesa rocks, resistivity dispersion, i.e., the decrease in resistivity and dielectric constant with frequency, should be more pronounced than that encountered in oil-field lithologies. Thus, one should anticipate that the recorded resistivity may be noticeably less than that indicated by the standard electric logging tools. If one wishes to use this resistivity in any water content calculation, precautions should be observed to insure that parameters such as formation factor and resistivity index are appropriately normalized. Dispersion curves for samples from various NTS lithologies have been published by Eberle and Bigelow (1973). Examples appropriate to the Rainier Mesa area are shown on figures 35 and 36. The tuff samples on figure 35 (all saturated) were obtained in a horizontal hole in the zeolitized tuff in U16a.06 tunnel. The porosities range from 28 to 30 percent, the low end of the range appropriate to the tunnel beds in Rainier Mesa. Dispersion curves for two water contents are also shown for a welded sample of the Tub Spring Member (fig. 36). Examples for other rock types may be found in the cited reference.

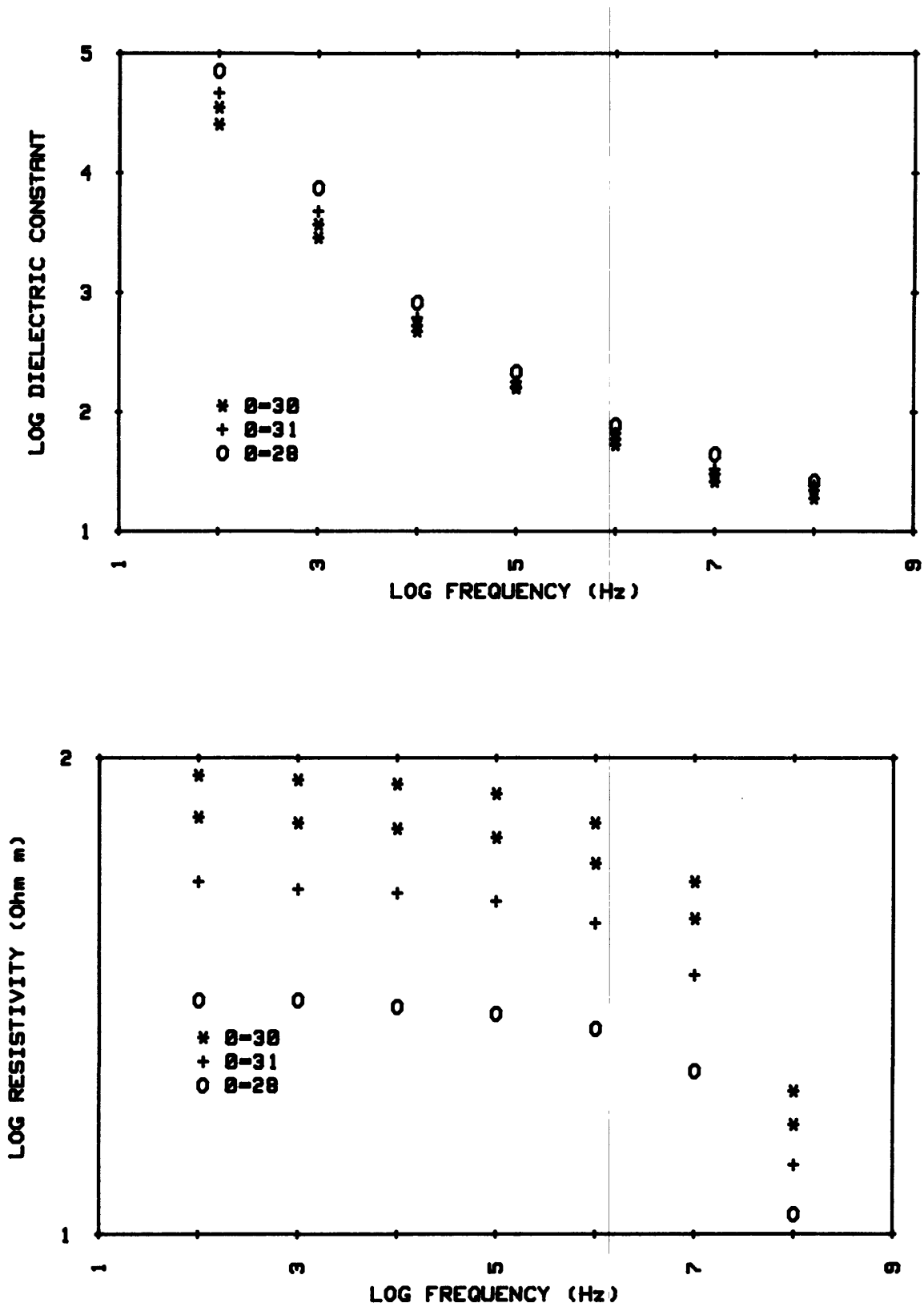


Figure 35.--Dielectric constant and resistivity as a function of frequency for four saturated zeolitized tuff samples. "0" indicates porosity of samples. (After Eberle and Bigelow, 1973).

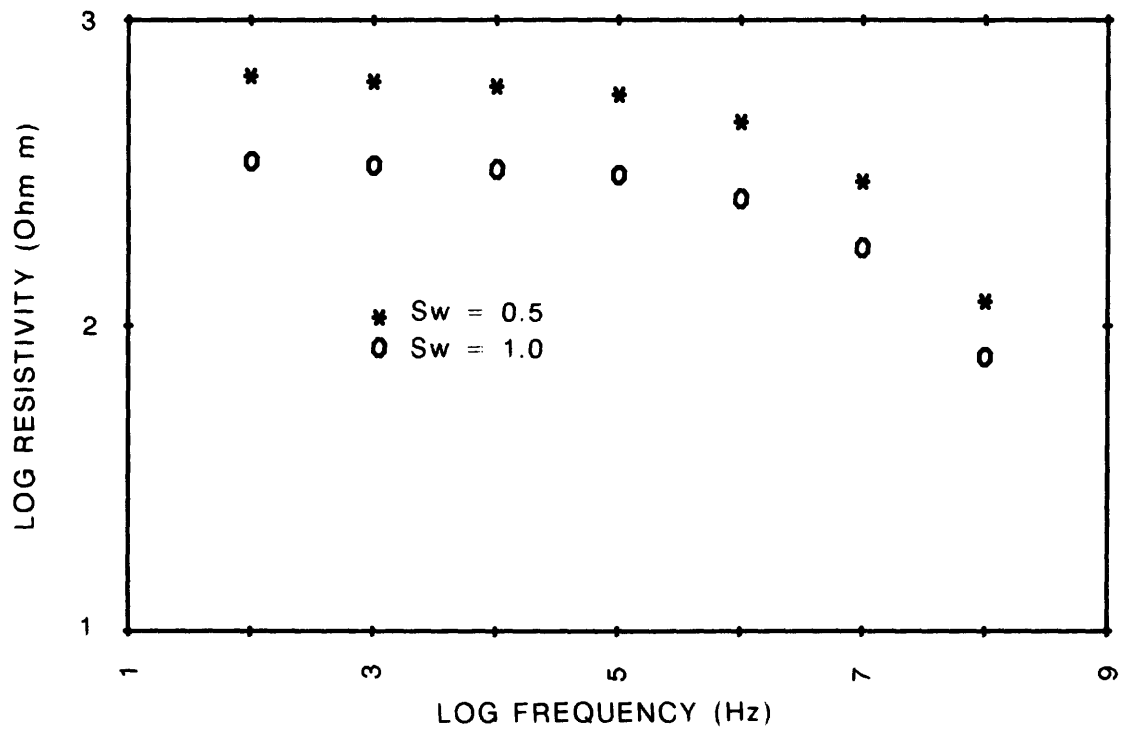
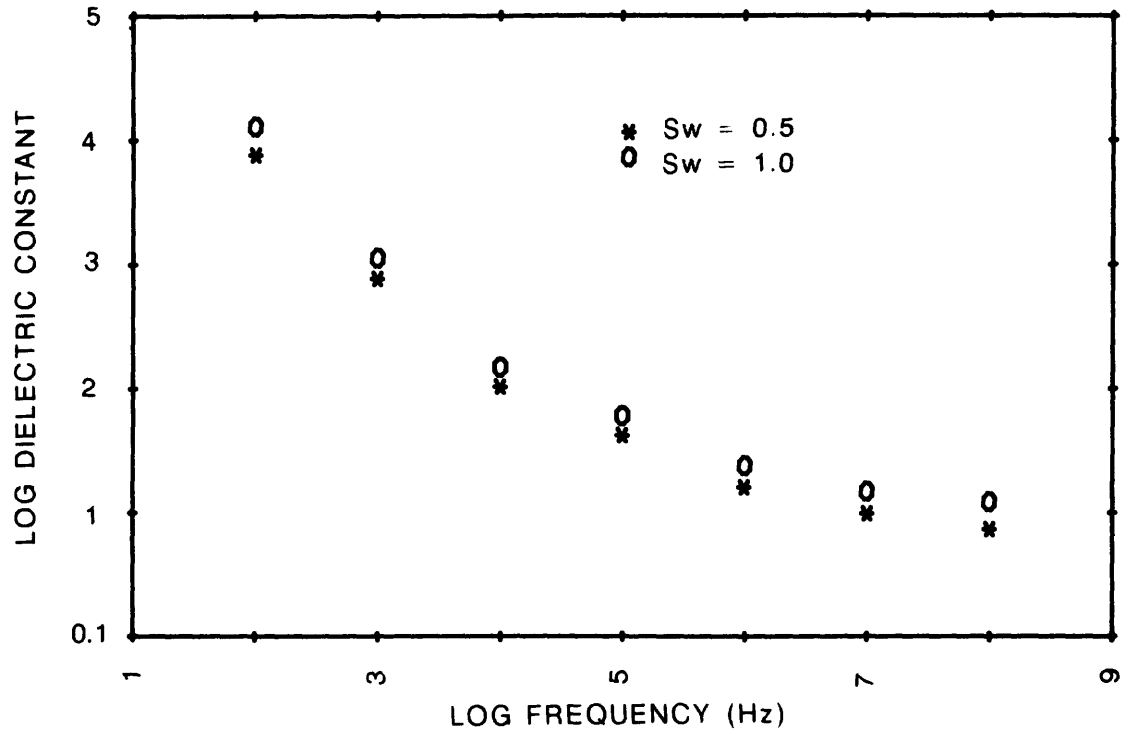


Figure 36.--Plots of dielectric constant and resistivity as a function of frequency for welded Tub Spring Member.

The dielectric constant tool is a shallow investigation tool, particularly at the higher frequencies, and thus is subject to the uncertainties of the extent of invasion. In the low MHz region, radii of investigation equivalent to the neutron log appear to be obtainable (Tittman, 1986). In the fresh water environment of Rainier Mesa, lower frequencies can probably be utilized without the adverse effects on attenuation and phase arising from the more saline pore waters found in petroleum lithologies at these frequencies. On the other hand, some neutron logs have been obtained in mud-filled holes in the unsaturated zone in Rainier Mesa clearly showing that the tuff is only partly saturated within the radius of investigation of the tool (Carroll, 1989). Thus, a high-frequency tool may be required if porosity is the desired output. Dielectric constant measured in the kilohertz frequency range has also been reported to be an indicator of the shaliness and the saturation of clayey sands (Hoyer and Rumble, 1976).

Additional details and references on the application of the dielectric constant to geophysical logging may be found in Tittman (1986) and Schlumberger (1987).

RESISTIVITY OF ROCKS IN RAINIER MESA AREA

In two previous reports dealing with velocity and density logging in Rainier Mesa (Carroll and Magner, 1988; Carroll, 1989) the statistical variation of these properties within individual lithologies were included and the values obtained were listed in appendices. This has not been done for electrical resistivity principally because of the absence of suitable information on mud resistivities in the individual boreholes. All R_m data listed on the logs examined for this report were almost universally obtained from the mud pit or tank. Thus the exact value to utilize with departure curves is unknown. The 4-in. borehole sizes generally drilled in Rainier Mesa necessitate the use of standard electric logs because resistivity tools with greater resolution available from commercial contractors are not generally compatible with these hole sizes. Thus standard electric logs were generally the only available resistivity devices employed over the historical period covered by this report. It is apparent that if resistivity is to become a quantitative tool in Rainier Mesa, the use of focused and induction tools needs to be explored for these slim holes.

Representative values of resistivity for the tuff units and comparisons of regional variations between similar units must await a study with greater control than this one. Based upon cursory examination, however, the average resistivity of the zeolitized zone is estimated as 50 ohm-meters, and that of the unsaturated zone beneath the caprock as 100 ohm-meters. These figures are considered accurate to about 20 percent.

The standard departure curves (Schlumberger, 1949) for determining true resistivity from the response of normal logs are based upon hole diameters about twice those used on Rainier Mesa. These curves (beds of infinite thickness, no invasion) indicate that a short-normal spacing for a 4-in. diameter hole of about 6 inches. For bed thicknesses in excess of about 17 ft this spacing will yield a good approximation to true resistivity for rock to mud resistivities of 20 to 1 or less. On the other hand, the standard 16-in. normal in a 4-in. hole is close to the peak of the departure curve, and yields higher than true resistivities by nearly 20 percent at a tuff to mud

resistivity ratio of 5 to 1. This increases as the resistivity contrast between tuff and mud increases. The use of a shorter long normal spacing would also allow the resistivities of thinner beds to be resolved and thus, some thought should be given to redesign of the normal log spacings for use in Rainier Mesa exploratory holes.

SUMMARY AND CONCLUSIONS

Examination of available data bearing on geophysical logging for electrical properties in vertical holes in the Rainier Mesa area results in a number of observations of utility in volcanic rocks. Several of these are fairly unqualified and can be utilized in future exploration in the area with considerable benefit. Other observations are less concrete and require additional laboratory or other field studies to pursue their usefulness or applicability to the tuffs in general. In the case of the parameters affecting resistivity behavior of the tuffs, although the questions on quantitative interpretation have not all been answered, it is felt that the directions to be pursued have been presented with considerably more succinctness than heretofore at Rainier Mesa and NTS. The following are the main observations of this investigation:

1) Aside from the usual characteristic signatures seen on electric logs due to low-porosity welded tuffs, there are character correlations within the bedded tuffs in the present tunnel testing areas which are diagnostic of the 3A/Tub Spring Member contact and subunits 3D and 4J. The 3A/Tub Spring horizon, characterized by a resistivity low, appears to be the most universal signature seen on these logs. Correlation signatures appear to become muted in the present westernmost drill holes in Rainier Mesa, and may be absent at the extreme north and south of the Rainier Mesa area.

2) The electric log does not appear to be particularly diagnostic in defining the top of zeolitization in many holes. However, electric logs penetrating this zone in northern Aqueduct Mesa appear to reflect this horizon, as does the n#2 hole in Rainier Mesa.

3) Bottom-hole temperatures obtained from electric logs in the Rainier Mesa area are not representative of the geothermal gradient in the area. In the deep volcanic sections removed from topographic effects, an estimate of the temperature at depth can be obtained from a combination of the geothermal gradient of 31 C/km determined by Lachenbruch and others (1987) in the Hagestad hole and the temperature of 20 C measured at tunnel level in N-tunnel.

4) A major unknown at NTS is the pore-water resistivity in the tuff, a value which cannot be obtained from existing measurements of fracture water. A pore-water resistivity of 35 ohm-meters has been derived from the water chemistry data of 18 samples from the t#3 hole. This is a value not greatly different from fracture water resistivity. Pore-water chemistry in the tuffs complicates log interpretation because it is not primarily NaCl and is composed of low total dissolved solids.

5) The observed electrical resistivity of tuffs in the Rainier Mesa area can be adequately described by the Waxman-Smits model if clay is ubiquitous in the tuff. If the ions in the clay double layer of the tuffs are as accessible

as they are in clayey sands, clay in amounts generally less than 5 percent appear to be generally sufficient to account for the resistivity observed in most zones. Clay in these amounts in both the partially saturated vitric tuff and in the saturated zeolitized tuff appears to be substantiated by available X-ray diffraction data. The high cation exchange capacity of clinoptilolite does not appear to yield anywhere near equivalent counterions in lowering the electrical resistivity of the tuffs compared with clays. To account for the ions indicated by these exchange capacities would require tuff resistivities an order of magnitude lower than presently observed. The dominance of clay as the primary mechanism in lowering resistivity, particularly at moderate to high clay contents, is supported by laboratory measurements on core from the Rainier Mesa area. In the presence of trace amounts of clay, the relative contribution of clinoptilolite counterions to the electrical resistivity in the zeolitized zone is unknown and requires further investigation. At best, however, it appears to be generally no greater than that from small amounts of clay. In the unsaturated zone, where zeolites are absent in significant amounts, clay must be the dominant mineral lowering electrical resistivity if pore-water resistivities are of the 35 ohm-meter magnitude indicated by the water chemistry from the t#3 hole.

6) The Waxman-Smits model predicts that the clay content per se bears no relationship to resistivity if the clay is distributed in a purely random fashion. This is because current conduction is via ion content in the available porosity, and weight clay may not necessarily be related to rock porosity. A wide range in resistivity, depending on porosity and clay content, is predicted at low clay contents. At high clay contents resistivity becomes less sensitive to clay and probably approaches a nearly constant value for the porosity ranges observed in the zeolitized tuff. Based on empirical observations on logs, a value of 2 to 8 ohm-meters appears to be the approximate limiting value recorded in the Rainier Mesa area, and this occurs at clay contents of less than 50 percent.

7) The empirical rule historically used in Rainier Mesa to determine clayey tuff zones based on observed resistivity, i.e., that zones exhibiting resistivities of less than 20 ohm-meters should be suspected of being clayey and those exhibiting resistivities of less than 10 ohm-meters should be suspected of potentially containing high clay contents, compares favorably with theory, given the uncertainty of some of the input parameters. Applying the Waxman-Smits model to the range of porosity and saturation available in the tuffs of Rainier Mesa suggests that this empirical rule is somewhat pessimistic at the lower porosities and saturations theoretically obtainable. If one postulates that clay cannot be present at depth in significant volumes unless both saturated and restricted to the the higher porosity ranges observed in the tuff, and (or) that the zeolites contribute counterions equivalent to trace amounts of clay to the resistivity, then this empirical rule is conservative.

8) Only one magnetic susceptibility and two induced polarization logs have been run in Rainier Mesa holes. The magnetic susceptibility log appears to yield lithologic correlations not recorded by other logs. Induced polarization logs yield noticeable response in the tuffs, however, the utility of these logs in deriving quantitative lithologic parameters requires laboratory investigation involving core.

9) The SP log often exhibits positive deflections in the volcanic rocks opposite several zones considered clayey. These deflections are opposite from what one would expect for saline pore water more resistive than the borehole mud, and are attributed to the effect of divalent cations in the ground water. Lost circulation coupled with the presence of divalent cations in the formation waters render successful interpretation of this log in terms of R_w or water chemistry difficult.

10) Although dielectric constant logs have not been run in Rainier Mesa holes, core measurements of the dielectric constant and resistivity in the range 100 Hz to 100 MHz indicate dispersion of a greater magnitude than seen in oil-bearing rocks, a phenomenon probably due to the higher resistivities prevalent in the fresh-water rocks of Rainier Mesa.

11) The 16- and 64-in. normal standard electric log spacings are not optimum for logging the 4-in. holes drilled in Rainier Mesa. If quantitative uses are to be made of resistivity, investigations of the applicability of focused and induction logs need to be pursued.

12) Uncertainties in the environmental corrections applicable to electric logs negate derivation of resistivities for specific units. The average resistivity of the unsaturated zone, exclusive of the caprock, can only be estimated at 100 ohm-meters and that of the zeolitized zone as 50 ohm-meters. These estimates are considered accurate within about 20 percent.

Finally, it appears that electric logging methods presently available may be a potent arsenal in deriving many mineralogic and physical-property parameters of the volcanic rocks. A major requirement in successfully applying these tools, however, lies in extensive laboratory investigations on samples.

REFERENCES CITED

- Alger, R.P., 1966, Interpretation of electric logs in fresh water wells in unconsolidated formations: Transactions 7th SPWLA Logging Symposium, Paper CC, 23 p.
- Alger, R.P., and Harrison, C.W., 1987, Improved fresh water assessment in sand aquifers utilizing geophysical well logs: 2nd International Symposium Minerals and Geotechnical Logging Society SPWLA, Proceedings, p. 99-118.
- Almon, W.R., 1979, A geologic appraisal of shaly sands: Transactions 20th SPWLA Annual Logging Symposium, Paper WW, 14 p.
- Amphlett, C.B., 1964, Inorganic ion exchangers: New York, Elsevier, 141 p.
- Arps, J.J., 1953, The effect of temperature on the density and electrical resistivity of sodium chloride solutions: Transactions American Institute of Mining and Metallurgical Engineers, v. 198, p. 327-330.
- Balch, S.J., Morris, W.A., Blohm, D., and Thuma, B., 1987, Interpretation of borehole magnetic data for mineral exploration and lithologic mapping: Proceedings 2nd International Symposium on Borehole Geophysics for Minerals, Geotechnical, and Groundwater Applications SPWLA, p. 179-188.
- Bates, R.L., and Jackson, J.A., 1980, Glossary of geology: Falls Church, VA, American Geological Institute, 749 p.
- Bath, G.D., 1968, Aeromagnetic anomalies related to remanent magnetism in volcanic rock, Nevada Test Site, in Eckel, E.B., ed., Geological Society of America Memoir 110, p. 135-146.

- Bish, D.L., and Vaniman, D.T., 1985, Mineralogic summary of Yucca Mountain, Nevada: Los Alamos National Laboratory Report LA-10543-MS, 55 p.
- Breck, D.W., 1973, Zeolite molecular sieves: Structure Chemistry and Use: New York, Wiley and Sons, 771 p.
- Brethauer, G.E., Magner, J.E., and Miller, D.E., 1980, Statistical evaluation of physical properties in Area 12, Nevada Test Site, using USGS/DNA storage and retrieval system: U.S. Geological Survey report USGS-474-309, 96 p.; available only from U.S. Department of Commerce, National Technical Information Service, Springfield, VA 22161.
- Bristow, Q., 1987, A multifrequency slim hole inductive conductivity and magnetic susceptibility probe: Proceedings 2nd International Symposium on Borehole Geophysics for Minerals, Geotechnical, and Groundwater Applications SPWLA, p. 217-226.
- Byers, F.M., 1962, Porosity, density, and water content data on tuff of the Oak Spring Formation from the U12e tunnel system, Nevada Test Site, Nevada: U.S. Geological Survey Open-File Report (TEI 811), 37 p.
- Campos, J.C., and Hilchie, D.W., 1980, The effects of sample grinding on cation exchange capacity measurements: Transactions 21st SPWLA Logging Symposium, Paper FF, 18 p.
- Carroll, R.D., 1989, Density logging and density of rocks in the Rainier Mesa area, Nevada Test Site: U.S. Geological Survey Open-File Report 89-239.
- Carroll, R.D., Cunningham, M.J., 1980, Geophysical investigations in deep horizontal holes drilled ahead of tunnelling: International Journal Rock Mechanics Mining Science, v. 17, p. 89-107.
- Carroll, R.D., Cunningham, M.J., and Muller, D.C., 1979, Geophysical logging and seismic investigations, in U.S. Geological Survey investigations in connection with the Mighty Epic event, U12n.10 tunnel, Nevada Test Site: U.S. Geological Survey report USGS-474-228, 191 p.; available only from U.S. Department of Commerce, National Technical Information Service, Springfield, VA 22161.
- Carroll, R.D., and Magner, J.E., 1988, Velocity logging and seismic velocity of rocks in the Rainier Mesa area, Nevada Test Site, Nevada: U.S. Geological Survey Open-File Report 88-380, 85 p.
- Carroll, R.D., and Muller, D.C., 1973, Techniques for the quantitative determination of alluvial physical properties from geophysical logs, southern Yucca Flat, Nevada Test Site: U.S. Geological Survey report USGS-474-175, 113 p.; available only from U.S. Department of Commerce, National Technical Information Service, Springfield, VA 22161.
- Claassen, H.C., and White, A.F., 1979, Application of geochemical kinetic data to ground-water systems, Part I, A tuffaceous-rock system in southern Nevada, in Jenne, E.A., ed., Chemical Modeling in Aqueous Systems: American Chemical Society Symposium Series, 93, p. 447-473.
- Clavier, C., Coates, G., and Dumanoir, J., 1977, Theoretical and experimental bases for the dual-water model for the interpretation of shaly sands: Annual Conference of Society of Petroleum Engineers, 52nd, Denver, SPE Paper 6859.
- _____, 1984, Theoretical and experimental bases for the dual-water model for interpretation of shaly sand: Journal of the Society Petroleum Engineers, v. 24, p. 153-167.
- Clebsch, Alfred, Jr., 1961, Tritium age of ground water at the Nevada Test Site, Nye County, Nevada: U.S. Geological Survey Professional Paper 424-C, p. C122-C125.

- Clebsch, Alfred, Jr., and Barker, F.B., 1960, Analysis of ground water from Rainier Mesa, Nevada Test Site, Nye County, Nevada: U.S. Geological Survey Open-File Report, (TEI-763), 22 p.
- Daniels, W.R., Wolfberg, K., Rundberg, R.S., and others, 1982, Summary report on the geochemistry of Yucca Mountain and environs: Los Alamos National Laboratory Report LA-9328-MS, 364 p.
- Desai, K.P., and Moore, E.J., 1969, Equivalent NaCl determination from ionic concentrations: *The Log Analyst*, v. 10, no. 3, p. 12-21.
- Doll, H.G., 1949, The SP log: Theoretical analysis and principles of interpretation: *Transactions American Institute Mining Engineers*, v. 179, p. 146-185.
- Dresser Atlas, 1982, Well logging interpretation techniques: Dresser Atlas, Dresser Industries, Inc., Houston, 211 p.
- Eberle, W.R., and Bigelow, R.C., 1973, Electrical dispersion characteristics of selected rock and soil samples from the Nevada Test Site: U.S. Geological Survey report USGS-474-162, 50 p.; available only from U.S. Department of Commerce, National Technical Information Service, Springfield, VA 22161.
- Edmundson, H., and Raymer, L.L., 1979, Radioactive logging parameters for common minerals: *Transactions 20th SPWLA Annual Logging Symposium*, Paper O, 20 p.
- Evers, J.F., and Iyer, B.G., 1975, A statistical study of the SP log in freshwater formations of northern Wyoming: *Transactions 16th SPWLA Logging Symposium*, Paper K, 8 p.
- Freedman, R., and Vogiatzis, J.P., 1986, Theoretical modeling of induced-polarization logging in a borehole: *Geophysics*, v. 51, no. 9, p. 1830-1849.
- Gibbons, A.B., Hinrichs, E.N., Hansen, W.R., and Lemke, R.W., 1963, Geology of the Rainier Mesa Quadrangle, Nye County, Nevada: U.S. Geological Survey Geologic Quadrangle Map GQ-215, scale 1:24,000.
- Gomez-Rivero, O., 1976, A practical method for determining cementation exponents and some other parameters as an aid in well log analysis: *The Log Analyst*, v. 27, no. 5.
- Gondouin, M., Tixier, M.P., and Simard, G.L., 1957, An experimental study on the influence of the chemical composition of electrolytes on the SP curve: *Transactions American Institute Mining Engineers*, v. 213, p. 58-72.
- Hay, R.L., and Sheppard, R.A., 1977, Zeolites in open hydrologic systems, in *Mineralogy and geology of natural zeolites*: Mineralogical Society of America, p. 93-102.
- Hearst, J.R., and Nelson, P.H., 1985, Well logging for physical properties: New York, McGraw-Hill, 571 p.
- Hill, H.J., and Milburn, J.D., 1950, Effect of clay and water salinity on electrochemical behavior of reservoir rocks; *Transactions American Institute on Mining and Metallurgical Engineers*, v. 207, p. 64-72.
- Hill, H.J., Shirley, O.J., and Klein, G.E., 1979, Boundwater in shaly sands--its relation to Qv and other formation properties: *The Log Analyst*, v. 20, no. 3, p. 3-19.
- Hoover, D.L., 1968, Genesis of zeolites, Nevada Test Site; in Eckel, E.B., ed., *Nevada Test Site: Geological Society of America Memoir 110*, p. 275-284.
- Hoyer, W.A., and Rumble, R.C., 1976, Dielectric constant of rocks as a petrophysical parameter: *Transactions 17th SPWLA Logging Symposium*, Paper O, 28 p.

- Jacobson, Roger L., Henne, Mark S., and Hess, John W., 1986, A reconnaissance investigation of hydrogeochemistry and hydrology of Rainier Mesa: University Nevada Desert Research Institute Pub. 45046, 54 p.
- Johnson, W.L., and Linke, W.A., 1977, Some practical applications to improve formation evaluation of sandstones in the MacKenzie delta: Formation Evaluation Symposium of Canadian Well Log Society, 6th, Paper R.
- Juhasz, I., 1979, The central role of Qv and formation water salinity in the evaluations of shaly formations: Transactions 20th SPWLA Annual Logging Symposium, Paper AA, 26 p.
- _____, 1981, Normalized Qv--the key to shaly sand evaluation using the Waxman-Smits equation in the absence of core data: Transactions 22nd SPWLA Annual Logging Symposium, Paper Z, 36 p.
- Keller, G.V., 1959a, Porosity, density, and fluid permeability of the Oak Spring Tuff, in Properties of Oak Spring Formation in Area 12 at the Nevada Test Site: U.S. Geological Survey Open-File Report (TEI-672).
- _____, 1959b, Measurements of water content in the Oak Spring tuff, in Properties of Oak Spring Formation in Area 12 at the Nevada Test Site: U.S. Geological Survey Open-File Report (TEI-672).
- _____, 1962, Electrical resistivity of rocks in the Area 12 tunnels, Nevada Test Site, Nye County, Nevada: Geophysics, v. 27, no. 2, p. 242-252.
- Knowlton, G.D., and McKague, L.H., 1976, A study of the water content in zeolitic tuffs from the Nevada Test Site: Lawrence Livermore National Laboratory Report UCRL-78013, 18 p.
- Lachenbruch, A.H., Marshall, B.V., and Roth, E.F., 1987, Thermal measurements in Oak Spring Formation at the Nevada Test Site, southern Nevada: U.S. Geological Survey Open-File Report 87-610, 19 p.
- Maldonado, Florian, Steele, S.G., and Townsend, D.R., 1979, Supplementary lithologic logs of selected vertical drill holes in Area 12, Nevada Test Site: U.S. Geological Survey report USGS-474-261, 61 p.; available only from U.S. Department of Commerce, National Technical Information Service, Springfield VA 22161.
- Ming, D.W., and Dixon, J.B., 1987, Quantitative determination of clinoptilolite in soils by a cation-exchange capacity method: Clays and Clay Minerals, v. 35, no. 6, p. 463-468.
- Ming, D.W., and Mumpton, F.A., 1989, Zeolites in soils, in Minerals in Soil Environments, 2nd Ed., Dixon, J.B., and Weed, S.B., eds.: Soil Science Society of America, 1264 p.
- Moore, J.E., 1962, Selected logs and drilling records of wells and test holes drilled at the Nevada Test Site prior to 1960: U.S. Geological Survey Open-File Report (TEI-804), 54 p.
- Mumpton, F.A., 1977, Natural zeolites, in Mineralogy and geology of natural zeolites: Mineralogical Society of America, p. 1-15.
- National Research Council, 1929, International Critical Tables, v. 6, New York, McGraw-Hill, 471 p.
- Nelson, P.H., Hansen, W.H., and Sweeney, M.J., 1982, Induced polarization response of zeolitic conglomerate and carbonaceous siltstone: Geophysics, v. 47, no. 1, p. 71-88.
- Olhoeft, G.R., 1986, Electrical conductivity, in Eighth Workshop on electromagnetic induction in the earth and moon, review papers: International Association Geomagnetism and Aeronomy Working Group 1-3, August 1986, University Neuchatel, p. 2-1 to 2-13.
- Ortiz, I., Van Gonten, W.D., and Osoba, J.S., 1972, Relationship of the electrochemical potential of porous media with hydrocarbon saturation: Transactions 13th SPWLA Logging Symposium, Paper P, 14 p.

- Patchett, J.G., 1975, An investigation of shale conductivity: Transactions 16th SPWLA Annual Logging Symposium, Paper U, 41 p.
- Patnode, H.W., and Wyllie, M.R., 1950, The presence of conductive solids in reservoir rock as a factor in electric log interpretation: Transactions American Institute Mining Engineers, v. 189, p. 47-52.
- Pawloski, G.A., 1981, Water contents of samples from the Nevada Test Site: Total free (natural state to 105 °C), and more tightly bonded (105-700 °C): Lawrence Livermore National Laboratory Report UCRL-53130, 18 p.
- Ransom, R.C., 1977, Methods based on density and neutron well logging responses to distinguish characteristics of shaly sandstone reservoir rocks: The Log Analyst, v. 28, no. 3, p. 47-62.
- Sargent, K.A., and Orkild, P.P., 1973, Geologic map of the Wheelbarrow Peak-Rainier Mesa Area, Nye County, Nevada: U.S. Geological Survey Miscellaneous Geologic Investigations Map I-754, scale 1:48,000.
- Schlumberger, 1949, Resistivity departure curves: Schlumberger, Ridgefield, CT, 121 p.
- _____, 1979, Log interpretation charts: Schlumberger, Ridgefield, CT, 97 p.
- _____, 1987, Log interpretation principles/applications: Schlumberger, Houston, TX, 198 p.
- Scott, J.A., Seeley, R.L., and Barth, J.L., 1981, A magnetic susceptibility well-logging system for mineral exploration: Transactions 22nd SPLWA Logging Symposium, Paper CC, 21 p.
- Smits, L.J.M., 1968, SP log interpretation in shaly sands: Journal of the Society Petroleum Engineers, v. 8, p. 123-136.
- Starkey, H.C., 1964, Determination of the ion-exchange capacity of a zeolitic tuff: U.S. Geological Survey Professional Paper 475-D, p. D93-D95.
- Sumner, J.S., 1976, Principles of induced polarization for geophysical exploration: New York, Elsevier, 277 p.
- Thomas, E.C., 1976, The determination of Qv from membrane potential measurements on shaly sands: Journal of Petroleum Technology, v. 28, p. 1087-1096.
- Thordarson, William, 1965, Perched ground water in zeolitized-bedded tuff, Rainier Mesa and vicinity, Nevada Test Site, Nevada: U.S. Geological Survey Open-File Report (TEI-862), 90 p.
- Tittman, Jay, 1986, Geophysical well logging, in Methods in Experimental Physics, v. 24: Geophysics: New York, Academic Press, 175 p.
- Tripp, A.C., and Klein, J.D., 1988, Departure curves for induced polarization well logging: The Log Analyst, v. 29, no. 2.
- U.S. Geological Survey, 1979, U.S. Geological Survey investigations in connection with the Mighty Epic event, U12n.10 tunnel, Nevada Test Site: U.S. Geological Survey report USGS-474-228, 191 p.; available only from U.S. Department of Commerce, National Technical Information Service, Springfield, VA 22161.
- Ucok, Hikmet, 1979, Temperature dependence of the electrical resistivity of aqueous salt solutions and solution-saturated porous rocks: University of Southern California Ph.D. dissertation, 154 p.
- van Olphen, H., 1977, An introduction to clay colloid chemistry, New York, John Wiley, 318 p.
- Vinegar, H.J., and Waxman, M.H., 1984, Induced polarization of shaly sands: Geophysics, v. 49, no. 8, p. 1267-1287.
- Waxman, M.H., and Smits, L.J.M., 1968, Electrical conductivities in oil-bearing shaly sands: Journal of the Society Petroleum Engineers, v. 243, no. 8, p. 107-122.

- Waxman, M.H., and Thomas, E.C., 1974, Electrical conductivities in oil bearing shaly sands: (I) The relation between hydrocarbon saturation and resistivity index; (II) The temperature coefficient of electrical conductivity: Journal of the Society Petroleum Engineers, v. 14, p. 213-225.
- White, A.F., Claassen, H.C., and Benson, L.V., 1980, The effect of dissolution of volcanic glass on the water chemistry in a tuffaceous aquifer, Rainier Mesa, Nevada: U.S. Geological Survey Water-Supply Paper 1535-Q, 34 p.
- Wiley, R., and Snoddy, M.L., 1986, Complex resistivity of shaly sands and minerals: The Log Analyst, v. 27, no. 5, p. 45-59.
- Worthington, P.F., 1985, The evolution of shaly sand concepts in reservoir evaluation: Log Analyst, v. 26, no. 1, p. 23-40.
- Zonge, K.L., Sauck, W.A., and Sumner, J.S., 1972, Comparison of time, frequency, and phase measurements in induced polarization: Geophysical Prospecting, v. 20, no. 3, p. 626-648.